DUVAR

2024

INNOVATIVE APPROACHES IN ENGINEERING SOLUTIONS

& Applied Studies

EDITORS:
PROF. DR. ARİF UZUN & ASST. PROF. DR. ERMAN ZURNACI

INNOVATIVE APPROACHES IN ENGINEERING SOLUTIONS & APPLIED STUDIES

Editors:

Prof. Dr. Arif UZUN

Asst. Prof. Dr. Erman ZURNACI

Innovative Approaches In Engineering Solutions & Applied Studies
Editors: Prof. Dr. Arif UZUN, Asst. Prof. Dr. Erman ZURNACI

Editor in chief: Berkan Balpetek
Cover and Page Design: Duvar Design
Printing : December -2024
Publisher Certificate No: 49837
ISBN:978-625-5551-01-6

853 Sokak No:13 P.10 Kemeraltı-Konak/İzmir
Tel: 0 232 484 88 68

www.duvaryayinlari.com
duvarkitabevi@gmail.com

TABLE OF CONTENTS

Chapter 1

MICROSTRUCTURE AND MECHANICAL PROPERTIES OF CU COPPER ALLOYS PRODUCED BY POWDER METALLURGY METHOD

Mehmet AKKAŞ[1]

[1] Assoc. Prof. Dr., Department of Mechanical Engineering/Faculty of Engineering and Architecture, Kastamonu University, Turkey, mehmetakkas@kastamonu.edu.tr, (ORCID: 0000-0002-0359-4743)

1. INTRODUCTION

Copper is a versatile element that can be alloyed with a variety of materials, including high-melting-point elements such as iron, chromium, and cobalt. The resulting copper-based alloys are utilized extensively across a broad spectrum of industrial sectors, encompassing applications such as components in gas turbines, medical devices, and nuclear systems. These alloys exhibit remarkable capabilities in addressing critical challenges associated with wear resistance, corrosion, and thermal fatigue [1]. The unique properties inherent to copper alloys are propelling the development of innovative formulations, particularly for machinery components such as bearings, gears, and cams, which are subjected to friction and wear during operational cycles. This necessitates an urgent demand for the continuous development of novel materials designed specifically to mitigate wear rates in modern engineering applications. Furthermore, tribological research is dedicated to the systematic analysis and exploration of phenomena related to friction, lubrication, and wear [2]. By investigating these elements, researchers aim to uncover pathways that can effectively reduce friction and wear in machine components. As technological advancements progress, traditional materials are increasingly being replaced by new materials that exhibit more specialized and superior characteristics. This shift underscores the critical need for ongoing development in raw materials within the industrial sector, particularly in the field of materials science. Researchers are directing their focus towards the investigation of innovative materials that demonstrate enhanced attributes compared to conventional natural and alloyed substances. These new composites, in contrast to traditional materials, are engineered to possess superior properties that meet contemporary demands [3-5].

Composite materials offer a multitude of advantages over their conventional counterparts. One of their most significant attributes is their lightweight nature, which is coupled with impressive strength and durability [6]. Specifically, copper alloys provide a range of benefits, including catalytic activity and compatibility with hydrogenation processes [7]. Additionally, electrolytic copper coatings have been effectively employed in various applications to reduce wear and friction, especially in abrasive environments. The utilization of powder metallurgy techniques for the production of copper-based alloys is a well-established practice [8]. Powder metallurgy encompasses a comprehensive suite of processes that include the generation, blending, and transformation of metal powders into finished products. This methodology is particularly advantageous for materials that exhibit poor forgeability and machinability. For example, the inherent challenges associated with forging high-strength alloys used in gas turbine disk fabrication have rendered powder metallurgy a more favorable alternative.

Furthermore, the ability to precisely control the particle size of the powders and minimize defects, such as gas voids, represents additional benefits of this production method [9-13].

As technological landscapes continue to evolve, there is a compelling imperative to enhance materials that serve as foundational components in industrial applications. Scientists and researchers in the materials domain are increasingly focused on the development of new substances that exhibit superior characteristics compared to traditional natural and alloyed materials. Such innovations have led to the creation of composite materials distinguished by their exceptional properties. Notably, composite materials provide numerous advantages over conventional materials, prominently featuring their lightweight composition in conjunction with superior strength [14-17].

Copper and its alloys are amenable to alloying with several elements, including iron, chromium, and cobalt, all of which possess elevated melting points. Copper-based alloys are employed in an array of industrial applications, which include critical components in gas turbines, medical devices, and nuclear systems. These alloys are adept at addressing issues of wear resistance, corrosion, and thermal fatigue, thereby facilitating the ongoing advancement of new copper-based formulations. The engineering of machine components such as bearings, gears, and cams—elements that experience mutual contact and wear—is of paramount importance [18-21]. Presently, there exists a substantial need for the innovation of new materials designed explicitly to reduce wear rates. In this context, tribological studies concentrate on various phenomena, including friction, lubrication, and wear, with the goal of identifying effective strategies to minimize friction and wear in mechanical components [23,23].

Owing to their remarkable properties—such as exceptional heat resistance, corrosion resistance, toughness, and mechanical strength—copper and its alloys are increasingly preferred as high-performance engineering materials across a multitude of fields, including aerospace, automotive, and biomedical applications [24]. In addition to industrial and medical applications, such as machinery components and construction materials, these materials are also employed in advanced applications encompassing electronics, aerospace technology, and everyday products like super-elastic eyeglass frames and mobile phone antennas. Recent years have also witnessed an increased utilization of copper alloys in robotics applications. Nonetheless, the industrial application of copper and its alloys faces challenges associated with their mechanical properties and wear resistance [25-29]. To overcome these challenges, the integration of molybdenum (Mo) and tungsten (W) particles into copper alloys via powder metallurgy techniques has been explored. This approach aims to significantly enhance both

the wear resistance and mechanical properties of the produced samples, thereby addressing a critical need within the industry.

In the course of this study, a thorough literature review revealed a conspicuous gap regarding the feasibility of producing copper composites reinforced with molybdenum and tungsten. Consequently, this research endeavors to fill the identified gap in the existing literature by investigating the production of molybdenum and tungsten-reinforced copper composites utilizing powder metallurgy techniques. The primary objective of this study is to provide valuable insights and contributions to the materials science field, particularly in the quest to develop high-performance copper-based alloys characterized by enhanced mechanical properties for a diverse range of industrial applications. This research holds the potential to facilitate advancements in material engineering, ultimately leading to the creation of innovative applications across various industries, enhancing both the functionality and durability of the resultant alloys in practical use.

2. EXPERIMENTAL STUDIES

Three distinct alloy compositions were prepared via powder metallurgy for subsequent experimental assessment. This synthesis process utilized high-purity copper (Cu), molybdenum (Mo), and tungsten (W) powders, each with an approximate purity of 99.9% and a particle size of 325 mesh. To tailor the properties of these alloys for experimental requirements, 20% by weight of Mo and 20% by weight of W were introduced into the base materials, enabling the targeted modification of their mechanical and physical attributes. To ensure homogeneity within the alloy powders, the constituent metal powders underwent a mechanical alloying process. This procedure involved mixing in a Retsch PM100 planetary ball mill, which operated at a rotational speed of 350 rpm for a duration of 5 hours. The planetary mill's design includes a tightly sealed powder chamber, which prevents contamination by isolating the powder from the external environment once enclosed. This isolation is crucial for maintaining the purity and consistency of the alloy during the milling process. After the mechanical alloying phase, the blended powders were transferred into a cold pressing mold for compaction. The cold pressing process employed a pressing pressure of 700 MPa to shape and densify the powder materials. This pressing procedure was performed with a Specac GS15011 hydraulic pellet press housed at the Central Research Laboratory of Kastamonu University. A cylindrical mold with a 13 mm diameter was chosen to ensure uniform sample geometry. Throughout the pressing operation, a constant pressure of 700 MPa was applied to achieve the required level of material densification and structural integrity, setting a

consistent baseline for subsequent material testing and analysis. The sintering of the powder samples was performed using an atmosphere-controlled heat treatment furnace located in the Metallurgy and Materials Engineering Laboratories at Kastamonu University. After compaction, the samples were sintered at a temperature of 1050°C under an argon atmosphere for 30 minutes. This controlled environment facilitated the formation of robust material bonds and promoted effective densification of the powders.

The complete sintering cycle lasted 270 minutes. To eliminate volatile substances, such as residual oils and other impurities within the samples, a gradual heating process was employed. The samples were heated from room temperature to the target sintering temperature of 1050°C at a controlled rate of approximately 10°C per minute, reaching the sintering temperature in 120 minutes. This gradual increase allowed for the controlled expulsion of contaminants without compromising the material structure. Upon reaching the sintering temperature, the samples were held isothermally at 1050 °C for 30 minutes. This holding period was critical for promoting diffusion and bonding at the particle level within the powder matrix, thereby enhancing the material's mechanical properties and microstructure uniformity. Following the holding phase, a controlled cooling process was applied to avoid thermal stresses that might otherwise impact the structural integrity of the samples. Over a period of 120 minutes, the samples were gradually cooled to room temperature within the controlled atmosphere of the furnace's cooling chamber. This careful cooling process further stabilized the internal structure of the sintered materials. Following the sintering process, the test samples were prepared for scanning electron microscopy (SEM) imaging through a series of meticulous metallographic procedures. These procedures included mounting in bakelite, incremental grinding, precision polishing, and targeted etching. Each sample was mounted individually in bakelite at a controlled temperature of 100°C, providing stability and ease of handling for subsequent preparation stages.

3. EXPERIMENTAL RESULTS AND EVALUATION

3.1. SEM-EDS Analysis Results of Samples

Scanning electron microscopy (SEM) imaging of Co-Mo-W alloys fabricated using the powder metallurgy method has been conducted, providing a detailed assessment of their microstructural features. A thorough examination of the SEM images presented in Figure 1 reveals a pronounced copper matrix that constitutes a significant component of the samples. In addition, the images demonstrate a uniform distribution of molybdenum (Mo) and tungsten (W) particles within the internal architecture of the alloy.

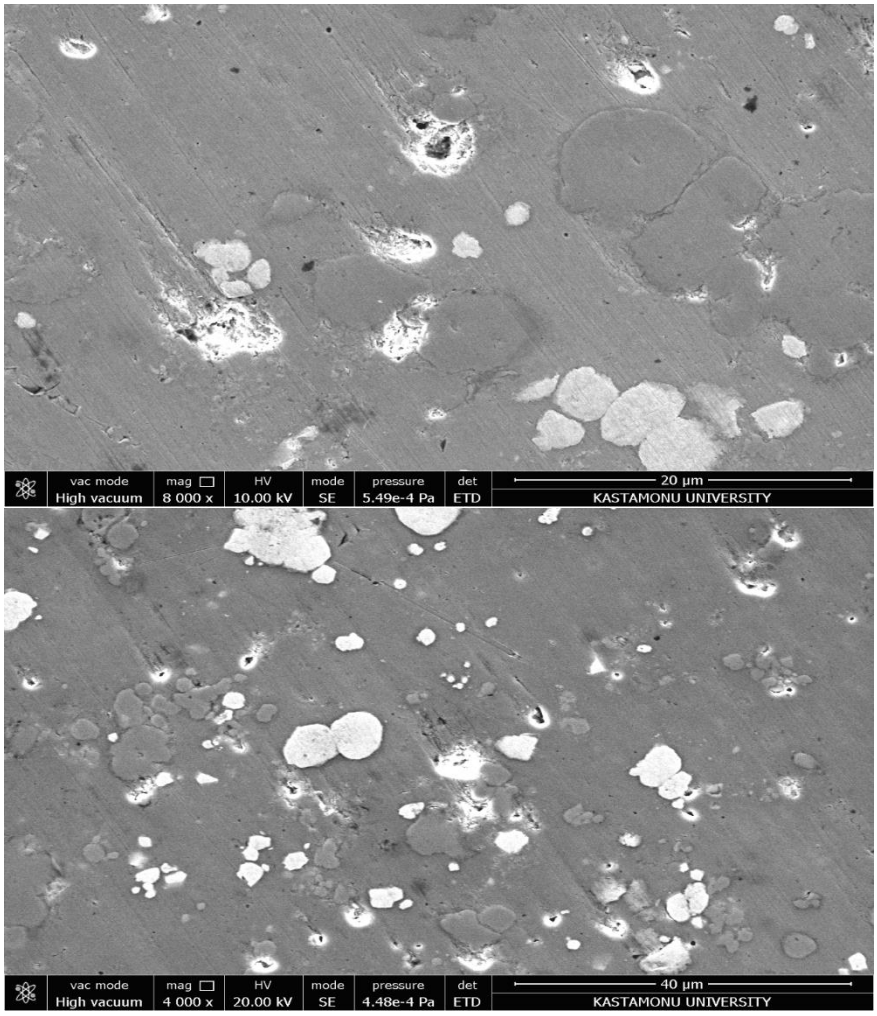

Figure 1. SEM images of the produced sample.

The produced samples show evidence of partial cracking and the occurrence of porosity, both of which are pivotal factors that can adversely affect their mechanical performance [30]. Importantly, the SEM analysis suggests that the introduction of Mo and W into the alloy composition is associated with a notable decrease in the overall levels of porosity. This reduction is particularly beneficial, as it implies an enhancement in the densification of the material, thereby bolstering its structural integrity [31-34]. Furthermore, the SEM images substantiate that the Mo and W particles are not only present but are also uniformly distributed throughout the microstructural framework of the alloys. This homogenous distribution is attributed to the successful implementation of mechanical alloying followed by sintering processes, which effectively promote the even dissemination of these particles within the copper matrix. The uniformity of Mo and W distribution is essential for the enhancement of the mechanical properties of the alloys, as it is likely to improve their strength and overall durability [35-39].

The insights derived from the scanning electron microscopy energy dispersive spectroscopy (SEM-EDS) analysis, as detailed in Figure 2 and summarized in Table I.. Provide robust evidence that the chemical compositions of the synthesized composite sample are in close accordance with the specified formulation parameters established prior to synthesis [40-42]. A particularly noteworthy observation is made from the EDS analysis at Spot 1, which indicates that the internal structure of the composite material comprises 75.15% copper (Cu), 0.14% molybdenum (Mo), and 24.71% tungsten (W). This finding illustrates the predominant role of copper in the composite's architecture. Furthermore, the assessment conducted at Spot 2 revealed a composition that consists entirely of 100% copper, highlighting a region within the sample where copper exists in its purest form. In contrast, the analysis at Spot 3 distinctly identified a composition that is composed entirely of 100% molybdenum, underscoring the presence of this critical alloying element within the matrix. Finally, the results obtained from Spot 4 indicated a composition of 5.87% Cu and 94.13% W, which suggests a significant presence of tungsten in this particular region, pointing to the alloy's multifaceted microstructural characteristics [43-47].

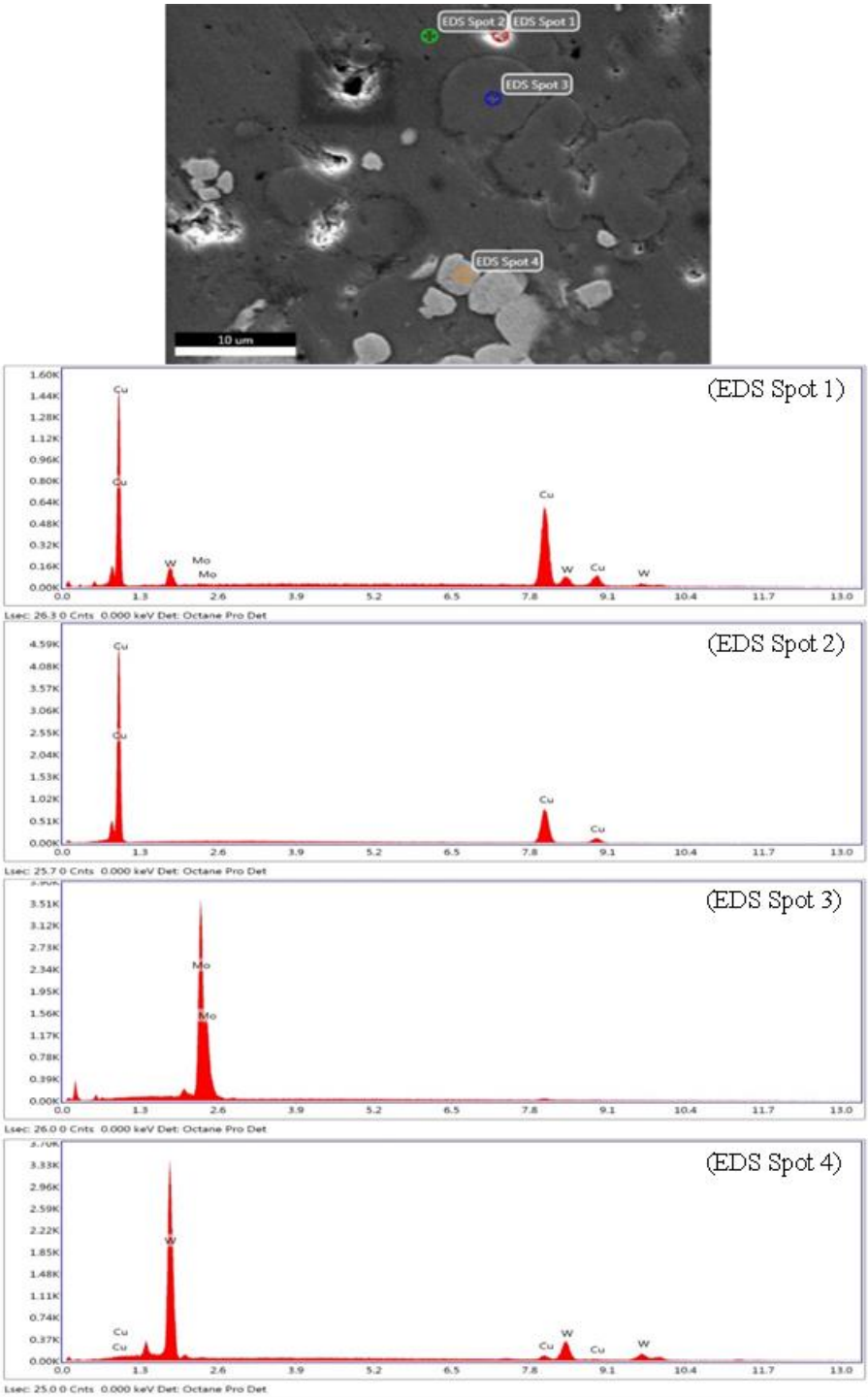

Figure 2. SEM-EDS analysis results of the produced sample.

Table I. EDS Spot analysis results of the produced sample.

EDS Spot	Element	Weight (%)
EDS Spot 1	Cu	75.15
	Mo	0.14
	W	24.71
EDS Spot 2	Cu	100
EDS Spot 3	Mo	100
EDS Spot 4	Cu	5.87
	W	94.13

The SEM-EDS results not only corroborate the hypothesis that the light gray regions observed in the SEM images represent the principal phase of the material but also reveal the complex and heterogeneous nature of the composite. The distinct chemical compositions identified at various locations throughout the sample shed light on the spatial distribution and arrangement of the alloying elements, revealing critical insights into how these factors influence the overall properties of the composite material. This extensive compositional analysis is paramount for understanding the intricate interplay between the microstructural features of the material and its resulting mechanical properties [48-51]. Such knowledge is vital for the advancement of optimization strategies and application methodologies concerning composite materials, with implications in both academic research and practical industrial applications. Moreover, gaining a more profound understanding of the relationships between composition and microstructure will significantly enhance the ability to engineer materials specifically tailored to meet diverse application requirements. This capability is particularly crucial in industries where performance and functionality are paramount, such as aerospace, automotive, and biomedical fields. By integrating the findings from this study into broader material science research, we can facilitate significant advancements in the development of innovative solutions across various engineering disciplines. Ultimately, this comprehensive knowledge base will contribute not only to the enhancement of existing materials but also to the creation of novel composites that can fulfill the demanding challenges presented by modern technological applications. Such developments will ensure that engineers and researchers can continue the boundaries of material performance, leading to groundbreaking applications in the future [52-56].

The hardness assessments were meticulously carried out along a defined linear trajectory across the surface of the sample, with measurements taken at precise intervals of 150 μm. This methodical approach ensured that the data collected accurately reflects the hardness distribution throughout the material. The results indicated that the microhardness of the sample was approximately 179 vickers, a value that signifies a substantial degree of hardness for the material in question. This notable increase in hardness can be primarily linked to the presence of hard phases, specifically carbides, which play a crucial role in enhancing the overall strength and wear resistance of the composite [57-60]. The introduction of alloying elements such as molybdenum (Mo) and tungsten (W) into the matrix has been instrumental in facilitating the formation of these hard phases. The solid solution strengthening and precipitation hardening mechanisms associated with these elements are likely responsible for the pronounced enhancement in the hardness values observed [58]. Moreover, the formation of these hard phases not only contributes to increased hardness but also impacts other mechanical properties, such as toughness and ductility, which are critical for various applications. The presence of carbides and other reinforcing phases within the microstructure effectively impedes dislocation movement, which is a primary mechanism of plastic deformation [60-65].

4. GENERAL RESULTS

In this comprehensive investigation, copper alloys incorporated with molybdenum (Mo) and tungsten (W) were successfully synthesized utilizing the advanced powder metallurgy technique. The parameters established for the production process included a cold pressing phase conducted at a pressure of 700 MPa, followed by a sintering phase at a temperature of 1050 ℃ for a duration of 30 minutes within an argon-controlled atmosphere. This methodology was meticulously designed to optimize the properties of the resultant materials. The produced samples underwent thorough analysis using state-of-the-art scanning electron microscopy-energy dispersive spectroscopy (SEM-EDS) and microhardness testing. The analysis yielded several significant findings, which are outlined as follows:

- The powder metallurgy approach effectively enabled the pressing and sintering of copper alloys containing Mo and W, demonstrating its potential as a reliable fabrication method for high-performance materials.
- A detailed examination of the SEM images reveals a notable trend: as the proportions of Mo and W within the alloys increased, there was a corresponding decrease in the porosity levels of the samples. This

observation is particularly significant, as lower porosity generally correlates with enhanced mechanical strength and integrity.

- The microhardness measurements conducted on the samples yielded a value of approximately 179 vickers. This substantial increase in hardness is closely linked to the presence of carbides and the formation of hard phases within the microstructure. The incorporation of Mo and W particles has facilitated the development of these hard phases, which directly contributes to the overall enhancement of hardness observed in the alloys.

REFERENCES

1. Liu, Q., Niu, B., Liu, L., Ren, R., Ni, J., Luo, N., ... & He, J. (2024). Microstructure evolution and property characteristics in hot-pressed Mo-W-Cu refractory functional alloys with varying tungsten content. *International Journal of Refractory Metals and Hard Materials*, *125*, 106859.
2. Akkaş, M. (2022). Synthesis and characterization of MoSi2 particle reinforced AlCuMg composites by molten salt shielded method. *Türk Doğa ve Fen Dergisi*, *11*(4), 11-17.
3. Shakunt, N. S., & Upadhyaya, A. (2024). Effect of Fe addition in W-Ni-Cu heavy alloy processed through powder metallurgy on microstructure and mechanical properties. *Journal of Alloys and Compounds*, *970*, 172578.
4. Uzun, A. (2019). Production of aluminium foams reinforced with silicon carbide and carbon nanotubes prepared by powder metallurgy method. *Composites Part B: Engineering*, *172*, 206-217.
5. Albartouli, A. B. M., & Uzun, A. (2023). Mechanical and electrical properties of graphene nanosheet reinforced copper matrix composites materials produced by powder metallurgy method. *Science of Sintering*, *55*(3), 399-411.
6. Kumar, N., Bharti, A., Dixit, M., & Nigam, A. (2020). Effect of powder metallurgy process and its parameters on the mechanical and electrical properties of copper-based materials: Literature review. *Powder Metallurgy and Metal Ceramics*, *59*, 401-410.
7. Gurusamy, P., Subash, P., Bejaxhin, A. B. H., & Ramanan, N. (2024, November). Mechanical Properties, Tribological MG Characteristics of Stir Cast Magnesium Metal Matrix Composites. In *Advances in Additive Manufacturing Technologies: Proceedings of the International Conference on Advances in Additive Manufacturing Technologies* (p. 60). CRC Press.
8. Jaiswal, A. K., Maji, B., Kumar, M., & Maity, J. (2024). Structure-Property Correlation of a Newly Synthesized 6351Al/Body-Centered Tetragonal Boron Nitride Composite. *Journal of Materials Engineering and Performance*, *33*(14), 7164-7193.
9. Akkaş, M. (2024). The Effect of Molten Salt on The Mechanical Properties and Microstructure of CuNiSi Alloys with Reinforced Fe. *Science of Sintering*, *56*(1).

10. Mishra, S. (2024). *Microstructural Modification to Enhance the Properties of Carbon Nanotube Reinforced Copper Composites* (Doctoral dissertation, IIT Kharagpur).

11. Manikandan, R. (2024). Effect of Mn addition in W-Ni-Cu heavy alloy processed through hot press sintering techniques on microstructure, microtexture and grain boundary character evolution. *Materials Characterization*, *210*, 113808.

12. Ujah, C. O., & Von Kallon, D. V. (2024). Characteristics of Phases and Processing Techniques of High Entropy Alloys. *International Journal of Lightweight Materials and Manufacture*.

13. Gurmaita, P. K., Pongen, R., & Gurmaita, S. K. (2024). A7075 alloy reinforced metal matrix composites fabricated through stircasting route: a review. *International Journal of Cast Metals Research*, 1-48.

14. Akkaş, M., K Tabonah, T. M., A Elfghı, A. M., & Özorak, C. (2023). Powder Metallurgıcal Fabrıcatıon Of Co Reınforced Cunısı Matrıx Composıtes: Mıcrostructural And Corrosıon Characterızatıon. *Technological Applied Sciences*, *18*(4), 64-74.

15. Özorak, C., Tabonah, T. M. K., & Akkaş, M. (2023). Production of CuNiSi Composites by Powder Metallurgy Method: Effects of Ti on the microstructural and corrosion properties. *European Journal of Technique (EJT)*, *13*(2), 88-93.

16. Vijaya Ramnath, B., Elanchezhian, C., Annamalai, R. M., Aravind, S., Sri Ananda Atreya, T., Vignesh, V., & Subramanian, C. (2014). Alumınıum Metal Matrıx Composıtes-A Revıew. *Reviews on Advanced Materials Science*, *38*(1).

17. Zhou, X., Jawad, A., Luo, M., Luo, C., Zhang, T., Wang, H., ... & Chen, Z. (2021). Regulating activation pathway of Cu/persulfate through the incorporation of unreducible metal oxides: Pivotal role of surface oxygen vacancies. *Applied Catalysis B: Environmental*, *286*, 119914.

18. Selvakumar, V., Muruganandam, S., Tamizharasan, T., & Senthilkumar, N. (2016). Machinability evaluation of Al–4% Cu–7.5% SiC metal matrix composite by Taguchi–Grey relational analysis and NSGA-II. *Sādhanā*, *41*, 1219-1234.

19. Akkaş, M., & Elfghı, A. M. A. (2022). TiB2 parçacık takviyeli alcumg kompozitlerin üretilebilirliğinin araştırılması. *Uluslararası Doğu Anadolu Fen Mühendislik ve Tasarım Dergisi*, *4*(2), 118-128.

20. Sodhi, G. S., & Kaur, J. (2001). Powder method for detecting latent fingerprints: a review. *Forensic science international*, *120*(3), 172-176.

21. Murugadoss, P., & Jeyaseelan, C. (2024). Enhancing tribo-mechanical and corrosion properties of A383 aluminum matrix composites through stir-cum-squeeze casting with marble dust and hexagonal boron nitride reinforcement. *Proceedings of the Institution of Mechanical Engineers, Part L: Journal of Materials: Design and Applications*, 14644207241235784.

22. Angelo, P. C., Subramanian, R., & Ravisankar, B. (2022). *Powder metallurgy: science, technology and applications*. PHI Learning Pvt. Ltd..

23. Chandramouli, R., Kandavel, T. K., Shanmugasundaram, D., & Kumar, T. A. (2007). Deformation, densification, and corrosion studies of sintered powder metallurgy plain carbon steel preforms. *Materials & design*, *28*(7), 2260-2264.

24. Sezgin, C. T., & Hayat, F. (2023). Investigation of corrosion behaviour of boronised cold rolled high manganese steel. International Journal of Materials and Product Technology, 66(2), 135-151.

25. Sezgin, C. T., & Hayat, F. (2022). The effects of boriding process on tribological properties and corrosive behavior of a novel high manganese steel. Journal of Materials Processing Technology, 300, 117421.

26. Hayat, F., & Sezgin, C. T. (2021). Wear behavior of borided cold-rolled high manganese steel. Coatings, 11(10), 1207.

27. Sezgin, C. T., & Hayat, F. (2020). The microstructure and mechanical behavior of TRIP 800 and DP 1000 steels welded by electron beam welding method. Soldagem & Inspeção, 25, e2526.

28. Akkaş, M., & Al, S. F. R. A. (2021). Effect of hot pressing and reinforcement of TiC and WC on the mechanical properties and microstructure of AlCuFeCrNi HEAs alloy. *Science of Sintering*, *53*(1), 19-35.

29. Dewangan, S. K., Kumar, D., Samal, S., & Kumar, V. (2021). Microstructure and mechanical properties of nanocrystalline AlCrFeMnNiWx (x= 0, 0.05, 0.1, 0.5) high-entropy alloys prepared by powder metallurgy route. *Journal of Materials Engineering and Performance*, *30*(6), 4421-4431.

30. Mohanty, S., Maity, T. N., Mukhopadhyay, S., Sarkar, S., Gurao, N. P., Bhowmick, S., & Biswas, K. (2017). Powder metallurgical processing of equiatomic AlCoCrFeNi high entropy alloy: Microstructure and mechanical properties. *Materials Science and Engineering: A*, *679*, 299-313

31. Wissuchek, F., Derby, B. K., & Misra, A. (2024). Heterogeneous Morphologies and Hardness of Co-Sputtered Thin Films of Concentrated Cu-Mo-W Alloys. *Nanomaterials*, *14*(18), 1513.

32. Zygmuntowicz, J., Łukasiak, A., Piotrkiewicz, P., & Kaszuwara, W. (2019). Al2o3-cu-mo hybrid composites: Fabrication, microstructure, properties. *Compos. Theory Pract*, *19*(2), 43-49.

33. Zhao, X., Zhong, Q., Zhai, P., Fan, P., Wu, R., Fang, J., ... & Li, W. (2022). Microstructure and Wear Resistance of Laser-Clad Ni–Cu–Mo–W–Si Coatings on a Cu–Cr–Zr Alloy. *Materials*, *16*(1), 284.

34. Xiao, L., Zhao, X., Zhong, Q., Zhai, P., Peng, Z., Su, H., ... & Cai, Z. Microstructure and Wear Resistance of Laser Cladding Ni-Cu-Mo-W-Si Coatings on Copper Alloys. *Zhenwu and Su, Heng and Xiao, Yuxiang and Zhang, yafang and Jiang, Yuxiang and Liu, Sainan and Cai, Zhenyang, Microstructure and Wear Resistance of Laser Cladding Ni-Cu-Mo-W-Si Coatings on Copper Alloys*.

35. Madej, M. (2019). Copper infiltrated high speed steel skeletons. *Archives of Materials Science and Engineering*, *98*(1).

36. Kuskov, K. V., Volkov, I. N., Skodich, N. F., Nepapushev, A. A., Arkhipov, D. I., & Moskovskikh, D. O. (2019, June). Study of structure of copper-based composite materials during the spark plasma sintering. In *IOP Conference Series: Materials Science and Engineering* (Vol. 558, No. 1, p. 012024). IOP Publishing.

37. Akkaş, M., & Boushiha, K. F. I. (2021). Investigation of wc reinforced cunisi composites produced by mechanical alloying method. *El-Cezeri*, *8*(2), 592-603.

38. Abedi, M., Sovizi, S., Azarniya, A., Giuntini, D., Seraji, M. E., Hosseini, H. R. M., ... & Mukasyan, A. (2023). An analytical review on Spark Plasma Sintering of metals and alloys: From processing window, phase transformation, and property perspective. *Critical reviews in solid state and materials sciences*, *48*(2), 169-214.

39. Dehestani, M., Sharafi, S., & Khayati, G. R. (2023). Electrodeposited FeCoNiWMo high entropy alloy/SiC nanocomposite coatings: Microstructure, mechanical properties and corrosion resistance. *Intermetallics*, *162*, 107988.

40. Govindaraju, M., & Balasubramanian, K. (2012). Vacuum Brazing of Precipitation Hardening Stainless Steel without Losing its Mechanical Properties. In *Brazing and Soldering 2012: IBSC Proceedings of 5th International Conference* (p. 281). ASM International.

41. Ahmadkhaniha, D., Kruemmling, J., & Zanella, C. (2022). Electrodeposition of high entropy alloy of Ni-Co-Cu-Mo-W from an aqueous bath. *Journal of The Electrochemical Society*, *169*(8), 082515.

42. Liu, S., Sun, Y., Zhai, P., Fan, P., Zhang, Y., Li, M., ... & Cai, Z. (2023). Microstructure and Properties of Nickel-Based Gradient Coatings Prepared Using Cold Spraying Combined with Laser Cladding Methods. *Materials*, *16*(4), 1627.

43. Ghosh, S. (2016). Microwave Processing of Composites, Glass-Ceramic Coatings and Metallic Alloys: An Overview. *Microwave Engineering of Nanomaterials: From Mesoscale to Nanoscale*, 141.

44. Akkaş, M. (2021). Production and characterization of boron carbide and silicon carbide reinforced copper-nickel composites by powder metallurgy method. *Materialwissenschaft und Werkstofftechnik*, *52*(1), 32-42.

45. Aghababaei Nejad, M., Soltanolkotabi, M., & Eslami Majd, A. (2018). Polarization investigation of laser-induced breakdown plasma emission from Al, Cu, Mo, W, and Pb elements using nongated detector. *Journal of Laser Applications*, *30*(2).

46. Li, L., Zhang, Q., Li, H., & Geng, D. (2023). Liquid metal catalyzed chemical vapor deposition towards morphology engineering of 2D epitaxial heterostructures. *Chemical Communications*, *59*(99), 14636-14648.

47. Ghosh, S. (2016). Microwave Processing of Composites, Glass-Ceramic Coatings and Metallic Alloys: An Overview. *Microwave Engineering of Nanomaterials: From Mesoscale to Nanoscale*, 141.

48. Liu, T., Chen, C., Liu, S., Chen, Z., Pu, Z., Huang, Q., ... & Zhang, G. (2024). Transition metal phosphides as noble-metal-alternative co-catalysts for solar hydrogen production. *Coordination Chemistry Reviews*, *521*, 216145.

49. Hooke, R. (2018). *Diffuse boundary layer effects on the properties of metal in metal matrix composites manufactured with the field assisted sintering technique* (Doctoral dissertation, Rutgers University-School of Graduate Studies).

50. Towobola, A. V. (2024). *Synthesis and Characterization of Ag and Cu doped DLC Thin Films for Anti-microbial Applications* (Doctoral dissertation, University of Saskatchewan Saskatoon Canada).

51. Abdelkhalek, A. S., Barakat, W. S., Abu-Oqail, A. M. I., Elkady, O. A., EL-Nikhaily, A., & Mohamed, A. Y. (2024). Mechanical and Physical Properties of Al/CNT/hBN Hybrid Composites produced via Powder

Metallurgy and Hot-Rolling Techniques. *Industrial Technology Journal*, *2*(1), 50-67.

52. Islak, S., Özorak, C., Sezgin, C. T., & Akkaş, M. (2016). Trd Yöntemiyle Supap Çeliği Yüzeyinde Üretilen Kaplamalarin Mikroyapi Ve Aşinma Özellikleri. Technological Applied Sciences, 11(3), 75-85.

53. Islak, S., Özorak, C., Sezgin, C. T., & Akkaş, M. (2016). Effect of boron on micro structure and microhardness properties of Mo-Si-B based coatings produced viatig process. Archives of Metallurgy and Materials, 61.

54. Thirumurugan, R., Padmanaban, M., Ramkumar, T., & Shanmugam, D. (2024). Investigation of mechanical and tribological behavior of Al-Ni-Co-MWCNT composites prepared by powder metallurgy technique. *Proceedings of the Institution of Mechanical Engineers, Part E: Journal of Process Mechanical Engineering*, 09544089241228942.

55. Gökçe, A., Fındık, F., & Kurt, A. O. (2011). Microstructural examination and properties of premixed Al–Cu–Mg powder metallurgy alloy. *Materials Characterization*, *62*(7), 730-735.

56. Wong-Ángel, W. D., Téllez-Jurado, L., Chávez-Alcalá, J. F., Chavira-Martínez, E., & Verduzco-Cedeño, V. F. (2014). Effect of copper on the mechanical properties of alloys formed by powder metallurgy. *Materials & Design*, *58*, 12-18.

57. Karakulak, E. (2017). Characterization of Cu–Ti powder metallurgical materials. *International Journal of Minerals, Metallurgy, and Materials*, *24*, 83-90.

58. Samal, C. P., Parihar, J. S., & Chaira, D. (2013). The effect of milling and sintering techniques on mechanical properties of Cu–graphite metal matrix composite prepared by powder metallurgy route. *Journal of alloys and compounds*, *569*, 95-101.

59. Moustafa, S. F., Abdel-Hamid, Z., & Abd-Elhay, A. M. (2002). Copper matrix SiC and Al2O3 particulate composites by powder metallurgy technique. *Materials Letters*, *53*(4-5), 244-249.

60. Wu, D., Wu, S. P., Yang, L., Shi, C. D., Wu, Y. C., & Tang, W. M. (2015). Preparation of Cu/Invar composites by powder metallurgy. *Powder Metallurgy*, *58*(2), 100-105.

61. Pingale, A. D., Owhal, A., Katarkar, A. S., Belgamwar, S. U., & Rathore, J. S. (2021). Recent researches on Cu-Ni alloy matrix composites through electrodeposition and powder metallurgy methods: A review. *Materials Today: Proceedings*, *47*, 3301-3308.

62.Çetin, T., & Akkaş, M. (2020). Effect of WC reinforced on microstructure and mechanical properties of CuAlMn alloys produced by hot pressing method. *European Journal of Technique (EJT)*, *10*(1), 173-183.

63. Hao, H., Mo, W., Lv, Y., Ye, S., Gu, R., & Yu, P. (2016). The effect of trace amount of Ti and W on the powder metallurgy process of Cu. *Journal of Alloys and Compounds*, *660*, 204-207.

64. Gohar, G. A., Manzoor, T., Ahmad, A., Raza, H., Farooq, A., Karim, I., ... & Asad, F. (2020). Synthesis and investigate the properties of Cu–Al–Ni alloys with Ag addition using powder metallurgy technique. *Journal of Alloys and Compounds*, *817*, 153281.

65. Somani, N., Sharma, N., Sharma, A., Gautam, Y. K., Khatri, P., & Solomon, J. A. A. (2018). Fabrication of Cu-SiC composites using powder metallurgy technique. *Materials Today: Proceedings*, *5*(14), 28136-28141.

Chapter 2

EFFECT OF ALLOYING ELEMENTS ON THE MICROSTRUCTURE EVOLUTION AND MECHANICAL PROPERTIES OF COPPER ALLOY COMPOSITE

Musa KILIÇ[1]

[1] Assoc. Prof. Dr., Beşiri Organized Industrial Zone Vocational School, Department of Machinery and Metal Technologies, Welding Technology Program, Batman University, Turkey, musa.kilic@batman.edu.tr (ORCID: 0000-0001-5808-6917)

INTRODUCTION

Copper alloys manufactured through powder metallurgy have garnered significant interest within the realm of advanced manufacturing technologies due to the unique advantages associated with this method [1]. Unlike conventional fabrication techniques such as casting, machining, and hot or cold pressing powder metallurgy stands out for its ability to exercise precise control over the chemical composition, grain structure, and homogeneity of alloyed materials [2]. This high level of control enables manufacturers to meticulously tailor material properties to meet specific performance demands, making an ideal approach for applications where improved mechanical and physical attributes are critical. This method not only enhances material uniformity but also enables the production of parts with complex geometries, offering a versatile alternative to traditional manufacturing [3]. A primary advantage of produced copper based composites lies in their enhanced material properties, especially in terms of wear resistance, corrosion resistance, and optimized surface qualities, including reduced friction and improved surface tension. These characteristics contribute significantly to the reliability, longevity, and functionality of copper based composites, making them indispensable in a variety of high performance engineering applications [4-8]. Furthermore, the capability of fabricate composite materials with specialized structural and functional properties has underscored their importance in modern engineering. One of the key characteristics of fabricated composites is their superior strength to weight ratio, which facilitates the development of lightweight, high strength materials [9-11]. This feature is crucial for applications demanding efficient material use and cost effective production, as it leads to reduced material consumption, decreased production costs, and lower operational expenses over time. Copper alloys, renowned for their combination of low density and high strength, have thus become vital components in advanced composite development, particularly for applications where mechanical resilience and lightweight properties are essential [12-15].

Copper alloys are renowned for their exceptional combination of high electrical conductivity and impressive mechanical strength, making them indispensable in a broad spectrum of industrial and electrical applications. These alloys, owing to their unique properties, are commonly utilized in the production of components that require both electrical efficiency and structural integrity, such as connectors, electrical railways, lead frames, and elastic conductive materials [16]. Their dual functionality, allowing them to conduct electricity while maintaining robustness under mechanical stress, positions them as essential materials in various advanced technological sectors, particularly in electrical engineering and manufacturing industries [17-19]. In the existing body of

research, numerous copper alloy compositions have been developed and optimized to meet the ever-evolving industrial demands for specific performance characteristics. These alloys are often engineered by incorporating various alloying elements, which serve to tailor the material properties for particular applications. Some of the most commonly added elements include nickel (Ni), silicon (Si), magnesium (Mg), iron (Fe), phosphorus (P), chromium (Cr), beryllium (Be), zinc (Zn), tin (Sn), and aluminum (Al). These elements, when introduced into the copper matrix, significantly influence the resulting properties of the alloy, enhancing aspects such as corrosion resistance, strength, hardness, and, in certain cases, thermal stability. By varying the types and quantities of these alloying elements, manufacturers are able to create copper-based materials that are optimized for specific functionalities, such as improved wear resistance, better formability, or enhanced resistance to high-temperature conditions [20-26]. The addition of nickel (Ni) and silicon (Si) to copper alloys, for instance, is known to improve both strength and corrosion resistance, making these alloys ideal for use in environments that demand both durability and conductivity. Similarly, magnesium (Mg) and tin (Sn) are often used to enhance the alloy's mechanical properties, while elements like zinc (Zn) and aluminum (Al) improve the overall workability and resistance to oxidation. These tailored compositions are increasingly critical as the demand for more advanced, efficient, and durable materials continues to rise in industries such as electronics, automotive, aerospace, and power generation [27-29]. Moreover, the study and development of copper alloys with these various alloying elements have led to a deeper understanding of the fundamental relationship between composition, microstructure, and performance characteristics. The precise control of alloy composition during the manufacturing process allows for the development of materials that are tailored not only for improved electrical performance but also for mechanical durability under challenging operational conditions. This balance of electrical and mechanical properties is a key factor in the widespread adoption of copper alloys in high-performance electrical and electronic components. As technology continues to advance, the development of new copper alloys, particularly those with enhanced mechanical properties or specialized electrical characteristics, will be pivotal in meeting the needs of industries that rely heavily on copper-based materials [30-33]. In this context, ongoing research into novel copper alloy formulations and their manufacturing processes remains crucial for ensuring the continued success and application of these materials in modern industrial systems and infrastructure. The purpose of this research is to examine the effects of incorporating cobalt and tungsten particles into copper alloys produced through powder metallurgy, with a focus on the resulting changes in

microstructure and mechanical properties. To systematically analyze these effects, copper based alloys were pressed under constant pressure and then sintered at a controlled temperature. These controlled processes allow for the comparison of microstructural changes and mechanical improvements across samples. Copper and its alloys are widely recognized for their exceptional properties, including high thermal conductivity, excellent corrosion resistance, and notable toughness, which make them ideal for demanding engineering sectors such as aerospace, automotive, and biomedical industries. In these fields, material reliability and resilience are paramount due to the extreme conditions and operational stresses involved [34-37]. Additionally, copper alloys are extensively used across a broad range of applications, from heavy machinery and construction materials to medical devices, consumer electronics, space exploration technology, flexible eyeglass frames, and even mobile antennas. The versatility of copper alloys is further demonstrated by their growing use in robotics, where they provide both structural support and conductivity essential for advanced mechanical functions. However, despite the significant advantages offered by copper alloys, certain limitations persist in terms of mechanical strength and wear resistance, particularly in high-demand industrial environments. To address these challenges, this study investigates the reinforcement of copper alloys with cobalt and tungsten particles through powder metallurgy, with the aim of enhancing the alloys' mechanical robustness and wear resistance. By achieving these improvements, the newly developed composite materials are expected to meet critical performance requirements in industrial applications. The anticipated enhancement in wear resistance and mechanical properties is poised to expand the utility of copper based composites across diverse engineering contexts, addressing the industrial need for more resilient and durable materials capable of enduring harsh operating conditions [38].

An in-depth review of existing literature reveals a notable gap in studies focused on the feasibility and effectiveness of producing copper-based composites reinforced with cobalt and tungsten. This study seeks to address this gap by creating a novel powder metallurgy based composite material with these reinforcing elements. The findings of this research hold significant potential for advancing the development of high-performance, durable composite materials tailored for challenging engineering applications. Furthermore, the results are expected to contribute valuable insights into optimizing the production processes of such composites, broadening their applicability across various industrial sectors. This contribution not only represents an advancement in material performance but also aligns with the goals of sustainable and efficient use of engineering materials. Ultimately, the production of copper, cobalt and tungsten

composites through powder metallurgy offers a promising solution for the development of materials capable of meeting the stringent demands of modern industrial applications, thus advancing the field of composite materials.

1. EXPERIMENTAL PROCEDURE

Three distinct alloy compositions were synthesized through powder metallurgy (PM) to facilitate a detailed experimental analysis. This synthesis employed high-purity copper, cobalt, and tungsten powders, each with a purity level of approximately 99.95% and an average particle diameter of 44 μm.. To tailor the material properties according to experimental objectives, cobalt and tungsten were added at a concentration of 25% by weight each to the base copper material. This composition strategy aimed to systematically enhance the mechanical and physical characteristics of the resulting alloys, allowing for targeted improvements in properties such as hardness, tensile strength, and wear resistance. To achieve optimal homogeneity within the alloy powders, a rigorous mechanical alloying procedure was conducted. In this process, the metal powders were thoroughly mixed in a Retsch PM100 planetary ball mill. The ball milling was set to rotate at a high speed of 500 revolutions per minute (rpm) for an extended period of 24 hours to ensure a well-distributed particle blend. This prolonged milling duration was critical to achieving effective bonding between the constituent metal powders at a microstructural level. The planetary ball mill used in this study is designed with a securely sealed powder chamber, effectively preventing any contamination by isolating the alloy powders from the external environment once sealed.

Figure 1. Retsch PM100 planetary ball mill device.

Following the mechanical alloying stage, the blended powders were transferred into a cold pressing mold to undergo compaction. This cold pressing operation utilized a high-pressure environment of 800 MPa, applied to consolidate and densify the powder particles into a cohesive, solid form. The pressing was conducted using a Specac GS15011 hydraulic pellet press located at Kastamonu University's Central Research Laboratory (see Figure 2b). To maintain uniformity in sample geometry, a cylindrical mold with a 20 mm diameter (depicted in Figure 2a) was chosen, allowing for consistent sample dimensions across all specimens. The use of 800 MPa as the pressing pressure was critical to achieve the necessary level of compaction, ensuring close particle packing and enhanced material cohesion. This high-pressure environment not only facilitates the reduction of porosity within the powder matrix but also aids in aligning particles closely, which is essential for achieving high density and structural integrity in the final compact. A constant pressure of 800 MPa was applied throughout the pressing process to create a standardized baseline for the material's physical properties, providing a uniform densification profile across samples. This consistency is particularly important, as it minimizes variability in the samples' mechanical properties, which in turn enhances the reliability of subsequent material testing and analysis.

Figure 2. a) Mold device b) Specac GS15011 brand pellet device.

The sintering process for the powder samples was carried out in an atmosphere controlled heat treatment furnace (Protherm) housed within the Metallurgy and Materials Engineering Laboratories at Kastamonu University (Figure 3). Following the compaction stage, each sample was subjected to a sintering temperature of 925 °C under a continuous argon atmosphere for a duration of 180 minutes. This carefully managed sintering environment was crucial for fostering the development of strong interparticle bonds and enhancing the densification of the powder matrix. Operating under an argon atmosphere served multiple purposes. Primarily, it minimized oxidation and prevented contamination of the

samples, which is essential for maintaining the purity of high-quality alloy systems. Argon, as an inert gas, creates an environment that supports uniform heat distribution, helping the particles within the powder to undergo effective diffusion bonding without compromising the material's structural integrity. The temperature of 925 °C was specifically chosen to facilitate atomic diffusion at the particle interfaces, promoting the consolidation of the powder particles into a cohesive solid structure. The sintering process not only allowed for the elimination of residual porosity but also played a pivotal role in enhancing the material's mechanical properties, such as hardness and tensile strength. By enabling the particles to coalesce and form continuous grain boundaries, sintering reinforces the overall structural homogeneity of the material, which is essential for achieving uniformity in properties across the entire sample. The extended sintering duration of 180 minutes ensured that adequate time was provided for complete phase formation and bond strengthening, resulting in a dense and robust microstructure that enhances the durability and performance of the alloy under operational stresses.

Figure 3. Protherm brand atmosphere controlled heat treatment furnace.

The complete sintering cycle extended over a period of 540 minutes. To effectively remove volatile substances, such as residual oils and impurities within the samples, a gradual and controlled heating approach was adopted. The temperature was incrementally raised from ambient to the target sintering temperature of 1050°C, at a controlled rate of approximately 5 °C per minute, reaching the desired temperature within 180 minutes. This gradual heating allowed for the effective release of contaminants, ensuring that the material structure remained intact and uncompromised throughout the process. Upon reaching the target sintering temperature, the samples were maintained

isothermally at 925°C for an additional 180 minutes. This holding period was crucial for facilitating diffusion and bonding at the particle level within the powder matrix, which is essential for enhancing both the mechanical properties and the uniformity of the microstructure. This dwell time allowed the particles to coalesce effectively, creating a dense and cohesive structure that contributes to the overall performance of the material.

Figure 4 illustrates the final sintered samples, highlighting the uniform morphology achieved through this meticulously managed sintering cycle. This controlled heating and cooling process ultimately resulted in a structurally sound material with enhanced properties, preparing it for subsequent testing and application in demanding engineering contexts.

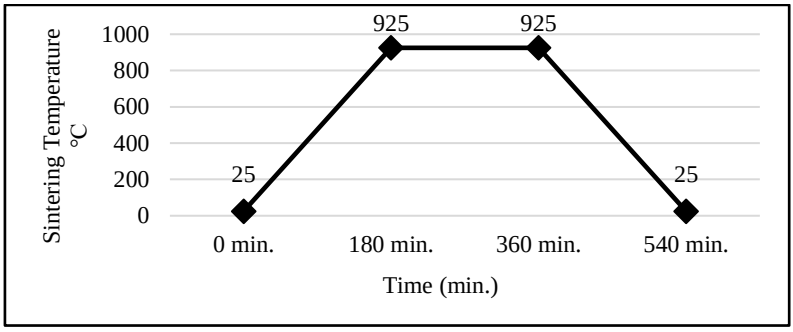

Figure 4. Sintering processes

Scanning electron microscopy (SEM) imaging through a series of meticulous metallographic procedures. Sample underwent a systematic grinding process with abrasive papers of increasingly finer mesh sizes, beginning at 120 mesh and advancing sequentially through 200, 400, 600, 800, 1000, 1200 and ultimately 2000 mesh. The samples were then polished using diamond suspensions with particle sizes of 3 µm and 1 µm, achieving a smooth, reflective surface necessary for detailed SEM analysis. The etched samples were then examined with a "FEI QUANTA 250 FEG" SEM at the Central Research Laboratories of Kastamonu University (see Figure 5). The SEM provided high-resolution images, enabling a detailed examination of the microstructure and morphology of the sintered material.

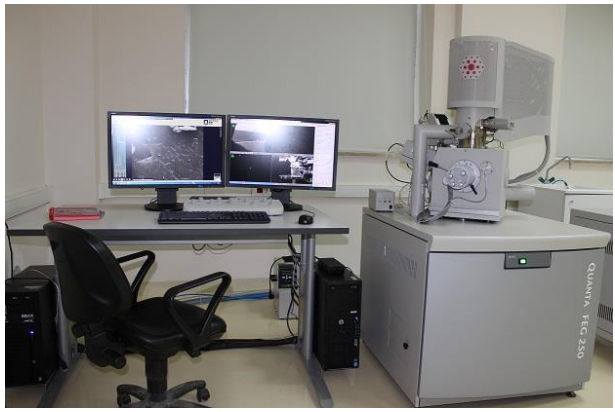

Figure 5. FEI QUANTA 250 FEG SEM analyzer.

The microhardness measurements were conducted using a SHIMADZU HMV-G21 microhardness tester (see Figure 6), which is housed within the Metallurgy and Materials Engineering Laboratory at Kastamonu University. This sophisticated instrument is specifically engineered to deliver highly accurate microhardness assessments through a controlled indentation process, allowing for detailed analysis of material properties.

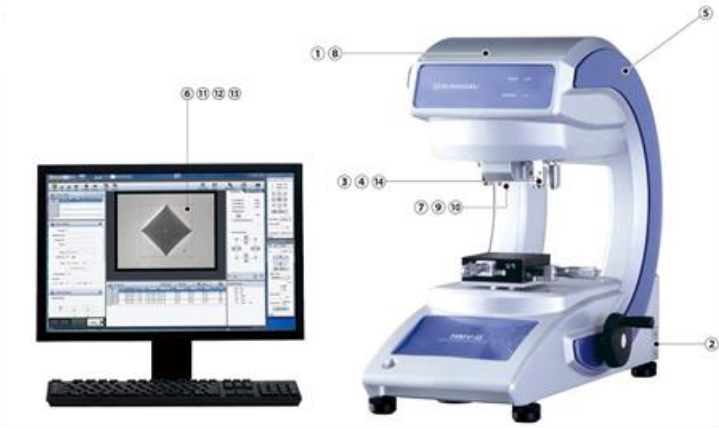
Figure 6. SHIMADZU HMV-G21 model microhardness tester.

The microhardness tests were carried out under a predetermined load of 0.025 kg, which was consistently applied for a duration of 15 seconds to ensure both the accuracy and repeatability of the indentation results. To enhance the reliability and statistical significance of the data collected, hardness measurements were meticulously taken from a minimum of 6 distinct locations across the surface of each sample. This methodological approach facilitated a detailed examination of

the hardness distribution, enabling an evaluation of both the uniformity and variability present within the microstructure of the sintered material.

2. EXPERIMENTAL RESULTS

2.1. Microstructure Evolution

A comprehensive microstructural analysis of the alloy produced via the powder metallurgy (PM) technique was conducted using scanning electron microscopy (SEM), providing valuable insights into the material's internal structure and phase distribution. SEM imaging allowed for a high-resolution visualization of the alloy's microstructural features, facilitating an in-depth examination of particle distribution, phase interactions, and matrix composition within the material. As observed in the SEM images shown in Figure 7, the alloy exhibits a well-defined copper matrix, which serves as the primary structural component and base phase of the samples. This copper matrix appears as a continuous phase, supporting the overall framework of the alloy and contributing significantly to its mechanical and thermal properties. The presence of a well-established copper matrix highlights the alloy's foundational structure, which is essential for achieving the intended performance characteristics [39].

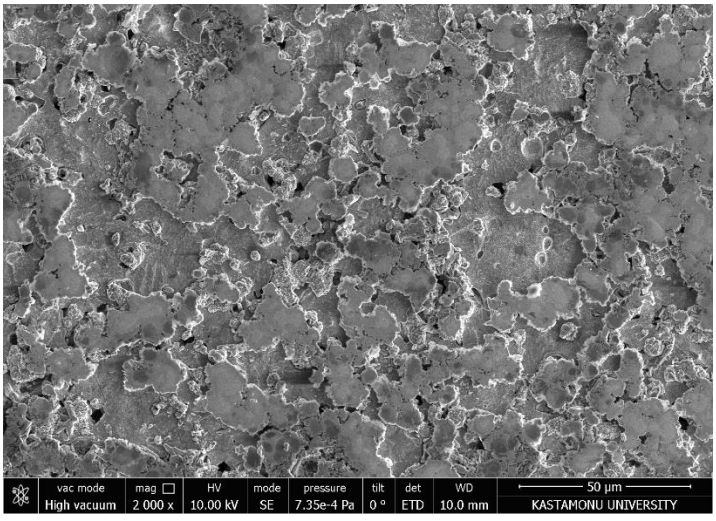

Figure 7. SEM images of the produced sample.

The SEM analysis further reveals the homogeneous dispersion of cobalt and tungsten particles embedded within the copper matrix. This uniform distribution is critical, as it enhances the alloy's overall stability and optimizes the mechanical properties by ensuring even load distribution across the material. Cobalt and tungsten particles appear consistently spaced within the copper matrix, forming

a stable composite architecture that minimizes the risk of localized stress concentrations and improves the material's resistance to mechanical wear and thermal degradation. Additionally, the even dispersion of cobalt and tungsten within the copper matrix enhances the alloy's bonding and cohesion at a microstructural level [40-43]. The particle distribution achieved through powder metallurgy is instrumental in promoting particle-to-particle interactions, resulting in a more resilient composite structure. The consistent integration of cobalt and tungsten particles within the copper matrix not only reinforces the mechanical strength of the alloy but also contributes to its improved corrosion resistance, wear resistance, and thermal stability—qualities that are particularly advantageous for applications in high-stress and high-temperature environments. Overall, the SEM analysis confirms that the powder metallurgy process has effectively facilitated the formation of a structurally sound, homogeneously reinforced copper-based alloy. The detailed microstructural insights gained through SEM imaging underscore the successful incorporation of cobalt and tungsten particles, validating the alloy's design as a composite material with tailored properties for demanding engineering applications. These findings are critical for advancing the development and optimization of PM-fabricated alloys, as they provide a clear understanding of the microstructural mechanisms that contribute to the enhanced performance of the material under practical operating conditions. The analysis of the fabricated samples reveals the presence of partial microcracking and porosity—two critical structural factors that can significantly influence the mechanical behavior and durability of the alloy under stress conditions [30]. These defects, particularly microcracks and voids, often serve as stress concentrators, potentially initiating early failure points that can compromise the alloy's overall resilience and performance [44-46].

The information obtained from scanning electron microscope energy dispersive spectroscopy (SEM-EDS) analysis is detailed in Figure 8.

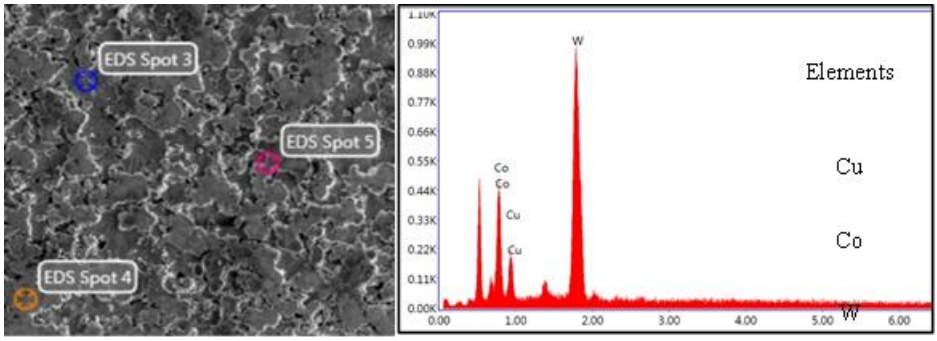

Figure 8. SEM-EDS analysis of the produced composite sample.

The reduction in porosity achieved through the alloying with cobalt and tungsten is not only beneficial for mechanical strength but also plays a vital role in improving the alloy's resistance to environmental factors such as corrosion and wear. A denser, less porous structure typically reduces the pathways through which corrosive agents might penetrate, thus extending the alloy's lifespan in corrosive or high-wear environments [47-51]. This densification effect, facilitated by the cobalt and tungsten additions, also contributes to higher thermal stability and improved overall structural integrity under operational stresses, further broadening the alloy's potential application scope in demanding engineering fields. Moreover, the observed reduction in porosity enhances the alloy's capability to maintain uniform stress distribution across its structure, thus minimizing the likelihood of localized stress build-up, which could otherwise lead to fracture initiation. The diminished porosity indicates a more uniform and well-integrated particle bonding within the copper matrix, highlighting the effectiveness of powder metallurgy techniques in producing alloys with tailored microstructural characteristics [52-55].

2.2. Microhardness Evolution

Figure 9 displays an in depth microhardness profile of the synthesized sample, offering valuable insights into the material's mechanical characteristics and reinforcing its potential for high-performance applications. This microhardness analysis was conducted meticulously along a pre-defined linear path across the sample's surface, with measurements recorded at regular intervals of 150 μm. This systematic sampling ensured that the collected data accurately represented the hardness distribution, providing a comprehensive view of the material's consistency and structural robustness [57,59].

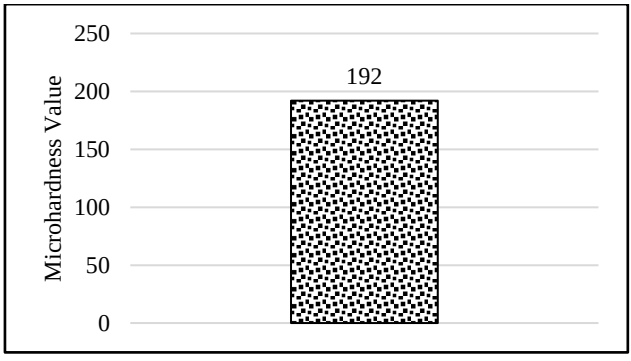

Figure 9. Microhardness graph of the produced sample.

The microhardness measurements revealed a mean value of approximately 192 Vickers, indicating a high degree of hardness for the synthesized composite material. This significant enhancement in hardness is primarily attributed to the formation of hard phases within the microstructure, notably carbides, which play a critical role in elevating the strength and wear resistance of the composite material [60-63]. These hard phases act as reinforcements within the alloy, bolstering its mechanical resilience and making it well-suited for applications requiring durability under intense mechanical loads. The integration of alloying elements, specifically cobalt and tungsten, into the base matrix has been instrumental in promoting the formation of these hard phases. This solid solution strengthening occurs when the alloying elements become part of the copper matrix, impeding dislocation motion and reinforcing the overall structure. Precipitation hardening, on the other hand, results from the formation of carbide phases, which further enhance the material's resistance to plastic deformation and mechanical wear. Beyond merely improving hardness, the development of these reinforcing phases contributes positively to other key mechanical properties, including toughness and ductility. By impeding dislocation movement an essential mechanism of plastic deformation the hard phases introduced through cobalt and tungsten additions increase the material's ability to withstand deformation under mechanical stress, which is essential for applications subjected to high wear and repeated impact. The presence of carbides, therefore, enhances both the material's hardness and its comprehensive mechanical stability. These findings emphasize the importance of precisely optimizing alloy composition and processing parameters in the synthesis of composite materials. The synergistic effects achieved by incorporating cobalt and tungsten not only enhance the microhardness but also help to customize the composite for specific high-stress applications. This tailored approach to alloy composition is crucial for developing advanced materials that meet the demands of various engineering fields, such as aerospace, automotive, and manufacturing, where durability and resistance to deformation are paramount. In conclusion, the data presented here provide an essential foundation for advancing material science, particularly in the domain of high-performance composites and alloys. The demonstrated influence of cobalt and tungsten on the mechanical properties of the synthesized composite highlights the potential for further research and development in this area, with the ultimate aim of achieving materials that offer optimal performance under challenging operational conditions. The comprehensive understanding of alloying and microstructural reinforcement mechanisms underscored by this study is invaluable for the continued innovation and enhancement of engineering materials designed for demanding environments [64].

3. CONCLUSIONS

This extensive study successfully explored the synthesis of copper alloys incorporated with cobalt and tungsten, employing the advanced technique of powder metallurgy. The production process was meticulously tailored to achieve optimal material properties, with a two-phase procedure involving cold pressing followed by sintering. During the cold pressing phase, a pressure of 800 MPa was applied to compact the alloy powders, ensuring adequate densification. This was followed by a sintering phase conducted at a temperature of 925 °C for 180 minutes under a controlled argon atmosphere. These carefully selected process parameters were designed to enhance the structural and mechanical properties of the resulting materials, ensuring their suitability for high-performance applications.

Effectiveness of Powder Metallurgy: The powder metallurgy technique proved to be a highly effective method for fabricating copper alloys reinforced with cobalt and tungsten. This approach successfully facilitated the pressing and sintering of these alloys, demonstrating the reliability of powder metallurgy for producing high-performance materials. The controlled sintering environment, maintained under an argon atmosphere, played a critical role in achieving the desired microstructural features, such as uniform particle distribution and minimized porosity, which are essential for ensuring the material's mechanical strength and durability. The sintering process, specifically the temperature and duration chosen, was instrumental in promoting optimal densification and interparticle bonding.

Microstructural Analysis and Porosity Reduction: The SEM images provided detailed visual evidence of the internal structure of the alloys, revealing a clear trend: as the content of cobalt and tungsten increased, the level of porosity within the alloy samples decreased significantly. This reduction in porosity is a crucial factor, as lower porosity is generally associated with enhanced mechanical properties such as strength and durability. The uniformity of the porosity distribution is indicative of the efficiency of the sintering and mechanical alloying processes, which are designed to promote homogenous material formation and prevent the formation of voids that could negatively affect the alloy’s performance. Furthermore, the SEM-EDS analysis confirmed that the cobalt and tungsten particles were evenly dispersed throughout the copper matrix, underscoring the successful incorporation of these alloying elements during the mechanical alloying phase and subsequent sintering process. This homogeneous distribution contributes to the material’s overall uniformity and mechanical integrity, which are vital for its reliability in demanding applications.

Microhardness Testing and Enhanced Mechanical Properties: The microhardness measurements taken across the sample surfaces revealed a notable increase in hardness, with the measured value reaching approximately 192 Vickers. This substantial enhancement in hardness is closely associated with the formation of hard phases, particularly carbides, within the alloy microstructure. The introduction of cobalt and tungsten particles played a key role in facilitating the formation of these hard phases, which are known to significantly improve the wear resistance and overall mechanical strength of the material. The formation of carbides and other hard phases is a well-established mechanism for strengthening alloys, as they hinder dislocation movement and provide resistance to plastic deformation, both of which are critical factors for materials used in applications subject to high stress, wear, and impact. As a result, the alloys produced in this study exhibit significantly improved mechanical properties, making them well-suited for use in environments where durability and resistance to wear are essential.

REFERENCES

1. Kestursatya, M., Kim, J. K., & Rohatgi, P. K. (2003). Wear performance of copper–graphite composite and a leaded copper alloy. *Materials Science and Engineering: A*, *339*(1-2), 150-158.
2. Nemani, A. V., Ghaffari, M., Bokati, K. S., Valizade, N., Afshari, E., & Nasiri, A. (2024). Advancements in additive manufacturing for copper-based alloys and composites: a comprehensive review. *Journal of Manufacturing and Materials Processing*, *8*(2), 54.
3. Zhang, X., Lei, Q., Meng, X., Cao, X., Yin, J., Zhou, S., ... & Jia, Y. (2024). Effect of TiC particle size on the microstructure and properties of CuCr-TiC composites manufactured by powder metallurgy. *Composite Structures*, *344*, 118323.
4. Akkaş, M. (2020). The mechanical and corrosion properties of WCCo–Al coatings formed on AA2024 using the HVOF method. *Materials Research Express*, *7*(7), 076515.
5. Jiang, H., Li, Y., Jiang, L., Zhang, X., Liu, X., Li, L., ... & Lei, Q. (2024). High strength and high conductivity Cu-Ta composites fabricated by powder metallurgy. *Materials Today Communications*, *38*, 108183.
6. Uzun, A. (2019). Production of aluminium foams reinforced with silicon carbide and carbon nanotubes prepared by powder metallurgy method. Composites Part B: Engineering, 172, 206-217.
7. Jiang, H., Li, Y., Jiang, L., Zhang, X., Liu, X., Li, L., ... & Lei, Q. (2024). High strength and high conductivity Cu-Ta composites fabricated by powder metallurgy. *Materials Today Communications*, *38*, 108183.
8. Albartouli, A. B. M., & Uzun, A. (2023). Mechanical and electrical properties of graphene nanosheet reinforced copper matrix composites materials produced by powder metallurgy method. Science of Sintering, 55(3), 399-411.
9. Hong, E., Kaplin, B., You, T., Suh, M. S., Kim, Y. S., & Choe, H. (2011). Tribological properties of copper alloy-based composites reinforced with tungsten carbide particles. *Wear*, *270*(9-10), 591-597.
10. Akkaş, M. (2024). The Effect of Molten Salt on The Mechanical Properties and Microstructure of CuNiSi Alloys with Reinforced Fe. *Science of Sintering*, *56*(1).
11. Gariba, A. M. M., Islak, S., Hraam, H. R. H., & Akkaş, M. (2022). Microstructural and mechanical properties of Ti-B4C/CNF functionally graded materials. *Metallography, Microstructure, and Analysis*, *11*(5), 736-745.

12. Shakunt, N. S., & Upadhyaya, A. (2024). Effect of Fe addition in W-Ni-Cu heavy alloy processed through powder metallurgy on microstructure and mechanical properties. *Journal of Alloys and Compounds*, *970*, 172578.
13. Xiong, S., Li, S., Wei, J., Zhou, H., Zhu, Q., Liu, B., & Zeng, L. (2024). Tuning heterogeneous geometric microstructure of Cu-based materials via powder metallurgy for improving high synergistic strengthening and electrical conductivity. *Materials Today Communications*, *38*, 108580.
14. Akkaş, M., K Tabonah, T. M., A Elfghı, A. M., & Özorak, C. (2023). Powder Metallurgical Fabrıcatıon of Co Reınforced CuNiSi Matrıx Composites: Microstructural and Corrosion Characterization. *Technological Applied Sciences*, *18*(4), 64-74.
15. Özorak, C., Tabonah, T. M. K., & Akkaş, M. (2023). Production of CuNiSi Composites by Powder Metallurgy Method: Effects of Ti on the microstructural and corrosion properties. *European Journal of Technique (EJT)*, *13*(2), 88-93.
16. Zhang, X., Lei, Q., Yin, J., Zhou, S., Xiao, Z., & Tang, Y. (2024). Ultrahigh strength CuCr/diamond composites fabricated by powder metallurgy. *International Journal of Refractory Metals and Hard Materials*, *122*, 106698.
17. Dong, D. Q., He, F. Y., Chen, X. H., Li, H., Shi, K. H., Xiong, H. W., ... & Zhang, L. (2024). Effect of tungsten carbide particles on microstructure and mechanical properties of Cu alloy composite bit matrix. *Journal of Iron and Steel Research International*, *31*(2), 519-530.
18. Akkaş, M., Hakan, A. Ş., & Polat, Ş. (2023). Effect of Ni: Si ratio on microstructure and properties of powder metallurgical Corson alloy. *Science of Sintering*, *55*(4), 425-436.
19. Masuda, C., & Tanaka, Y. (2006). Fatigue properties of Cu–Cr in situ composite. *International journal of fatigue*, *28*(10), 1426-1434.
20. Gain, A. K., & Zhang, L. (2016). Interfacial microstructure, wettability and material properties of nickel (Ni) nanoparticle doped tin–bismuth–silver (Sn–Bi–Ag) solder on copper (Cu) substrate. *Journal of Materials Science: Materials in Electronics*, *27*, 3982-3994.
21. Yan, H., Zhang, J., Zhang, P., Yu, Z., Li, C., Xu, P., & Lu, Y. (2013). Laser cladding of Co-based alloy/TiC/CaF2 self-lubricating composite coatings on copper for continuous casting mold. *Surface and Coatings Technology*, *232*, 362-369.

22. Madhusudan, S., Sarcar, M. M. M., & Rao, N. B. R. M. (2016). Mechanical properties of Aluminum-Copper (p) composite metallic materials. *Journal of applied research and technology*, *14*(5), 293-299.
23. Uddin, S. M., Mahmud, T., Wolf, C., Glanz, C., Kolaric, I., Volkmer, C., ... & Fecht, H. J. (2010). Effect of size and shape of metal particles to improve hardness and electrical properties of carbon nanotube reinforced copper and copper alloy composites. *Composites Science and Technology*, *70*(16), 2253-2257.
24. Roa, F., & Way, J. D. (2003). Influence of alloy composition and membrane fabrication on the pressure dependence of the hydrogen flux of palladium− copper membranes. *Industrial & engineering chemistry research*, *42*(23), 5827-5835.
25. Caligulu, U., Durmus, H., Akkas, M., & Sahin, B. (2021). Microstructure and mechanical properties of Ni matrix B4C reinforced functionally graded composites. *Science of Sintering*, *53*(4), 475-484.
26. Akkaş, M., & Elfghı, A. M. A. (2022). TiB2 parçacık takviyeli alcumg kompozitlerin üretilebilirliğinin araştırılması. *Uluslararası Doğu Anadolu Fen Mühendislik ve Tasarım Dergisi*, *4*(2), 118-128.
27. Singh, B. B., & Balasubramanian, M. (2009). Processing and properties of copper-coated carbon fibre reinforced aluminium alloy composites. *journal of materials processing technology*, *209*(4), 2104-2110.
28. Gan, Y. X., Solomon, D., & Reinbolt, M. (2010). Friction stir processing of particle reinforced composite materials. *Materials*, *3*(1), 329-350.
29. Dong, L., Chen, W., Zheng, C., & Deng, N. (2017). Microstructure and properties characterization of tungsten–copper composite materials doped with graphene. *Journal of Alloys and Compounds*, *695*, 1637-1646.
30. Girish, B. M., Basawaraj, B. R., Satish, B. M., & Somashekar, D. R. (2012). Electrical resistivity and mechanical properties of tungsten carbide reinforced copper alloy composites. *International Journal of Composite Materials*, *2*(3), 37-42.
31. Akkaş, M., & Al, S.F.R.A. (2021). Effect of hot pressing and reinforcement of TiC and WC on the mechanical properties and microstructure of AlCuFeCrNi HEAs alloy. *Science of Sintering*, *53*(1), 19-35.
32. Sudagar, J., Lian, J., & Sha, W. (2013). Electroless nickel, alloy, composite and nano coatings–A critical review. *Journal of alloys and compounds*, *571*, 183-204.

33. Tu, J. P., Yang, Y. Z., Wang, L. Y., Ma, X. C., & Zhang, X. B. (2001). Tribological properties of carbon-nanotube-reinforced copper composites. *Tribology Letters*, *10*, 225-228.
34. Hayajneh, M., Hassan, A. M., Alrashdan, A., & Mayyas, A. T. (2009). Prediction of tribological behavior of aluminum–copper based composite using artificial neural network. *Journal of Alloys and Compounds*, *470*(1-2), 584-588.
35. Islak, S., Özorak, C., Sezgin, C. T., & Akkaş, M. (2016). Trd Yöntemiyle Supap Çeliği Yüzeyinde Üretilen Kaplamalarin Mikroyapi Ve Aşinma Özellikleri. Technological Applied Sciences, 11(3), 75-85.
36. Ma, W., & Lu, J. (2011). Effect of sliding speed on surface modification and tribological behavior of copper–graphite composite. *Tribology Letters*, *41*, 363-370.
37. Islak, S., Özorak, C., Sezgin, C. T., & Akkaş, M. (2016). Effect of boron on micro structure and microhardness properties of Mo-Si-B based coatings produced viatig process. Archives of Metallurgy and Materials, 61.
38. Rhee, K. Y., Han, W. Y., Park, H. J., & Kim, S. S. (2004). Fabrication of aluminum/copper clad composite using hot hydrostatic extrusion process and its material characteristics. *Materials Science and Engineering: A*, *384*(1-2), 70-76.
39. Akkaş, M., Islak, S., & Özorak, C. (2018). Corrosion and wear properties of Cu-TiC composites produced by hot pressing technique. *Celal Bayar University Journal of Science*, *14*(4), 465-469.
40. Xia, L., Jia, B., Zeng, J., & Xu, J. (2009). Wear and mechanical properties of carbon fiber reinforced copper alloy composites. *Materials Characterization*, *60*(5), 363-369.
41. Tu, J. P., Wang, N. Y., Yang, Y. Z., Qi, W. X., Liu, F., Zhang, X. B., ... & Liu, M. S. (2002). Preparation and properties of TiB2 nanoparticle reinforced copper matrix composites by in situ processing. *Materials Letters*, *52*(6), 448-452.
42. Roa, F., & Way, J. D. (2005). The effect of air exposure on palladium–copper composite membranes. *Applied surface science*, *240*(1-4), 85-104.
43. Zhou, S., Zhang, T., Xiong, Z., Dai, X., Wu, C., & Shao, Z. (2014). Investigation of Cu–Fe-based coating produced on copper alloy substrate by laser induction hybrid rapid cladding. *Optics & Laser Technology*, *59*, 131-136.

44. Ma, Z. Y., & Tjong, S. C. (2000). High temperature creep behavior of in-situ TiB2 particulate reinforced copper-based composite. *Materials Science and Engineering: A*, *284*(1-2), 70-76.
45. Akkaş, M., & Boushiha, K. F. I. (2021). Investigation of wc reinforced cunisi composites produced by mechanical alloying method. *El-Cezeri*, *8*(2), 592-603.
46. Veillère, A., Heintz, J. M., Douin, J., Chandra, N., & Silvain, J. F. (2009). Copper alloy/Carbon heat sink composite materials elaborated by a powder metallurgy process. In *ICCM-17-17th International Conference on Composite Materials*. International Committee on Composite Materials.
47. Frommeyer, G., & Wassermann, G. (1975). Microstructure and anomalous mechanical properties of in situ-produced silver-copper composite wires. *Acta Metallurgica*, *23*(11), 1353-1360.
48. Akhtar, F., Askari, S. J., Shah, K. A., Du, X., & Guo, S. (2009). Microstructure, mechanical properties, electrical conductivity and wear behavior of high volume TiC reinforced Cu-matrix composites. *Materials characterization*, *60*(4), 327-336.
49. Akkaş, M., Boushiha, K. F. I., & Tabonah, T. M. K. (2021). Toz metalurjisi yöntemi ile WC Takviyeli CuNiSi kompozitlerin üretimi ve karakterizasyonu. *İmalat Teknolojileri ve Uygulamaları*, *2*(1), 41-48.
50. Abyzov, A. M., Kidalov, S. V., & Shakhov, F. M. (2012). High thermal conductivity composite of diamond particles with tungsten coating in a copper matrix for heat sink application. *Applied Thermal Engineering*, *48*, 72-80.
51. Lloyd, J. C., Neubauer, E., Barcena, J., & Clegg, W. J. (2010). Effect of titanium on copper–titanium/carbon nanofibre composite materials. *Composites science and technology*, *70*(16), 2284-2289.
52. Çetin, T., & Akkaş, M. (2020). Effect of WC reinforced on microstructure and mechanical properties of CuAlMn alloys produced by hot pressing method. *European Journal of Technique (EJT)*, *10*(1), 173-183.
53. Akkaş, M. (2021). Production and characterization of boron carbide and silicon carbide reinforced copper-nickel composites by powder metallurgy method. *Materialwissenschaft und Werkstofftechnik*, *52*(1), 32-42.
54. Deshpande, P. K., & Lin, R. Y. (2006). Wear resistance of WC particle reinforced copper matrix composites and the effect of porosity. *Materials Science and Engineering: A*, *418*(1-2), 137-145.
55. Bident, A., Delange, F., Labrugere, C., Debiemme-Chouvy, C., Lu, Y., & Silvain, J. F. (2024). Fabrication and characterization of copper and copper

alloys reinforced with graphene. *Journal of Composite Materials*, *58*(1), 109-117.

56. Arkusz, K., Pasik, K., Nowak, M., & Jurczyk, M. (2024). Structural, Electrical and Corrosion Properties of Bulk Ti–Cu Alloys Produced by Mechanical Alloying and Powder Metallurgy. *Materials*, *17*(7), 1473.
57. Akkaş, M. (2022). Synthesis and characterization of MoSi2 particle reinforced AlCuMg composites by molten salt shielded method. *Türk Doğa ve Fen Dergisi*, *11*(4), 11-17.
58. Boggarapu, V., Sreekanth, P. R., & Peddakondigalla, V. B. (2024). Microstructure, mechanical and tribological properties of Al/Cu functionally graded material fabricated through powder metallurgy. *Journal of Engineering Research*, *12*(3), 502-510.
59. Maheshwari, M., Singh, K. P., Agarwal, S., Gautam, R. K. S., Raja, A. R., & Singh, S. (2024, February). An overview of nano-particle reinforced copper metal matrix composites. In *AIP Conference Proceedings* (Vol. 3007, No. 1). AIP Publishing.
60. Zhai, Z., Dong, H., Li, D., Wang, Z., Sun, C., & Chen, C. (2024). Effect of TiC Particles on the Properties of Copper Matrix Composites. *Inorganics*, *12*(4), 120.
61. Sezgin, C. T., & Hayat, F. (2023). Investigation of corrosion behaviour of boronised cold rolled high manganese steel. International Journal of Materials and Product Technology, 66(2), 135-151.
62. Sezgin, C. T., & Hayat, F. (2022). The effects of boriding process on tribological properties and corrosive behavior of a novel high manganese steel. Journal of Materials Processing Technology, 300, 117421.
63. Hayat, F., & Sezgin, C. T. (2021). Wear behavior of borided cold-rolled high manganese steel. Coatings, 11(10), 1207.
64. Sezgin, C. T., & Hayat, F. (2020). The microstructure and mechanical behavior of TRIP 800 and DP 1000 steels welded by electron beam welding method. Soldagem & Inspeção, 25, e2526.

Chapter 3

HIGH ENTROPY ALLOYS (HEAS): A NEW GENERATION OF METALLIC MATERIALS

Cihangir Tevfik SEZGİN[1]

[1] Dr. Öğr. Üyesi, Kastamonu Üniversitesi Kastamonu Meslek Yüksekokulu, Makine ve Metal Teknolojileri, ORCID: 0000-0002-1916-9901

1. Introduction

In recent years, high entropy alloys (HEAs) have emerged as a groundbreaking development in materials science, challenging the traditional concepts of alloy design with their multi-component and highly mixed structures. Conventional alloys are typically designed with a primary element as the base, to which smaller amounts of other elements are added. For instance, stainless steel is produced by adding elements like nickel, chromium, and molybdenum to a primary iron base. However, high entropy alloys consist of at least five different elements combined in equal or similar proportions, with no dominant base element. This innovative alloying approach pushes the boundaries of conventional alloy design, offering a completely new perspective to materials science.

The discovery of HEAs is rooted in the role of entropy in thermodynamics. In traditional alloys, thermodynamic stability is achieved through low entropy, meaning that specific phases remain stable around primary components. HEAs, on the other hand, benefit from high entropy to stabilize multiple phases within a complex composition. This unique influence of entropy helps occure stable microstructures, significantly affecting the stability of the alloy's structure. Moreover, thanks to the vast combinations of elements available for HEAs, they can achieve exceptional performance in terms of both mechanical and thermal properties.

These next-generation materials are known for their resilience, high-temperature resistance, corrosion resistance, and low density, making them extremely promising for various industries. For example, the aerospace and defense industries have shown significant interest in HEAs for applications that require high strength and durability at elevated temperatures. Additionally, the chemical industry finds them suitable for resisting corrosive environments.

Research into high entropy alloys has highlighted their significance not only in academic contexts but also in commercial and industrial applications. Studies exploring HEA production techniques, element combinations, and application areas are steadily increasing. The design of these alloys aims to harness the thermodynamic advantages of high entropy to achieve extraordinary properties, which is why they are often referred to as “designer alloys.”

This chapter will delve into the fundamentals of high entropy alloys, including their microstructural characteristics, production methods, thermodynamic framework, mechanical and chemical properties. The discovery of high entropy alloys has ushered in an exciting wave of innovation in materials science, offering a robust alternative to traditional alloying approaches.

2. High Entropy Alloys: Fundamental Concepts

Recently, high entropy alloys (HEAs), also referred to as multi-component alloys, have attracted considerable interest due to their distinct compositions, microstructures, and adaptable properties. These alloys are typically composed of at least five elements in equal or nearly equal ratios, forming a solid solution [1-4]. The near-equal proportions of multiple elements occure high mixing entropy, which reduces the likelihood of intermetallic phase formation and instead favors the development of simple solid solutions with face-centered cubic (FCC), body-centered cubic (BCC), or a combination of these crystal structures [5-7].

HEAs exhibit remarkable toughness, exceptional resistance to softening at high temperatures [8], significant ductility [1], strong fatigue resistance [9], outstanding wear resistance [10, 12], high hardness [11-13], and hihg corrosion resistance [14-16].

In a thermodynamic system under isothermal and isobaric conditions, the system strives to minimize Gibbs free energy (G), meaning that equilibrium is achieved when "G" reaches its lowest value. Therefore, the free energy of a system is given by the following relation [6]:

$$G=H-TS \quad (1)$$

Here, "H" represents enthalpy, "S" represents entropy, "G" represents free energy, and "T" represents temperature. It can be seen that the enthalpy and entropy of the system at a given temperature are directly related to establishing equilibrium. To predict the equilibrium phase of an alloy, the free energy change during the transition from elemental state to other states can be compared, allowing identification of the phase with the lowest mixing free energy. Equation (1) can be related to changes in free energy, enthalpy, and entropy between the elemental and mixed states as follows [6]:

$$\Delta G_{mix}=\Delta H_{mix}-T\Delta S_{mix} \quad (2)$$

According to the stated Boltzmann hypothesis, the mixing entropy of an n-element equimolar alloy in transition from the elemental to a random solution state can be calculated by the following equation [6]:

$$\Delta Smix=Rln(n) \quad (3)$$

The “R” in Equation 3 (8.31 J/K·mol) is the gas constant [17]. According to the literature, the result of ΔS_mix gives rise to three types of entropy-based alloys: low-entropy alloys, medium-entropy alloys, and high-entropy alloys. High entropy alloys (HEA) are defined as alloys that have a mixing entropy higher than 1.5R. These alloys are composed of at least five principal elements in equal or nearly equal proportions. Alloys with a mixing entropy of 1R to 1.5R are categorized as medium-entropy alloys (MEAs) [18-20], whereas those with mixing entropy below 1R are considered low-entropy alloys (LEAs) [21-23], which includes most conventional alloys [17]. Figure 1 shows the classification of alloy based on mixing high entropy alloys.

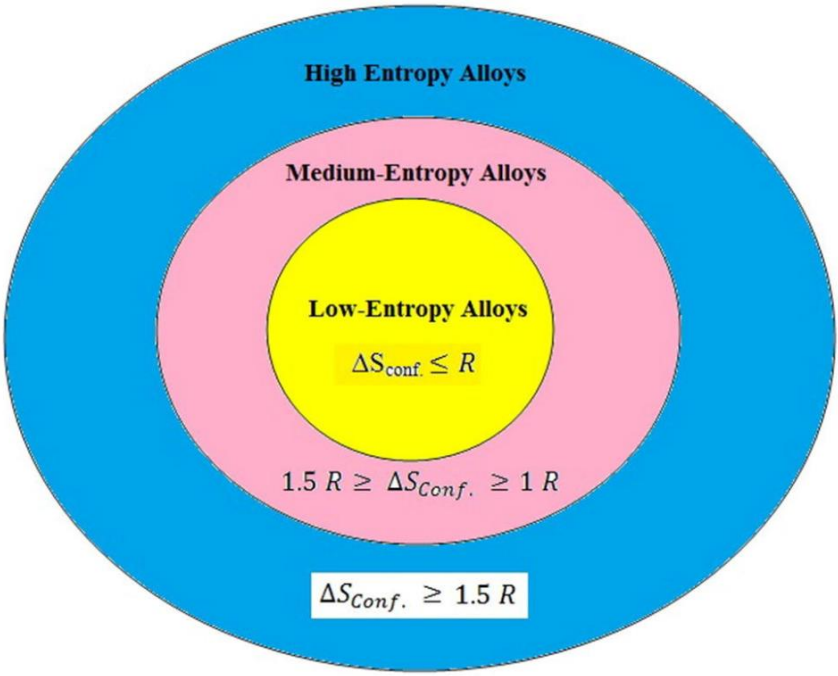

Figure 1. The classification of alloy based on mixing high entropy alloys [24]

3. Manufacturing of High Entropy Alloys

3.1. Powder Metallurgy

Although there are numerous production methods for high entropy alloys, this section discusses a few of the most commonly used methods. Products manufactured using the powder metallurgy method are transformed into higher-performance products compared to those produced by conventional manufacturing methods [25,26]. Powder metallurgy is perhaps the most

commonly used method in the production of high entropy alloys [27-30]. In powder metallurgy, the transformation of powder particles into a final product begins with the cold pressing process. The cold pressing process involves producing powders and consolidating them by compressing the particles into a single piece, known as the green compact, using a pressing tool at room temperature. In cold uniaxial pressing, the prepared powder is loaded into a die positioned between two punches. These punches then apply pressure in a single direction, compacting the powder particles through uniaxial compression. After the cold press, the process continues with sintering, as the products have weak bonds that can break into small pieces under even slight stress. Through sintering, powder particles bond to each other at high temperatures via a mechanism known as 'necking.' This enables the final product to attain the desired geometric and mechanical properties. Sintering is a densification method in which powder particles are compacted and shaped by applying heat below their melting or liquefaction point, typically in an inert gas atmosphere [26]. Figure 2 shows the schematic of sintering process.

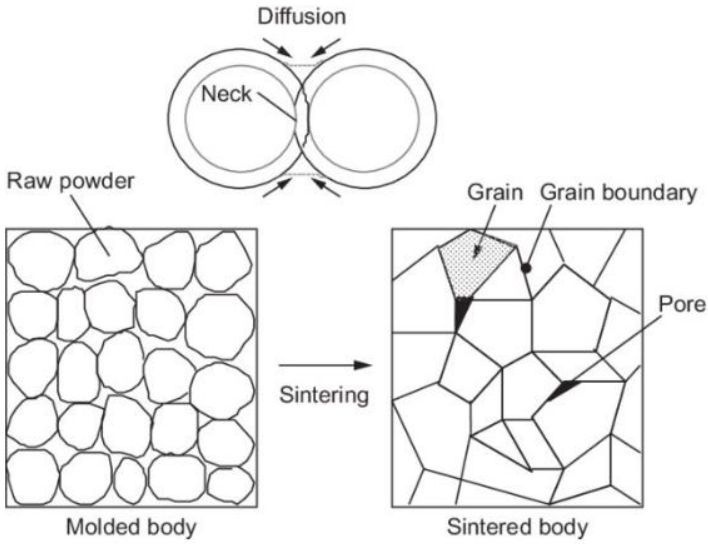

Figure 2. The schematic of sintering process [36]

Gas atomization is a technique where molten metals are directly converted into solid powder particles using a gas or liquid stream. A typical gas atomization setup has two main stages: first, the furnace chamber, where the metal powders (called the charge) are melted under a vacuum to reach the required temperature; second, the atomizing chamber, where the molten metal flows from the tundish through a nozzle at its base. As the molten metal flows by gravity through the

tundish, the atomizing nozzle breaks the liquid stream into fine droplets with a high-pressure gas or water jet, which rapidly solidify into powder particles [31,32]. The particle size of the metal powders is influenced by factors such as the cooling distance, coolant pressure and velocity, coolant flow rate, liquid flow rate and velocity, impingement angle, superheat, surface tension of the metal, and its melting range [33]. It has been observed that the mechanical properties of high entropy alloy powders produced by gas atomization are improved. In a study, researchers produced CoCrFeMnNi HEA powder with gas atomization and then make samples by use mechanical alloying. The findings showed that this HEA exhibited strong mechanical properties, with a tensile strength of approximately 1.0 GPa and a ductility around 6%, along with nanocrystalline structures when compared to the gas atomization route alone [34]. In antother research, a non-equiatomic $CrFeCoNiMo_{0.2}$ HEA was synthesized and evaluated its mechanical performance at 600–1100 °C. The added Mo contributed to higher activation energy, lattice distortion, and grain refinement, resulting in beneficially improved mechanical properties [35].

3.2. Melting and Casting Techniques

We can also produce a HEA with conventional production such as melting crude metals. One of the most important of these is the arc melting method. The arc melting process includes low energy consumption, time efficiency, and reduced porosity of products. In arc melting process, alloy ingots are placed in metallic crucibles and melted using a tungsten electric arc under an inert argon atmosphere, after the chamber is vacuumed to prevent oxidation. The alloy ingots are repeatedly melted by the arc melting process and then solidified by a coolant positioned beneath the metallic crucible to ensure uniformity within the alloy. In the arc melting method, metal powders can also be used instead of metal ingots [33].

Another melting HEA production method is vacuum induction melting. This process involves heating electrically conductive materials using electromagnetic induction, which occurs a magnetic field. It induces an electrical current, known as an Eddy current, within the conductive materials, which is then used to heat them. The ingot placed inside the crucible furnace resists the input current, causing the magnetic field to form through the conducting materials, rapidly melting them from the inside. However, the most important disadvantage of this method is re-melted the ingots several times to achieve a homogeneous HEA. [37,38]. During the final melting stage, the molten HEAs are poured into the desired mold and allowed to solidify. This melting process must be performed under a high vacuum. Figure 3 shows this process.

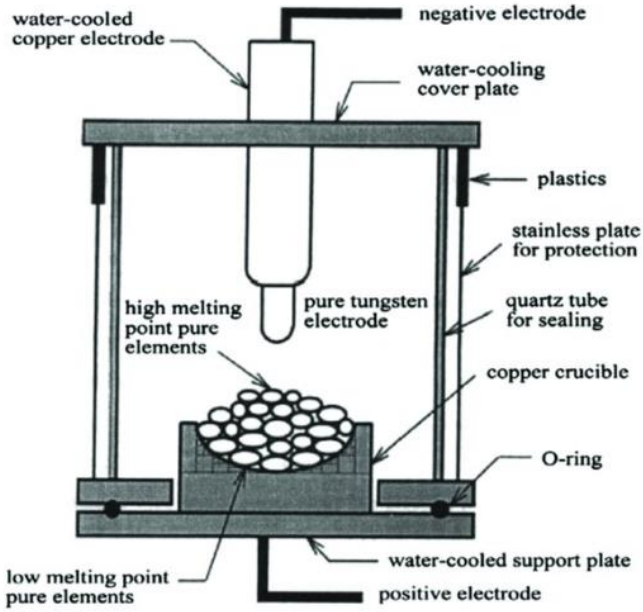

Figure 3. Vacuum arc melting process [39]

The vacuum induction melting process offers the benefits of precise control over heating and cooling rates, in contrast to the arc melting process, as well as achieving better homogeneity. Additionally, the vacuum media helps prevent oxidation [33].

4. Properties of High Entropy Alloys

In high entropy alloys, the added alloying elements have various effects. The mechanical properties of the alloy can be influenced, examples of which include increased hardness, improved ductility, high fracture toughness, and enhanced strength [40]. Additionally, studies in the literature have clarified how the added metals influence the mechanical properties of high entropy alloys by affecting the microstructure through changes in crystal lattice structure, diffusion effects of elements, and lattice energies.

Studies in the literature show that the presence of aluminum [41], as well as metals and alloys with face-centered cubic (FCC) lattice structures, such as Ni-Al and Cr-Fe [42], encourages high entropy alloys to form in the same lattice structure. Additionally, research indicates that adding elements like aluminum [43], vanadium [44], and cobalt [45] to high entropy alloys increases the hardness of the resulting alloy. The improvement of ductility and strength in high entropy alloys can be achieved through heat treatments [46,47].

Conclusions

High entropy alloys (HEAs) represent a transformative advancement in materials science, breaking away from conventional alloy design with their multi-component configurations and reliance on high entropy to stabilize complex structures. This unique alloying approach has shown the potential to significantly enhance mechanical and thermal properties. Through various production techniques, such as powder metallurgy, gas atomization, arc melting, and vacuum induction melting, HEAs can be optimized to meet the demands of high-performance applications.

HEAs exhibit superior strength, hardness, ductility, and corrosion resistance, alongside remarkable thermal stability. These attributes make them highly desirable for industries such as aerospace, defense, and chemical processing, where materials are subjected to extreme conditions. The incorporation of elements like aluminum, vanadium, and cobalt, along with appropriate heat treatments, has proven effective in further improving the mechanical performance and structural integrity of HEAs. Moreover, the adaptability of HEAs, owing to their complex microstructures and the diversity of possible element combinations, underscores their potential for extensive future research and practical applications.

In summary, the study and application of high entropy alloys open new avenues for alloy design, providing innovative solutions to challenges in engineering and industrial applications. Continued research will be crucial in exploring additional element combinations, refining production processes, and understanding the thermodynamic and microstructural factors that influence their performance. HEAs have established themselves as a promising material class with the potential to redefine industry standards, advancing materials science into a new era of alloy innovation.

REFERENCES

[1]. Gludovatz, B., Hohenwarter, A., Catoor, D., Chang, E. H., George, E. P., & Ritchie, R. O. (2014). A fracture-resistant high-entropy alloy for cryogenic applications. Science, 345(6201), 1153-1158.

[2]. Zhang, Y., Zuo, T. T., Tang, Z., Gao, M. C., Dahmen, K. A., Liaw, P. K., & Lu, Z. P. (2014). Microstructures and properties of high-entropy alloys. Progress in materials science, 61, 1-93.

[3]. Cantor, B., Chang, I. T. H., Knight, P., & Vincent, A. J. B. (2004). Microstructural development in equiatomic multicomponent alloys. Materials Science and Engineering: A, 375, 213-218.

[4]. Yeh, J. W., Chen, S. K., Lin, S. J., Gan, J. Y., Chin, T. S., Shun, T. T., ... & Chang, S. Y. (2004). Nanostructured high-entropy alloys with multiple principal elements: novel alloy design concepts and outcomes. Advanced engineering materials, 6(5), 299-303.

[5]. Wu, J. M., Lin, S. J., Yeh, J. W., Chen, S. K., Huang, Y. S., & Chen, H. C. (2006). Adhesive wear behavior of AlxCoCrCuFeNi high-entropy alloys as a function of aluminum content. Wear, 261(5-6), 513-519.

[6]. Erdogan, A., & Zeytin, S. (2019). Yüksek Entropili Alaşımlar: Prensipler Ve Alaşım Tasarımı. Niğde Ömer Halisdemir Üniversitesi Mühendislik Bilimleri Dergisi, 8(2), 1160-1178.

[7]. Santodonato, L. J., Zhang, Y., Feygenson, M., Parish, C. M., Gao, M. C., Weber, R. J., ... & Liaw, P. K. (2015). Deviation from high-entropy configurations in the atomic distributions of a multi-principal-element alloy. Nature communications, 6(1), 5964.

[8]. Wu, W. H., Yang, C. C., & Yeh, L. W. (2006, November). Industrial development of high-entropy alloys. In Annales de Chimie-Science des materiaux (Vol. 31, No. 6, p. 737). Paris; New York: Masson, 1978-.

[9]. Hemphill, M. A., Yuan, T., Wang, G. Y., Yeh, J. W., Tsai, C. W., Chuang, A., & Liaw, P. K. (2012). Fatigue behavior of Al0. 5CoCrCuFeNi high entropy alloys. Acta Materialia, 60(16), 5723-5734.

[10]. Lee, C. P., Chen, Y. Y., Hsu, C. Y., Yeh, J. W., & Shih, H. C. (2007). The effect of boron on the corrosion resistance of the high entropy alloys Al0. 5CoCrCuFeNiB x. Journal of the Electrochemical Society, 154(8), C424.

[11]. Fan, X., Qu, R., & Zhang, Z. (2021). Relation between strength and hardness of high-entropy alloys. Acta Metallurgica Sinica (English Letters), 34(11), 1461-1482.

[12]. Samoilova, O., Shaburova, N., Moghaddam, A. O., & Trofimov, E. (2022). Al0. 25CoCrFeNiSi0. 6 high entropy alloy with high hardness and improved wear resistance. Materials Letters, 328, 133190.

[13]. Yılmaz, A. M., Çiçek, H., Duran, S., Gülten, G., & Efeoğlu, İ. (2024). Investigation of hardness, tribological and adhesion properties of TiAlNiVN HEA films heat treated at different temperatures. Tribology International, 197, 109739.

[14]. Wu, P., Gan, K., Yan, D., Fu, Z., & Li, Z. (2021). A non-equiatomic FeNiCoCr high-entropy alloy with excellent anti-corrosion performance and strength-ductility synergy. Corrosion Science, 183, 109341.

[15]. Hsu, Y. J., Chiang, W. C., & Wu, J. K. (2005). Corrosion behavior of FeCoNiCrCux high-entropy alloys in 3.5% sodium chloride solution. Materials Chemistry and Physics, 92(1), 112-117.

[16]. Hsu, Y. J., Chiang, W. C., & Wu, J. K. (2005). Corrosion behavior of FeCoNiCrCux high-entropy alloys in 3.5% sodium chloride solution. Materials Chemistry and Physics, 92(1), 112-117.

[17]. Carroll, R., Lee, C., Tsai, C. W., Yeh, J. W., Antonaglia, J., Brinkman, B. A., ... & Dahmen, K. A. (2015). Experiments and model for serration statistics in low-entropy, medium-entropy and high-entropy alloys. Scientific reports, 5(1), 16997.

[18]. Akkaş, M. (2024). The Effect of Molten Salt on The Mechanical Properties and Microstructure of CuNiSi Alloys with Reinforced Fe. Science of Sintering, 56(1).

[19]. Akkaş, M., K Tabonah, T. M., A Elfghı, A. M., & Özorak, C. (2023). Powder Metallurgıcal Fabrıcatıon Of Co Reınforced Cunısı Matrıx Composıtes: Mıcrostructural And Corrosıon Characterızatıon. Technological Applied Sciences, 18(4), 64-74.

[20]. Özorak, C., Tabonah, T. M. K., & Akkaş, M. (2023). Production of CuNiSi Composites by Powder Metallurgy Method: Effects of Ti on the microstructural and corrosion properties. European Journal of Technique (EJT), 13(2), 88-93.

[21]. Tun, K. S., Nahata, A., Vincent, S., & Gupta, M. (2023). Development of a low entropy, lightweight, multicomponent, high performance (Hardness+ Strength+ Ductility) magnesium-based alloy. JOM, 75(2), 459-469.

[22]. Kaneko, T., & Suzuki, M. (2003, July). Automotive applications of magnesium alloys. In Materials science forum (Vol. 419).

[23]. Tun, K. S., Kumar, A., & Gupta, M. (2019). Introducing a high performance Mg-based multicomponent alloy as an alternative to Al-alloys. Frontiers in Materials, 6, 215.

[24]. Sharma, P., Dwivedi, V. K., & Dwivedi, S. P. (2021). Development of high entropy alloys: A review. Materials Today: Proceedings, 43, 502-509.

[25]. Akkaş, M., Hakan, A. Ş., & Polat, Ş. (2023). Effect of Ni: Si ratio on microstructure and properties of powder metallurgical Corson alloy. Science of Sintering, 55(4), 425-436.

[26]. Akkaş, M., & Elfghı, A. M. A. (2022). TiB2 parçacık takviyeli alcumg kompozitlerin üretilebilirliğinin araştırılması. Uluslararası Doğu Anadolu Fen Mühendislik ve Tasarım Dergisi, 4(2), 118-128.

[27]. Qiu, X. W. (2013). Microstructure and properties of AlCrFeNiCoCu high entropy alloy prepared by powder metallurgy. Journal of Alloys and Compounds, 555, 246-249.

[28]. Zhang, B., Huang, Y., Dou, Z., Wang, J., & Huang, Z. (2024). Refractory high-entropy alloys fabricated by powder metallurgy: Progress, challenges and opportunities. Journal of Science: Advanced Materials and Devices, 100688.

[29]. Hidayati, R., Kim, J. H., Kim, G., Yun, J. H., & Rhyee, J. S. (2024). Powder metallurgical process to enhance the critical current density and critical magnetic field in high entropy alloy superconductors. Current Applied Physics.

[30]. Nagarjuna, C., Sharma, A., Lee, K., Hong, S. J., & Ahn, B. (2023). Microstructure, mechanical and tribological properties of oxide dispersion strengthened CoCrFeMnNi high-entropy alloys fabricated by powder metallurgy. journal of materials research and technology, 22, 1708-1722.

[31]. Akkaş, M., & Boz, M. (2019). Investigation of the compressibility and sinterabilty of AZ91 powder production and particle production by gas atomisation method. Journal of magnesium and alloys, 7(3), 400-413.

[32]. Em Akra, K. M., Akkaş, M., Boz, M. U. S. T. A. F. A., & Seabra, E. (2020). The production of AZ31 alloys by gas atomization method and its characteristics. Russian Journal of Non-Ferrous Metals, 61, 332-345.

[33]. Alshataif, Y. A., Sivasankaran, S., Al-Mufadi, F. A., Alaboodi, A. S., & Ammar, H. R. (2020). Manufacturing methods, microstructural and mechanical properties evolutions of high-entropy alloys: a review. Metals and Materials International, 26, 1099-1133.

[34]. Liu, Y., Wang, J., Fang, Q., Liu, B., Wu, Y., & Chen, S. (2016). Preparation of superfine-grained high entropy alloy by spark plasma sintering gas atomized powder. Intermetallics, 68, 16-22.

[35]. Wang, J., Liu, Y., Liu, B., Wang, Y., Cao, Y., Li, T., & Zhou, R. (2017). Flow behavior and microstructures of powder metallurgical CrFeCoNiMo0. 2 high entropy alloy during high temperature deformation. Materials Science and Engineering: A, 689, 233-242.

[36]. Uchino, K. (2017). Manufacturing methods for piezoelectric ceramic materials. In Advanced Piezoelectric Materials (pp. 385-421). Woodhead Publishing.

[37]. Icin, K., Sunbul, S. E., Erdogan, A., & Doleker, K. M. (2023). A comparative study on the surface degradation mechanisms of arc melted and laser remelted CoCrFeNiAl0. 5Nb0. 5 HEA. Surface and Coatings Technology, 463, 129534.

[38]. Joseph, J., Jarvis, T., Wu, X., Stanford, N., Hodgson, P., & Fabijanic, D. M. (2015). Comparative study of the microstructures and mechanical properties of direct laser fabricated and arc-melted AlxCoCrFeNi high entropy alloys. Materials Science and Engineering: A, 633, 184-193.

[39]. Zhang, Y., Zuo, T. T., Tang, Z., Gao, M. C., Dahmen, K. A., Liaw, P. K., & Lu, Z. P. (2014). Microstructures and properties of high-entropy alloys. Progress in materials science, 61, 1-93.

[40]. Meyers, M. A., & Chawla, K. K. (2008). Mechanical behavior of materials. Cambridge university press.

[41]. Li, C., Li, J. C., Zhao, M., & Jiang, Q. (2010). Effect of aluminum contents on microstructure and properties of AlxCoCrFeNi alloys. Journal of Alloys and Compounds, 504, S515-S518.

[42]. Pradeep, K. G., Wanderka, N., Choi, P., Banhart, J., Murty, B. S., & Raabe, D. (2013). Atomic-scale compositional characterization of a nanocrystalline AlCrCuFeNiZn high-entropy alloy using atom probe tomography. Acta Materialia, 61(12), 4696-4706.

[43]. Tsai, M. H., & Yeh, J. W. (2014). High-entropy alloys: a critical review. Materials Research Letters, 2(3), 107-123.

[44]. Chen, M. R., Lin, S. J., Yeh, J. W., Chuang, M. H., Chen, S. K., & Huang, Y. S. (2006). Effect of vanadium addition on the microstructure, hardness, and wear resistance of Al 0.5 CoCrCuFeNi high-entropy alloy. Metallurgical and Materials Transactions A, 37, 1363-1369.

[45]. Hsu, C. Y., Wang, W. R., Tang, W. Y., Chen, S. K., & Yeh, J. W. (2010). Microstructure and mechanical properties of new AlCoxCrFeMo0. 5Ni High-Entropy Alloys. Advanced Engineering Materials, 12(1-2), 44-49.

[46]. Senkov, O. N., Senkova, S. V., & Woodward, C. J. A. M. (2014). Effect of aluminum on the microstructure and properties of two refractory high-entropy alloys. Acta Materialia, 68, 214-228.

[47]. Senkov, O. N., Scott, J. M., Senkova, S. V., Meisenkothen, F., Miracle, D. B., & Woodward, C. F. (2012). Microstructure and elevated temperature properties of a refractory TaNbHfZrTi alloy. Journal of Materials Science, 47, 4062-4074.

Chapter 4

DRIVE MECHANISMS AND STICK-SLIP PHENOMENON IN PRECISION MANUFACTURING MACHINES

Engin NAS[1]

[1] Assoc. Prof. Dr., Engin Pak Cumayeri Vocational School, Düzce University, Düzce, Turkey
https://orcid.org/0000-0002-4828-9240

1. CNC Control Systems

In today's technological age, traditional machine tools have been replaced by computer-controlled machine tools. One of the most important reasons for this is to minimize the loss of time and money by producing the workpieces to be made precisely and quickly. With the advancing technological developments, machines are constantly modified and improved. CNC-controlled machine tools allow the production of much more precise workpieces compared to traditional machines. The most critical elements affecting this precision are the drive mechanisms of the machine. Let's compare the movement given to the table of traditional machine tools with the movement given to the CNC-controlled machine tool. There is a standard movement mechanism in the conventional machine, while this mechanism in the CNC-controlled machine allows the production of more precise parts in terms of measurement precision thanks to the ball screw system. Today, scientists continue their studies to increase this precision even more by developing different drive mechanisms. In this study, firstly, information is given about the electric motors that move the machine. Then in the next stages, information is provided about the servo mechanisms that move the machine table or spindles, the ball screws that enable the machines to move, and the parameters that we will use to minimize the errors that occur during sudden stops and starts in the machines, and how to make a selection that is suitable for the design system.

A control system is a device or group of devices used to manage, command, direct, or regulate a system's behavior [1]. Given a certain input, a control system is made up of subsystems or facilities that work together to produce the required output with the desired performance [2]. The cutting tool in contemporary production machine tools carries out two fundamental tasks: chip removal and part movement. The servo system is supported by the system that performs this function. The regulation function is required to maintain the controlled item in the intended position when the external distribution is present in maneuver control. A common illustration of point-to-point control is placing a drill bit in a machining center. In tracking control, a controlled tool is moved along a desired trajectory, minimizing the error during the trajectory transition. An example of tracking control is the milling of circular workpieces [2].

A DC motor is used as a power set to drive the feed mechanism in the servo system. Compared with the AC motor control, the drive circuit of the DC motor is more straightforward and more reliable. In addition, the speed adjustment accuracy and dynamic response characteristics of the DC motor are more ideal than those of AC, with higher speed adjustment accuracy and an extensive speed range [2].

The components in two-axis machines are as follows.

1.1. Linear guides

They are precise devices made to turn a movement or torque into thrust, controlling the actual physical movement of any mechanism on a production line. A base, a saddle, set screws, and a flat rib make up linear guides. When subjected to unexpected loads, linear guides are highly resilient [1].

Some of the advantages of using linear guides are:

i.It is simple to transport goods weighing various weights, from little loads to several hundred kilos.

ii.Items can be carried between 2.5 millimeters and 1.5 meters.

iii.They move the load rapidly to its final location.

iv.The final positioning can be measured in microns, which are millionths of a meter, because they precisely place weights [2].

Industries that require linear guideways for high levels of precision in manufacturing [3]:

(a) Machine tool assembly and industrial robots

(b) Production of fiber optic and photonic components

(c) Manufacturing of semiconductors and electronic devices

(d) Manufacturing medical equipment [1].

1.2. Ball bearing slides

A kind of linear slide frequently seen in industrial equipment. Four rods hold the two rows of balls on either side of the base together in ball-bearing slides. The purpose of the two rows of balls is to roll along the rods and remove play from the slides, resulting in precise, low-friction action [1].

1.3. Dovetail slides

Typically constructed of cast iron, dovetail slides can also be manufactured of stainless steel and hard-coated aluminum. Like any bearing, dovetail slides consist of a fixed linear base and a moving carrier block. The dovetail slide has a v-shaped or dovetail slide-shaped protruding channel corresponding to the linear base of the carrier block. When the dovetail slide is inserted into its base's channel, it locks to the linear axis of the carrier channel and allows free linear movement [2].

Unlike ball-bearing slides, dovetail slides have direct contact between the base and the saddle. Due to this contact, more effort is required to move the saddle and slow down the acceleration rates. The contacting surfaces affect a larger area compared to other types of slides, allowing dovetail slides to be used in heavy-load applications and different industrial areas [1].

1.4. Machine slides

Machine slides are mostly used to perform linear motion on conventional and CNC machines. Several components are required to move the machine slide, such as AC/DC motor, ball bearing slide and roller slide. Machine slides can have one, two, or more axes. Standard machine slides include linear guide, reinforced road, and tail slides [2].

1.5. Roller slides

They employ rollers that travel between four parallel, semi-flat bars that encircle the rollers and cross at a 90-degree angle. The rollers are situated on the base and the upper carriage, respectively, between "V" grooved roller-bearing races. Crossed roller slides absorb more shocks and support twice as much weight as ball-bearing slides. They can also be layered to produce multi-axis linear motion. Because roller slides may be modified for many applications, they are incredibly adaptable [1].

1.6. Cylinder tables

Cylinder tables are the quietest type of table with bearings and consist of a longitudinally aligned front and rear sliding surface. The lifting arms are pivoted on the bearing bar to secure them to the rear support group [2].

1.7. XY table

Motor mounting plates, couplings, ball screws, a sizable base, and a top plate are among the forces and plates that make up XY tables. The force travels constantly in a linear motion along the plate while sliding over it on frictionless air bearings. This is due to the linear motor modules, usually two to four in number, which react to currents.

In XY tables, the tracks influence rigidity, load capacity, and straight-line accuracy, while the drive mechanisms determine speed and smoothness. Resolution, accuracy, and repeatability are additional crucial elements for XY tables. XY tables are usually mounted horizontally. Since XY tables are widely used in the industry, there is no such thing as unavailability in terms of supply [1].

The two primary varieties of electric motors are direct current (DC) and alternating current (AC). The uses and purposes of the two kinds of motors are distinct. We use both DC and AC electric motors on a daily basis. DC motors brought about a major shift in the manufacturing of various items. The introduction of AC motors altered people's perceptions of motors because of its amazing potential for starting power. Servo systems and other applications needing precise speed control frequently use DC motors [2].

2. Types of Control in CNC Machine Tools

Over the past few decades, digital and computer technologies have become increasingly important in engineering. By boosting engineering productivity, improving product quality, and building databases pertaining to production processes, these systems—which assist the development, research, production, and optimization processes—have grown to be an essential component of today's industry [4] .

Some subsystems that aid in the proper operation of machines use auxiliary drives. The performance, precision, speed, efficiency, and cost of machines are typically significantly improved by the use of such drives. They enable the processing of parts with more intricate geometric shapes under more demanding conditions.

Auxiliary drives in various machine tool classes can differ based on the central units' organization, configuration, and other characteristics. CNC systems operate auxiliary drives and carry out the operating modes that the control panels specify. This is accomplished with the use of the pertinent ladder diagrams stored in the CNC system's programmable controller [5, 6].

The drive system includes auxiliary drives for the cooling system, metering lubrication, hydraulic system, tool storage, and fixed positioning unit. Each of these drives has unique qualities that must be considered throughout the development, implementation, operation, and real-world application stages. The following is a formulation of the fundamental specifications for the auxiliary drives of the machines being studied:

- automatic control
- quick arrival at the desired position
- smooth operation
- potential for reverse control
- minimal energy consumption
- options for both automatic and manual start and stop
- the ability to set the lubricants in the ideal amounts
- trouble-free chip removal
- automatic subsystem operation
- subsystem blocking
- guaranteeing the workpiece's immobility during processing
- making sure the machine has the lubrication and cooling it needs
- compactness
- safety and economy.

The earliest models of lathes were made to be able to be operated by the hands. At the beginning of their production, the rotating spindle, which was controlled by a pedal, was later replaced by electric motors. Manually operated lathes still have their slide movements controlled by humans. The brain serves as the core control unit in classic lathes, while the limbs and legs are servo motors, the eyes and ears are sensors. Microprocessor technological advancements have replaced operator skills with digital system control, eliminating the need for manually controlled movements. In general, there are three categories into which CNC lathe control types fall [7].

1) Control of spindle speed
2) Control of slide movements
3) Control of slide positions

2.1 Spindle Speed Control

The drive mechanism that will move the spindle provides the necessary power for the system to operate at the desired accuracy in line with the process to be performed. The spindle drive mechanism in numerical control lathes should compensate for the friction losses caused by mechanical power transmission and ensure the system operates efficiently. For example, the drive mechanism should be given high power output to provide constant power in high chip removal by increasing the feed at a low cutting speed. As an additional illustration, with lathes, the cutting speed must be maintained while the chips are being removed from the workpiece's diameter, there must be a system that will allow the spindle speed to reach the desired speed with each reduction in diameter. In numerical control lathes, servo-electric motors must be used so that the drive mechanisms can perform the functions described above. These are direct (DC) electric and alternating (AC) electric motors. Speed is provided by changing the voltage in DC motors and by changing the source frequency in AC motors.

2.2 Slide Movement Control

In computer-controlled lathes (CNC), the progress speed of the slide movements is continuously controlled precisely. The most basic function of CNC lathes is to provide precise and fully automatic movement. Slide movements of computer-controlled lathes are performed with DC and AC servo electric motors.

2.3. Slide Position Control

The slides that move the workpiece in the lathe or milling machine are controlled by alternating (AC) and direct (DC) motors. In direct current motors, the speed depends on the main voltage and current intensity. The speed is directly proportional to the voltage given to the motor and inversely proportional to the

excitation current. The motor torque depends only on the excitation current and the armature (rotating part of the direct current machine) current intensity. Increasing the speed is achieved by reducing the excitation current with a rheostat (a device that changes the resistance of the conductor). This change is made according to the power required for the machine. Since DC motors can be used in most modern machines by changing the input voltage, the desired speed can be obtained and a constant cutting speed can be provided.

There are also machine tools operating with AC motors. Asynchronous and short-circuit AC motors, especially squirrel cage motors, are generally used in machine tools. AC motors require a step drive system with a range of spindle speeds. In the design of CNC machine tools, drive motors are traditionally used for rotational motion and ball screw shafts for table movement. In machine tools, slip-ring asynchronous motors are also used to protect the network and the motor from high starting currents. Asynchronous motors are suitable for frequent stopping and starting. The frequency is changed to increase the speed of these motors above 3000 rpm [8-10].

3. Drive Mechanisms

The electric drive system is subjected to strong demands from various mechanical processes, necessitating the best choice of motors, power converters, sensors, and mechanical gears. A spindle, auxiliary, and feed drives are part of the machine tools' drive system. Feed drives are used to quickly and precisely move tools and workpieces to the correct coordinates [6]. Spindle drives significantly impact the overall machine's performance and quality while also contributing to creating workpieces. Other systems and procedures that guarantee the efficient operation of machine tools use auxiliary drives.

Adding the right auxiliary drives can sometimes greatly increase efficiency, accuracy, cost, and performance. Additionally, it can allow workpieces with more intricate geometric shapes to be mechanically processed. Several variations of machine tool drive systems use alternating current (AC) and direct current (DC) motors. The behavior of these systems in different transient and steady-state operating modes can be thoroughly studied using computer modeling [6]. This great opportunity isn't always practical or feasible in industrial and laboratory settings.

Gravity and friction are the two most common forces encountered in mechanics. The first has been studied in every era, while the second has been largely neglected. The advent of conventional and CNC machines operating to very close tolerances under a wide range of conditions has shown that our understanding of the sliding process is inadequate. For instance, nuclear power plants' heat

exchanger pumps and jet engines are resulting in lubricating issues that have never been seen before. As a result, scientists have recently reexamined the rules of friction and discovered unexpected discoveries. The force of friction is defined by three rules: (1) the friction force is proportional to the load or pressure that one solid body applies to the other; (2) the force is independent of the area of contact; and (3) the force is independent of the sliding speed. Leonardo da Vinci articulated the first two laws, which were later rediscovered in the 1690s by Guillaume Amontons, a French engineer supported by the Royal French Academy of Sciences [11] .

Charles Augustin de Coulomb, a French scientist best renowned for his electrostatic studies, first proposed the third law in 1785 [12]. It is claimed that the coefficient of friction for any given material must always be the same and that friction only varies with the applied load. With a maximum variance of 10%, the first and second laws are often applicable. Studies have revealed that friction is not unaffected by sliding speed, though. A. Morin, a Frenchman, postulated in 1835 that there must be two friction coefficients since the friction force preventing two bodies from sliding at rest is stronger than the friction force after they have moved. These are categorized as kinetic for moving surfaces and static for stationary surfaces.

4. Stick-Slip phenomenon

A well-known illustration of vibration caused by friction is stick-slip behavior. It typically manifests as unstable motion during the machine's starting and stopping phases in dry friction, boundary lubrication, and mixed lubrication situations. All mechanical systems exhibit stick-slip behavior, which is also expected and seriously damaging. Examining stick-slip behavior and offering preventative measures are essential to comprehending vibrations caused by friction and have significant ramifications for the advancement of industry [13].

Many researchers have found that both static and kinetic coefficients change due to their studies. It has been observed that the kinetic coefficient decreases as the sliding speed increases. The static coefficient, on the other hand, is stated to depend to some extent on the length of time that the surfaces are in contact; therefore, the friction coefficient for any pair of surfaces is grouped under two headings: the static coefficient, which depends on the contact time, and the kinetic coefficient, which depends on the sliding speed. The deterioration of friction, i.e., the rapid change of the friction force, has given rise to the "Third Law" of stick-slip.

A common occurrence seen in friction tests is stick-slip. It happens when two objects in touch oscillate in speed between zero and a finite value. Two primary

conditions must be met for the stick-slip phenomenon (SS) to occur [14]. A common occurrence in day-to-day living is stick-slip. It is typically identified by the sound it produces. The squeaking of bicycle wheels, the rattling of window sills, the severe vibrating of drawbridges, chalk on the board, melody from an instrument, and noise from lubricated-less doors are all typical instances of stick-slip.

1. Because μs > μk (s = static, k = kinetic), the coefficient of friction is variable.

2. The system is adaptable enough to accommodate variations in the sliding body's speed.

In general, stick-slip is an undesirable behavior in most cases, and stick-slip has areas of use. A violinist does his best to encourage stick-slip by rosining his bow to produce music. A metal cutting tool must slide smoothly on the material. The cutting surface will be rough and irregular when a stick-slip occurs during sliding. It is observed that the sound that appears in the drive mechanism of a gramophone is spread into the environment in a distorted way [12].

There are three main methods to improve stick-slip in unwanted places. First, the sliding speed can be changed. This sometimes means slowing down and sometimes speeding up. For example, if a car's tires turn a corner quickly, they squeak, but if the turn is slow, they do not squeak; on the other hand, a door that squeaks when opened slowly may be silent when opened quickly. Second, reducing the stored energy in systems whose intermittent oscillation causes stick-slip is necessary. For example, hardening the spring will achieve this goal. Lubricating the sliding surfaces is the third and most popular technique.

A lubricant forms a soft film with much less frictional resistance than the surface of a metal. As the surfaces slide, the lubricant film gradually wears away and the parts of the metal surfaces come into contact. As long as the lubricant film coverage is 90% or higher, stick/slip slippage cannot occur. However, when the lubricant film coverage drops to 75%, stick/slip becomes very likely. The squeak that arises at this stage is a warning because it serves as a warning that the lubricant needs to be replaced. In this case, using a quality lubricant will prolong the stick-slip phenomenon. Some poor-quality lubricants never achieve even 90% coverage, no matter how much is applied [12]. Mechanical systems experience friction, a physical phenomenon that typically negatively impacts their motion, including stick-slip oscillations, steady-state errors, and poor tracking and contouring capabilities. Understanding the friction behavior of a mechanical system is typically the foundation for creating an effective friction model. However, because a variety of parameters, including the material, lubricant, and surface texture of the bodies in contact, influence friction behavior, modeling friction is difficult [15].

Although stick-slip is a natural condition of the machines used in machining production, studies are being carried out in the field of engineering to reduce this condition. With the studies carried out by scientists working in this field, even if stick-slip cannot be eliminated, it can be reduced to a minimum level. With the reduction of this condition, an increase in product quality and a decrease in production costs will occur.

References

[1] Wan NGAH, Design and analysis a control system for 3 axis mechanism machine, (2009).

[2] Muhammad Hayyul Sohaimi, Development Controller for 2 Axis Mechanism Machine, in, UMP, 2012.

[3] Liang Heong Lim, Design and Fabrication of Three Axis Mechanism with AC Servo Motor in Application of Personal Computer Numerical Control, in, UMP, 2007.

[4] Marin Zhilevski.;Mikho Mikhov, Control Device for a Type of Machine Tools, in: 2020 International Conference Automatics and Informatics (ICAI), IEEE, 2020, pp. 1-5.

[5] Tomoya Fujita.;Atsushi Matsubara.;Daisuke Kono.;Iwao Yamaji, Dynamic characteristics and dual control of a ball screw drive with integrated piezoelectric actuator, Precision Engineering, 34 (2010) 34-42.

[6] Mikho Mikhov.;Marin Zhilevski, Study and performance improvement of the drive systems for a class of machine tools, in: MATEC Web of Conferences, EDP Sciences, 2019, pp. 05003.

[7] A. Demir, "Cnc Takım Tezgahları Nelerdir", https://makineteknikk.tr.gg, (Accessed Dec. 5, 2024)

[8] Yusuf Altintas, Manufacturing automation: metal cutting mechanics, machine tool vibrations, and CNC design, Cambridge university press, 2012.

[9] Girish Kumar Singh, Induction machine drive condition monitoring and diagnostic research—a survey, Electric Power Systems Research, 64 (2003) 145-158.

[10] Erol Türkeş.;Sezan Orak, Takım Tezgahı Tasarımında Elektrik Motoru Seçimi, Journal of Science Technology of Dumlupınar University, (2008) 105-116.

[11] Thurmon E Lockhart, An integrated approach towards identifying age-related mechanisms of slip initiated falls, Journal of Electromyography Kinesiology, 18 (2008) 205-217.

[12] Ernest Rabinowicz, Stick and slip, Scientific American, 194 (1956) 109-119.

[13] Yixiao Lu.;Dong Han.;Qidi Fu.;Xi Lu.;Yan Zhang.;Zhiyong Wei.;Yunfei Chen, Experimental investigation of stick-slip behaviors in dry sliding friction, Tribology International, 201 (2025) 110221.

[14] R Kovar.;BS Gupta.;Z Kus, Stick-slip phenomena in textiles, in: Friction in Textile Materials, Elsevier, 2008, pp. 95-173.

[15] Syh-Shiuh Yeh.;Hsin-Chun Su, Development of friction identification methods for feed drives of CNC machine tools, The International Journal of Advanced Manufacturing Technology, 52 (2011) 263-278.

Chapter 5

INVESTIGATION OF MICROSTRUCTURAL AND MECHANICAL PROPERTIES OF MO-CONTAINING POWDER METAL STEELS AFTER SINTERING, DEFORMATION AND HEAT TREATMENT

Mehmet Akif ERDEN[1]
Harun ÇUĞ[2]

[1] Prof. Dr., Karabuk University, Engineering Faculty, Department of Medical, Karabük, Turkey
https://orcid.org/0000-0003-1081-4713
[2] Assoc. Prof. Dr., Karabuk University, Engineering Faculty, Department of Mechanical, Karabük, Turkey
https://orcid.org/0000-0002-6322-4269

The purpose of this work is to examine the mechanical and microstructural characteristics of powder metal (PM) steels with varying molybdenum (Mo) contents following the sintering, hot rolling, and heat treatment procedures. A high-precision balance was utilised to weigh the powders used in the study, and a three-axis mixer without balls was employed to homogenise them. After being sintered at 1375 °C in an environment consisting of 95% nitrogen and 5% hydrogen, the samples were hot-rolled at an 80% plastic deformation rate. The heat treatments applied both before and after rolling resulted in notable alterations to the material's microstructure. It was shown that the sintering process significantly reduced the grain size in the samples with 2% and 4% Mo due to an increase in the Mo ratio. Specifically, samples with 2% Mo had an average grain size of 2 μm, whereas samples with 4% Mo had a grain size of 1 μm. The development of precipitates like MoC(N) and their suppression of grain boundary movement have been linked to this reduction in grain size. The microstructure developed fine ferrite and pearlite grains as a result of hot rolling and later normalisation heat treatments. According to microstructural investigations, heat treatments and deformation increased density while decreasing porosity. The materials' mechanical qualities improved as a result of this circumstance. Properties including hardness, strength, and resistance to wear were all improved by the reduction in pores and the rise in precipitates. Nevertheless, following the normalisation procedure, a little reduction in hardness and wear resistance was noted. In addition to providing crucial information on how deformation and heat treatments can optimise the materials' performance attributes, this work has thoroughly uncovered the effects of Mo alloy on microstructural and mechanical properties.

1. Introduction

One significant technique for creating complexly formed, high-performance materials is powder metallurgy (PM). By regulating the microstructure, this technique has benefits for enhancing mechanical qualities, particularly in steels. Powder metal components become denser and have fewer micropores thanks to the sintering process. According to the literature, the microstructure is greatly impacted by the sintering temperature and environment [1, 2]. A common element in alloy steels, molybdenum (Mo) is recognised for its ability to refine grain size and improve hardness and strength. Precipitates containing Mo give microstructural control by stopping grain boundaries from moving. Mo enhances ferrite nucleation by forming high-stress areas at grain boundaries, as demonstrated [3]. Steels' mechanical qualities, such their strength and hardness, are enhanced by this technique.

Steels containing Mo frequently develop MoC and MoN precipitates during the sintering process. Grain growth is restricted by these precipitates, which do not dissolve even at high temperatures. The sintering environment has a major impact on the microstructure and precipitate formation [4]. According to reports in the literature, the inclusion of Mo limits the movement of grain boundaries, resulting in a finer structure [5]. Phases like ferrite and pearlite can generate fine grains in the microstructure of steels by hot rolling and related deformation operations. Following deformation, this mechanism is linked to larger nucleation zones. High deformation rates provide a finer structure, according to Inagaki (1997), who looked at how the amount of deformation affected nucleation mechanisms [5-7]. This circumstance is crucial for enhancing mechanical qualities.

The toughness and strength of materials made with PM are adversely affected by pores. The material's mechanical qualities deteriorate as the pore ratio rises. Li (2009) demonstrated that hot deformation and heat treatments can improve the material density and decrease the pore ratio [8]. Mechanical performance is positively impacted by increasing density. The impact of precipitates that occur in steels containing Mo on mechanical characteristics has been well examined in the literature. MoC(N) precipitates build up inside and at grain boundaries, reducing dislocation motion and boosting strength. Steels' hardness and resistance to wear are enhanced as a result [6-8]. By ensuring a uniform distribution of ferrite and pearlite phases in the material microstructure, the normalisation process aids in the optimisation of mechanical properties. Nevertheless, after normalisation, some research has found a minor drop in hardness and wear resistance [7-10]. The distribution of precipitates and the material's internal tensions upon deformation are related to this circumstance.

The purpose of this research is to examine the mechanical and microstructural characteristics of powder metal (PM) steels with varying molybdenum (Mo) contents following the sintering, hot rolling, and heat treatment procedures. Grain size, porosity, density, and precipitate formation in steels were to be assessed in relation to Mo addition and deformation operations. Understanding how these processes affect mechanical characteristics and identifying the mechanisms for improving steel performance through microstructure optimisation were also goals.

2. Materials and Methods

In this work, sintering, hot rolling, and heat treatment techniques were used to manufacture powder metal (PM) steels with varying molybdenum (Mo) contents and analyse their mechanical and microstructural characteristics. The chemical

compositions listed in Table 1 were followed in the preparation of the powders used in the experiments, ensuring that they contained iron (Fe), molybdenum (Mo), and carbon (C). A RADWAG AS-60-220 C/2 precision balance with a 0.01% sensitivity was used to weigh the powders. To create a homogenous mixture, the weighted powders were combined for an hour in a three-axis mixer of the Turbula brand without balls. In an environment-controlled tube furnace of the Protherm PTF 16/75/610 brand, the produced powder mixes were sintered for one hour at 1375 °C in a 95% nitrogen-5% hydrogen mixed gas atmosphere. The samples were carefully chilled to room temperature following the sintering procedure.

Following sintering, samples with an 80% plastic deformation rate were subjected to a hot rolling procedure. The samples were preheated for 30 minutes at 1150 °C in a Protherm brand heat treatment furnace prior to rolling. The technique of hot rolling was continued until 80% distortion was achieved. Following the completion of the hot rolling procedure, the samples were heated to 950 °C for 60 minutes and then left to cool in an air-conditioned environment. This procedure was used to guarantee that the ferrite and pearlite phases in the samples' microstructure were uniform. In order to examine the samples' microstructure, an etching procedure was performed using a 3% Nital solution. Using an optical microscope (OM) and a scanning electron microscope (SEM), microstructures were thoroughly inspected. The precipitates' chemical compositions and distributions were examined using energy dispersive X-ray spectroscopy (EDS).

On microscope images, grain sizes were quantified, and the impact of the Mo ratio was assessed. The Archimedes principle was used to determine the samples' densities, and the impact of heat treatment and deformation on the densities was examined. A Vickers hardness tester was used to evaluate hardness, and a rotary disc tester was used to test wear resistance. The results were assessed in light of the microstructural alterations. These techniques allowed for a thorough analysis of the impact of various Mo ratios and applied process parameters on the mechanical and microstructural characteristics of PM steels.

Table 1. Chemical elements of PM steels

Samples	Graphite (%wt)	Mo (%wt)	Fe (%wt)
Sample 1 (%80 Deformation)	0.55	2	Rest
Sample 2 (%80 Deformation)	0.55	4	Rest
Sample 3 (%80 Deformation+ 950℃ 1 h+normalization)	0.55	2	Rest
Sample 4 (%80 Deformation+ 950℃ 1 h+normalization)	0.55	4	Rest

3. Results and discussion

The mechanical and microstructural characteristics of powder metal (PM) steels with varying molybdenum (Mo) contents following sintering, hot rolling, and heat treatment procedures were examined in this work. Specifically, the impacts of deformation operations and Mo addition on mechanical performance, precipitate formation, porosity, and grain size were thoroughly investigated. The results offer crucial information for PM steel optimisation and are in line with previous research in the field.

Microstructure pictures of samples that have been sintered and 80% plastically distorted are shown in Figure 1. These pictures show how the molybdenum (Mo) content and various manufacturing steps affect the microstructure. First, the average grain size of the sintered sample with 2% Mo was found to be around 2 μm when the microstructure was analysed (Figure 1a). This structure can be linked to the fact that MoC(N) precipitates that are created during the sintering process restrict grain development and stop grain boundary movement. By controlling the sintering environment and temperature, it was found that the pores were uniformly distributed and contributed a specific density [11-14].

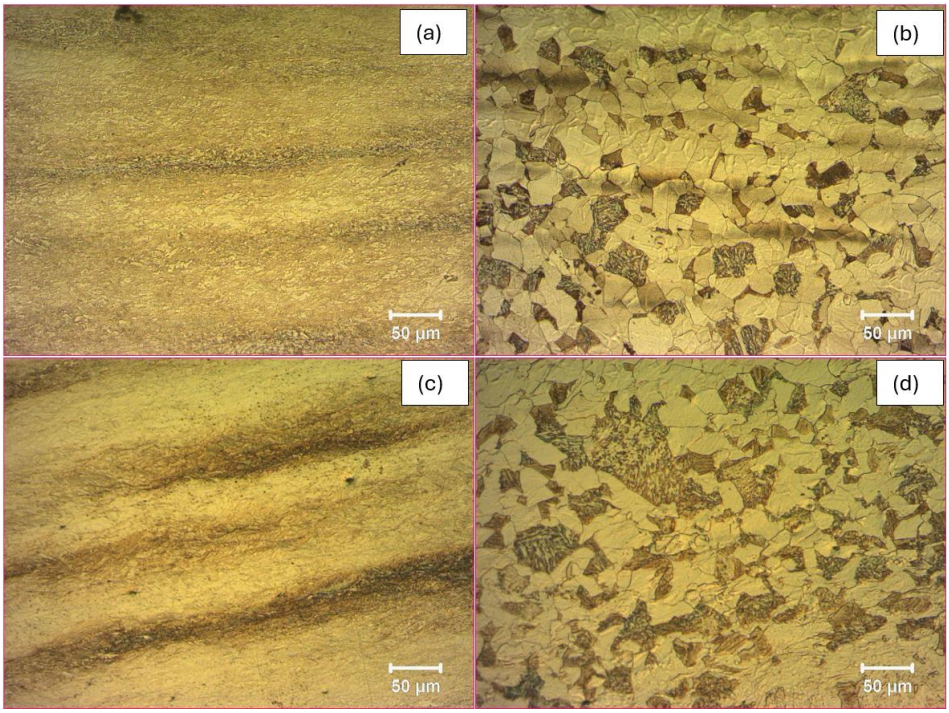

Figure 1. Microstructure images of TM steels with different molybdenum ratios sintered at 1400ºC for 1 hour in a 95% Nitrogen-5% Hydrogen mixed gas atmosphere, 200X. (a- Sample 1 (%80 Deformation), b- Sample 2 (%80 Deformation), c- Sample 3 (%80 Deformation+950°C 1 hour+ normalization), d- Sample 4 (%80 Deformation+950°C 1 hour+ normalization)

It was found that the average grain size in the microstructure of the sintered sample with 4% Mo dropped to about 1 µm (Figure 1b). This condition can be explained by the fact that a larger Mo ratio strengthens the barrier mechanism at grain borders and causes more precipitation generation. Grain boundary stabilisation and an increase in nucleation sites are the outcomes of increasing Mo addition, according to the research [17, 18]. Upon examining the microstructure following the hot rolling operation, samples that were 80% deformed showed the formation of finer and more uniform grains in the ferrite and pearlite phases (Figure 1c and Figure 1d). This circumstance can be linked to the fact that nucleation is encouraged during recrystallisation by the rise in dislocation density that occurs during deformation. Furthermore, it was found that deformation raises density and decreases porosity ratio.

Fine ferrite and pearlite grains were found to have a more regular structure in the microstructure that was produced following the normalisation procedure. Figure 1 illustrates how the combination of heat treatment and deformation decreased the material's porosity, improving its mechanical qualities. The findings unequivocally show how deformation and the addition of Mo reduce grain size and increase precipitate formation in PM steels [15-17].

Table 2. Hardness and porosity of samples.

Samples	**Hardness (0.5Hv)**	**Porosity (%)**
Sample 1 (%80 Deformation)	375	0.63
Sample 2 (%80 Deformation)	672	0.88
Sample 3 (%80 Deformation+ 950℃ 1 h+normalization)	241	0.58
Sample 4 (%80 Deformation+ 950℃ 1 h+normalization)	288	0.82

The link between the microstructure, hardness, and porosity of the samples with varying Mo ratios was closely investigated based on the findings shown in Figure 1 and Table 2. First, Sample 1, which was hot rolled and sintered, had a hardness value of 375 HV and included 97.45% Fe, 2.0% Mo, and 0.55% C. This hardness value demonstrates that the sample's structure is more uniform and that the Mo addition produces a microstructure that bolsters the grain size reduction effect. The high hardness value of Sample 1 was a result of its uniform microstructure and low porosity quantity (0.63%). The material becomes tougher because to the inhibitory effects of the Mo addition on the precipitates' grain boundaries [18-22].

Sample 2 has a hardness value of 672 HV and contains 0.55% C, 4% Mo, and 97.45% Fe. The porosity of this sample is 0.88% based on the information in Table 2. Grain size decreased and hardness rose dramatically in this sample as the Mo ratio increased due to the concentration of MoC and MoC(N) precipitates at the grain boundaries. Even while the porosity increased the material's hardness, it might have had adverse consequences on certain mechanical properties.

However, this sample's high hardness value indicates that the mechanical properties were enhanced by the Mo addition.

When the microstructure of Samples 3 and 4 was examined after the hot rolling process, it was seen that the ferrite and pearlite phases of both samples showed a homogeneous distribution, but the hardness values and porosity ratios showed differences. While the hardness of Sample 3 was 241HV, the porosity ratio was 0.58%. Since this sample has a lower Mo ratio, its hardness value is lower than Sample 2. In addition, as the sample with the lowest porosity ratio, it is seen that the porosity effect on the mechanical properties of Sample 3 is the least. Nevertheless, Sample 3's homogeneous microstructure and low porosity rate demonstrate that it offers superior machinability over the other samples, even with its low hardness value [22-24].

Sample 4's porosity rate was determined to be 0.82%, and its hardness was evaluated at 375 HV. This sample is thought to have a somewhat inferior mechanical performance because of its higher porosity rate, even if its hardness value is comparable to that of Sample 1, which has a lower Mo content. This scenario is related to the fact that the pores prepare the ground for fracture development and produce stress concentration spots within the material. According to Table 2's statistics, the hardness value rises with increasing Mo content and falls with increasing porosity rate. Therefore, one of the key elements influencing the materials' performance is the microstructural structures of the samples, namely the equilibrium between hardness and porosity rates [25,26].

4. General results

In this work, the effects of sintering, hot rolling and heat treatment methods on the microstructure, hardness and porosity of powder metal steels with varied molybdenum (Mo) content were examined. The results demonstrate that the characteristics of the material are significantly impacted by the Mo concentration and processing conditions. Below is a summary of the study's primary findings:

- It was found that Sample 1 with 2% Mo had a sintered hardness of 375 HV, while Sample 2 with 4% Mo had a hardness of 672 HV.
- The sintered samples' porosity ratios were determined to be 0.88% for Sample 2 and 0.63% for Sample 1.
- Grain size: The average grain size was measured to be 2 μm in the sample containing 2% Mo and 1 μm in the sample containing 4% Mo. It was found that the grain size reduced as the Mo level increased.

- Hot rolling effect: It was shown that samples that were 80% distorted had smaller grains and more uniform distributions of the ferrite and pearlite phases.
- Interaction between porosity and hardness: Porosity and hardness were shown to be inversely related; samples with reduced porosity had greater hardness values.
- Effect of precipitates: It was found that MoC and MoC(N) precipitates collected at the grain borders as the Mo concentration rose, inhibiting grain development and raising hardness.

References

1. Vassouf AR, Akgün M, Erden MA. Evaluation of the mechanical properties and machinability of chromium and molybdenum-added powder metallurgy steels. Proceedings of the Institution of Mechanical Engineers, Part E: Journal of Process Mechanical Engineering. 2024;238(2):674-686.
2. M. A. Erden, S. Gündüz, H. Karabulut, M. Türkmen, "Wear behaviour of sintered steels obtained using powder metallurgy method", Mechanıka. 2017, 23(4): 574–580
3. A.G. Yirik, S. Gündüz, D. Taştemür, M.A. Erden, "Microstructural and Mechanical Properties of Hot Deformed AISI 4340 Steel Produced by Powder Metallurgy", Science of Sintering, 55 (2023) 45-56
4. S. Wang, L.G. Hou, J.R. Luo, J.S. Zhang, L.Z. Zhuang, "Characterization of hot workability in AA 7050 aluminum alloy using activation energy and 3-D processing map", J.Mater.Process, 225, 110-121 (2015).
5. German, R. M. Powder Metallurgy Science. Metal Powder Industries Federation, 1994.
6. Upadhyaya, G. S. Sintered Metallic and Ceramic Materials: Preparation, Properties, and Applications. John Wiley & Sons, 2000.
7. Inagaki, I. (1997). Grain refinement by thermomechanical processing in steel. ISIJ International, 37(6), 556–563.
8. Li, H., et al. (2009). Effect of forging speed on microstructure of H13 steel. Materials Science and Engineering A, 506(1-2), 150–157.
9. Hodgson, P. D., & Gibbs, R. K. (1992). Influence of deformation on ferrite grain size. Journal of Materials Processing Technology, 31(3), 317–327.
10. Lagneborg, R., & Zajac, S. (1996). Precipitation and dispersion strengthening of microalloyed steels. Materials Science Forum, 223-224, 3–10.
11. Bhadeshia, H. K. D. H. (2001). Bainite in Steels: Theory and Practice. IOM Communications.
12. Bhat, V. (1990). Structure-property relationships in sintered steels. Metallurgical Transactions A, 21(8), 2137–2143.
13. I. Tamura, C. Ouchi, T. Tanaka, H.Sekine, Thermomechanical Processing of HighStrength Low-Alloy Steels; Butterworth-Heinemann, Oxford, 1988.
14. J.M. Chilton, M.J. Roberts, "Microalloying effects in hot-Rolled low-Carbon steels finished at high temperatures",Metall. Trans. A, 11 (1980) 1711.

15. A. Skowronek, D. Woźniak, A. Grajcar, “Effect of Mn Addition on Hot-Working Behavior and Microstructure of Hot-Rolled Medium-Mn Steels” Metals 2021, 11(2), 354.
16. M.A. Erden, M. Akgün, Proceedings of the Institution of Mechanical Engineers, Part C: Journal of Mechanical Engineering Science, 236(10) (2022) 5455.
17. Erden MA, Taşçi MT. The effect of Ni on the microstructure and mechanical properties of Nb-V microalloyed steels produced by powder metallurgy. J Polytech 2016; 19: 611–616.
18. M. A. Erden, F. G. Uzun, M. Akgün, and H. Gökçe, “Influence of Ti and Nb addition on the microstructure, mechanical, and machinability properties of 316L stainless steel fabricated by powder metallurgy,” Mater. Test., vol. 65, no. 8, pp. 1237–1253, 2023
19. M.A.Erden, B. Ayvacı, “The Effect on Mechanical Properties of Pressing Technique in PM Steels” Acta Phys. Pol. A, 135 (2019) 1078.
20. Jaakko Hannula, David Porter, Antti Kaijalainen, Jukka Kömi “Evaluation of Mechanical Properties and Microstructures of Molybdenum and Niobium Microalloyed Thermomechanically Rolled High-Strength Press Hardening Steel”, JOM, 71: 2405–2412, (2019)
21. M.A. Erden, “Effect of C Content on Microstructure and Mechanical Properties of Nb-V Added Microalloyed Steel Produced by Powder Metallurgy Method” European Journal of Science and Technology, 5 (9) (2016) 44.
22. S. Gündüz, H. Karabulut, M.A. Erden, M. Türkmen, “Microstructural effects on fatigue behaviour of a forged medium carbon microalloyed steel”, Mater. Test., 55 (2013) 865.
23. A. Rajeshkannan, K.S.Pandey, S. Shanmugam, R. Narayanasamy, “Deformation behaviour of sintered high carbon alloy powder metallurgy steel in powder preform forging”, Mater.Des.,29(2008) 1862.
24. M.A. Erden, A.M. Erer, Ç. Odabaşi, S. Gündüz, “The investigation of the effect of cu addition on the Nb-V microalloyed steel produced by powder metallurgy”, Sci. Sinter., 54 (2022) 153.
25. M.Elitaş, M. A. Erden, “Toz Metalürjisi Yöntemi ile Üretilen 316L Östenitik Paslanmaz Çeliğin Kaynaklanabilirliğinin İncelenmesi”, Bilecik Seyh Edebali University Journal of Science, 9:2, (2022) 947.
26. M.A. Erden, “Presleme basıncının toz metalürjisi ile üretilen alaşımsız çeliklerin mikroyapı ve mekanik özelliklerine etkisi”, OHU J. Eng. Sci., 6 (1) (2017) 257

Chapter 6

DEVELOPMENT AND CHARACTERIZATION OF GRAPHENE REINFORCED POLYAMIDE COMPOSITES FOR AEROSPACE AND DEFENCE APPLICATIONS

İbrahim KARTERİ[1,2]

[1] (ORCID: 0000-0001-8913-6753)Kahramanmaras¸ Istiklal University, Faculty of Elbistan Engineering Department of Energy Systems Engineering, Kahramanmaras¸, Türkiye
[2] Kahramanmaras¸ Istiklal University, Institute of Graduate Education, Department of Materials Science and Engineering, Kahramanmaras¸, Türkiye

1. INTRODUCTION

Since the physical and chemical properties of engineering plastic materials used recently can be changed, it is important to produce them as materials according to demand. In particular, these engineering plastic materials are lightweight, easy to produce, resistant to many chemicals and can be used in every field of industry due to their properties such as changing the desired properties [1,2].

Graphene-doped composite materials are increasingly used in many industries with their mechanical properties. These composite materials are especially preferred in aerospace applications due to their high strength-to-weight ratios and improved durability. They have the potential to increase fuel efficiency and overall performance by reducing the weight of aircraft and spacecraft. The addition of graphene material to engineering plastics provides resistance to environmental degradation while increasing thermal conductivity. Such properties make graphene-reinforced composites essential for areas where harsh conditions exist, such as the defence industry. Synthesis methods vary depending on the desired properties of the final material and each method offers certain advantages. However, despite the potential of graphene-reinforced composites, there are some technical and economic challenges. Problems such as scalability in production, cost-effectiveness and homogeneous distribution of graphene in the polymer matrix need to be solved. Future research should focus on overcoming these challenges and developing innovative formulations that maximise the advantages of graphene by optimising synthesis methods [3-7].

In conclusion, the development and characterization of engineering plastics by incorporating graphene into them has the potential to create a new generation of materials, especially in materials used in the aerospace and defence sectors. Ongoing research in this area will not only further advance our scientific understanding, but also pave the way for innovative applications that take advantage of the remarkable properties of graphene-reinforced composites.

2. MATERIAL AND METHOD

In order to investigate the properties of PA-Graphene blends, nanocomposite material samples were firstly supplied and this study was carried out using Graf Nano Technological Materials Company's laboratory. During this sample preparation, PA and graphene were used as matrix material and filler. Sample samples were produced from the prepared nanocomposite materials and investigations were carried out. Graphene material with graphene purity 99.5, bulk density 0.05 g/cm3 and thickness 5-8 nm was used. Graphene, the nano material used in this study, was prepared for the combination of 0.5 and 1 percent

by weight by providing thermo plastic materials. With the help of precision scales and mixers, graphene-added engineering plastic mixtures were formed at different ratios. The granulated plastic and powdered graphene were mixed dry with a mechanical mixer and then deposited into the filling chamber of the extruder machine. Here, the extruder machine, which has a 5-stage temperature control point, was monitored from the PLC screen where the temperature and pressure of the material were controlled, and pellet production was carried out by sending it to the chopper unit for pellet production. The prepared nanocomposite material mixture was placed in the hopper of the plastic injection moulding machine. Then, the machine was sent to the test moulds under regular heat and pressure and the cooling process was carried out. Thus, PA-Graphene (0.5 and 1% wt) composite material was produced by injection moulding machine. During the injection moulding process, the process parameters were adjusted to achieve optimum structural integrity and mechanical properties. During the injection moulding process, the processing temperatures of the injection moulding machine were varied to obtain flawless samples. Using the injection moulding process, samples were prepared for the analysis of the properties of the materials.

In order to analyse the Electronic-Electrical properties, Test Frequency between 4 Hz and 8 Mhz, measurement signal between 10mV ~ 5V rms, 1 ms High speed measurement, Touch Panel and ±0,05% High Accuracy were performed with Hioki branded measuring device. Shore D hardness measurements of the produced PA-Graphene (0.5 and 1% wt) composite materials were carried out. This method involves measuring the penetration depth of a tapered steel indenter into the sample surface. Due to the characteristics of the tested PA-Graphene (0.5 and 1% wt) composite material samples, the indentation hardness was tested on the Shore D scale with a scale of 0 to 100 Shore degrees. The dimensions of the composite specimens obtained by the injection moulding method were 7 mm thick specimens.

3. RESULTS AND DISCUSSION

Figure 3.1 shows the average hardness plot of PA-Graphene 0.5 and 1 wt.% composite materials. Based on the hardness (Shore D) values of two composite materials containing polyamide (PA) and graphene, PA-Graphene (0.5 wt%) Average Hardness: 73.4 and PA-Graphene (1 wt%) Average Hardness: 74.6. When analysed in terms of hardness between these two composite materials, increasing the proportion of graphene from 0.5% to 1% led to an increase in the hardness value of the composite. This indicates that graphene improves the mechanical properties of the material and creates a stiffer structure. Graphene is known for its high mechanical strength and hardness. Increasing the proportion

of graphene strengthens the bonds in the internal structure of the material, creating a more durable and rigid composite. This increase can be explained by the fact that the polyamide matrix interacts better with graphene and forms a stronger structure. The main reason for the difference in stiffness between both composites is the increase in graphene ratio. Looking at the graph in **Figure 3.1**, increasing the amount of graphene increased the hardness of the composite material. This clearly shows the contribution of graphene to mechanical properties such as hardness and durability.

Table1. Dielectric results of PA and Graphene doped composites

%wt Additive to Graphene	**Dielectric constant (έ) 100 kHz**	**Dielectric constant (έ) 1 MHz**	**Dielectric loss (ε˝) 100 kHz**	**Dielectric loss (ε˝) 1 MHz**	**Loss tangent (tanδ) 100 kHz**	**Loss tangent (tanδ) 1 MHz**
0	4.24	3.85	2.19	1.21	0.49	0.33
0.5	5.01	3.92	2.52	1.28	0.52	0.35
1	5.23	4.04	3.47	1.38	0.67	0.37

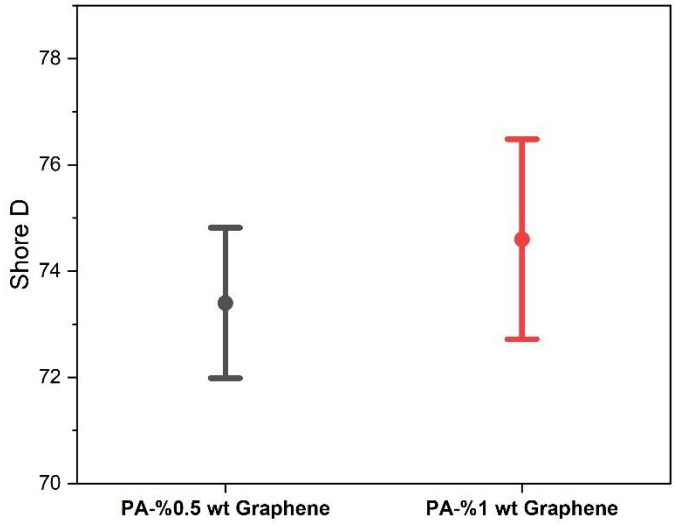

Figure 3.1. Hardness graph of PA-Graphene 0.5 and 1 wt% composite materials.

In this study, graphene doped PA (Polyamide (PA) composite materials were produced. PA-Graphene composite materials were obtained by injection moulding machine by adding 0.5 and 1 wt% Graphene to the produced PA engineering plastic material. An impedance analyser was used to determine the dielectric properties of the PA-Graphene composite materials. The frequency dependence of the dielectric properties of PA-Graphene composites was determined by capacitance, dielectric constant (ε‘), dielectric loss (ε’) and dielectric loss angle (tanδ) between 100kHz and 2MHz at room temperature. The 1MHz constant frequency dielectric constant values of the PA-Graphene composite materials produced at room temperature at 0, 0.5 and 1 wt% GNPs ratios were found to be 3.85, 3.92 and 4.04, respectively. The obtained results clearly show that the dielectric parameters are frequency dependent. **Table 1** shows the dielectric results of PA and graphene doped composites.

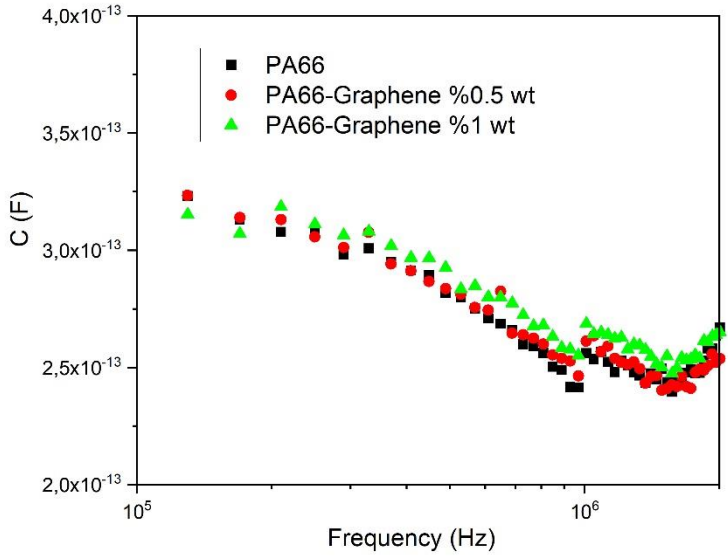

Figure 3.2. Frequency dependent capacitance graph of PA and Graphene doped composites.

Figure 3.2 shows the frequency dependent capacitance plot of PA and Graphene doped composites. The addition of graphene to the composite significantly affects the electrical properties of the material. The capacitance of the pure PA (polyamide) matrix depends only on the dipole polarisation of the polymer chains without additives. The composite with the highest proportion of graphene results in the formation of conductive graphene networks, which leads to a further increase in capacitance. The large surface area of graphene allows the electric field to be stored more efficiently. As the graphene ratio increases, the electrical conductivity and dielectric constant of the composite increases. This allows the composite to have higher capacitance values. Graphene increases the capacitance values by increasing the load carrying capacity and supporting the polarisation mechanisms of the polymer matrix. In the frequency dependent capacitance graph of PA and graphene doped composites, it is expected that the capacitance values of all materials decrease as the frequency increases. However, the increase in graphene content increases the capacitance values of the composites. When Figure 3.2. is analysed, it is seen that the composite containing 0% graphene has the lowest capacitance while the composite containing 1% graphene has the highest capacitance value. This is due to the high surface area

and conductive properties of graphene positively affecting the dielectric properties of the PA matrix.

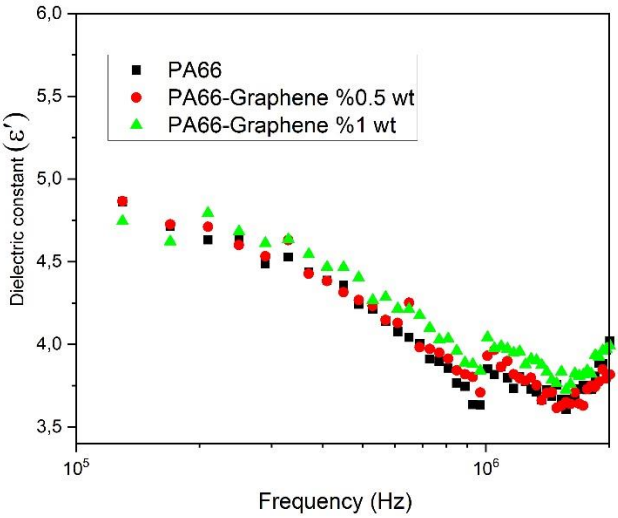

Figure 3.3. Frequency dependent dielectric constant plot of PA and Graphene doped composites.

Figure 3.3 shows the frequency dependent dielectric constant graph of PA and graphene doped composites. In the frequency dependent dielectric constant graph of PA and graphene doped composites, it is expected that the dielectric constant values decrease as the frequency increases. While the composite containing 0% graphene has the lowest dielectric constant, the composite containing 1% graphene reaches the highest dielectric constant. This is due to the high surface area and conductive properties of graphene, which favourably affect the dielectric properties of the PA matrix.

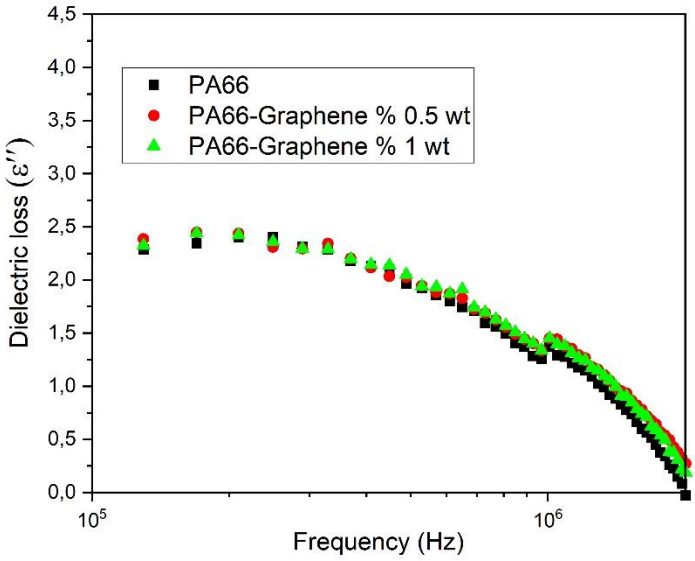

Figure 3.4. Frequency dependent dielectric loss plot of PA and Graphene doped composites.

Figure 3.4 shows the frequency dependent dielectric loss graph of PA and graphene doped composites. The frequency dependent dielectric loss graph of PA (polyamide) and graphene doped composites can be interpreted similarly to the dielectric constant graph. In the frequency dependent dielectric loss graph of PA and graphene doped composites, it is expected that the dielectric losses decrease as the frequency increases. However, increasing the graphene content may slightly increase the dielectric losses of the composites. While the composite containing 0% graphene has the lowest dielectric loss, the composite containing 1% graphene can reach the highest dielectric loss. However, these changes may not be as pronounced as in the dielectric constant and may remain at a lower level. This may be due to the limited effect of the conductive properties of graphene on energy loss.

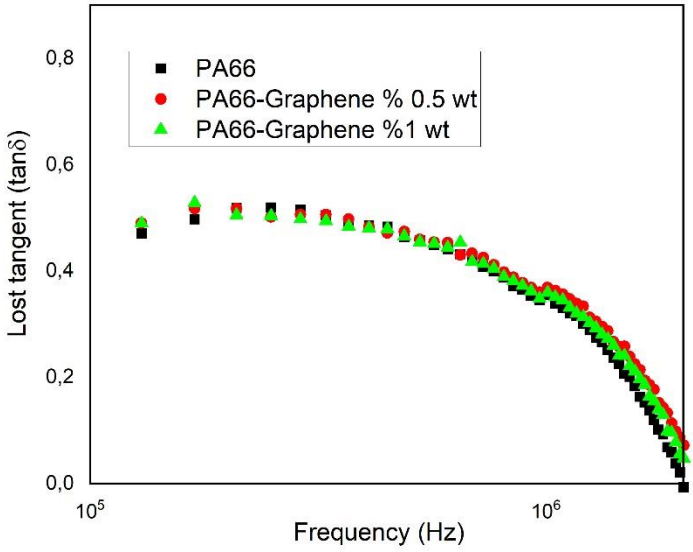

Figure 3.5. Frequency dependent loss tangent plot of PA and Graphene doped composites.

Figure 3.5 shows the frequency dependent loss tangent plot of PA and graphene doped composites. The decrease observed in the frequency dependent loss tangent plot of PA and graphene doped composites can be interpreted in a similar way to the trends in the dielectric loss and dielectric constant plot. The loss tangent (tan δ) expresses the ratio of the dielectric loss of a material to its dielectric constant and is considered as a measure of energy loss. The frequency dependent loss tangent plot of PA and graphene doped composites provides an important indicator to understand the dielectric properties and energy loss of the material. The decrease in loss tangent values as the frequency increases indicates that the material is expected to lose less energy in high frequency applications. It is observed that graphene doping can slightly enhance this effect and improve the dielectric performance of the composite material. The decrease in the frequency dependent loss tangent plot of PA and graphene doped composites indicates the frequency sensitivity of the dielectric performance of the material and energy loss. Graphene doping can improve this performance and help the material to work more efficiently in high frequency applications.

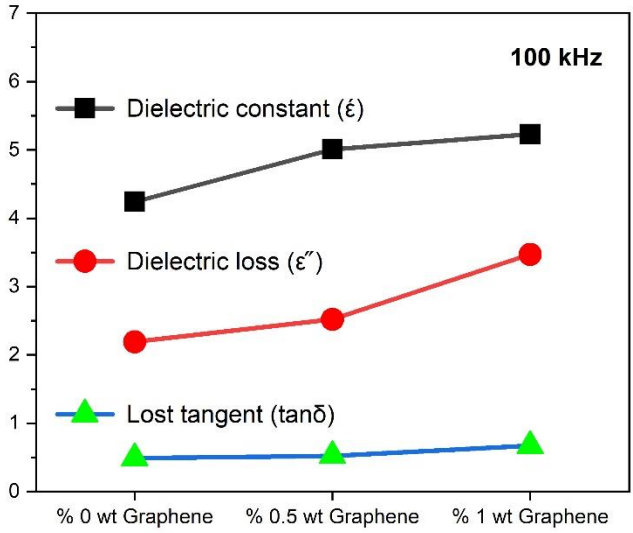

Figure 3.6. Plot of the loss tangent, dielectric loss and dielectric constant of PA and Graphene doped composites at 100 kHz frequency.

Figure 3.6 shows the loss tangent, dielectric loss and dielectric constant graph of PA and graphene doped composites at 100 kHz frequency. These changes observed at 100 kHz frequency of PA and graphene doped composites clearly show the effects of graphene on the dielectric loss and dielectric constant of the material. It is observed that as the graphene content increases, the dielectric loss and dielectric constant values increase, but the loss tangent value changes very little. This indicates that graphene affects the electrical performance of the material, especially in terms of energy loss, and this effect varies depending on the frequency.

4. CONCLUSION AND SUGGESTIONS

This study presents various characterisation results of composite materials produced by doping graphene into polyamide (PA) matrix.The PA-Graphene composites were characterised by high melting temperatures (263°C) and increasing hardness values with increasing graphene content. Graphene doping can improve the mechanical strength and hardness of the material, thereby improving its use in industrial applications. Frequency dependent changes in dielectric properties were investigated. An increase in dielectric constant and capacitance values was observed with increasing graphene content. This indicates

that the high surface area and conductive properties of graphene positively affect the electrical performance of the composite material. Frequency dependent dielectric loss and loss tangent analyses revealed that graphene doping has a limited effect on the energy loss properties of the composite material. It was observed that the dielectric losses increased with increasing graphene content, but the loss tangent values remained relatively constant. These findings indicate that the mechanical and electrical properties of PA-graphene composites can be optimised by properly selecting the graphene doping and can increase their usability in various industrial applications.

Acknowledgements

This research was partly supported by Graf Nano Technological Materials Industry and Trade Ltd. Co. Additionally, author would like to thank Kahramanmaras Istiklal University Scientific Research Projects Coordination Unit (Project No: 2022/3-3 LTP) for their financial supports

REFERENCES

1. Andrady, A. L., & Neal, M. A. (2009). Applications and societal benefits of plastics. *Philosophical Transactions of the Royal Society B: Biological Sciences*, *364*(1526), 1977-1984.
2. North, E. J., & Halden, R. U. (2013). Plastics and environmental health: the road ahead. *Reviews on environmental health*, *28*(1), 1-8.
3. Almansoori, A., Balázsi, K., & Balázsi, C. (2024). Advances, Challenges, and Applications of Graphene and Carbon Nanotube-Reinforced Engineering Ceramics. *Nanomaterials*, *14*(23), 1881.
4. Dahiya, M., & Bansal, S. A. (2022). Graphene-reinforced nanocomposites: synthesis, micromechanics models, analysis and applications–a review. *Proceedings of the Institution of Mechanical Engineers, Part C: Journal of Mechanical Engineering Science*, *236*(16), 9218-9240.
5. Mahenran, T., & Rajammal, V. K. K. N. (2022). Mechanical and Morphological Investigation of Aluminium 7075 Reinforced with Nano Graphene/Aluminium Oxide/Inconel Alloy 625 Using Ultrasonic Stir Casting Method. *Revue des Composites et des Materiaux Avances*, *32*(4), 181.
6. Baraheni, M., Hoseini, A. M., & Najimi, M. R. (2024). Investigation on carbon fiber-reinforced polymer combined with graphene nanoparticles subjected to drilling operation using response surface methodology and non-dominated sorting genetic algorithm-II. *Proceedings of the Institution of Mechanical Engineers, Part E: Journal of Process Mechanical Engineering*, 09544089241230160.
7. Almansoori, A., Balázsi, K., & Balázsi, C. (2024). Advances, Challenges, and Applications of Graphene and Carbon Nanotube-Reinforced Engineering Ceramics. *Nanomaterials*, *14*(23), 1881.

Chapter 7

INNOVATIVE AUTOMOTIVE STEELS: A COMPREHENSIVE REVIEW

Cihangir Tevfik SEZGİN[1]

[1] Dr. Öğr. Üyesi, Kastamonu Üniversitesi Kastamonu Meslek Yüksekokulu, Makine ve Metal Teknolojileri, ORCID: 0000-0002-1916-9901

1. Introduction

The steel industry has long been a cornerstone of industrial development, with steels being essential in a vast array of applications, from construction and transportation to energy and defense sectors. Traditionally, the development of steels focused on optimizing the properties of carbon steel, stainless steel, and alloy steels to meet the demands of various applications. However, the increasing need for advanced materials with higher strength, improved toughness, and enhanced corrosion resistance, particularly for high-performance applications, has led to the advent of "new generation steels." These novel materials offer a range of enhanced mechanical and chemical properties that conventional steels cannot provide.

New generation steels, such as Advanced High Strength Steels (AHSS), Twinning-Induced Plasticity (TWIP) steels, and Transformation-Induced Plasticity (TRIP) steels, have gained significant attention in both academic and industrial research. These steels have been developed through innovative alloying techniques, thermomechanical processing, and advanced heat treatments to achieve tailored microstructures. Unlike traditional steels, new generation steels often achieve their high strength and ductility through mechanisms like phase transformation, twinning, and controlled dislocation motion, making them suitable for demanding applications that require lightweight, high-strength materials.

Furthermore, with global priorities shifting toward sustainability and energy efficiency, the role of new generation steels in reducing carbon emissions and conserving resources has become more prominent. These materials not only help to reduce the weight of structures and vehicles, thereby improving fuel efficiency, but they also offer durability and longevity in service, which contribute to lower lifecycle costs and reduced environmental impact.

This comprehensive review explores the fundamental characteristics of new generation automotive steels, examining their development, microstructural features, mechanical and chemical properties, and specific applications. By analyzing the progress in alloy design and processing methods, this paper aims to provide a thorough understanding of the technological advancements in automotive steel and the future potential of these cutting-edge materials.

2. Necessity of Steel For Design Of Automotive Body

Climate change and global warming are among the primary threats to ecological sustainability. One of the main contributors to this, and perhaps the most significant, is automotive usage. In recent years, the automotive industry has conducted extensive research and development (R&D) activities aimed at

reducing vehicle weights to lower emission levels, and these efforts continue today. Reducing vehicle weight plays a critical role in decreasing emission levels, as it directly lowers fuel consumption, thereby reducing the emission of environmentally harmful gases. However, this reduction in weight must not compromise passenger safety in the event of an accident. In 2023, a total of 1,314,136 traffic accidents occurred on our country's road network. Of these accidents, 1,079,065 were property damage-only accidents, while 235,071 were accidents resulting in fatalities or injuries. Among the accidents involving fatalities or injuries, 83.1% occurred within residential areas, and 16.9% took place outside residential areas.

A total of 6,548 people lost their lives, and 350,855 people were injured in traffic accidents. As a result of the 235,071 fatal and injury-causing traffic accidents that occurred in Turkey in 2023, 2,984 individuals died at the scene, while 3,564 people, after being injured and transported to healthcare facilities, succumbed to the effects of the accident within 30 days. On average, in 2023, there were 644 fatal or injury-causing traffic accidents, 18 deaths, and 961 injuries per day on the country's roads [1].

As a result, there has been a notable increase in R&D activities focusing on steel materials, the primary materials used in the automotive industry.

The automotive sector constantly evolves to meet the demands for more environmentally friendly, fuel-efficient, and safer vehicles. At the forefront of this evolution is the improvement of materials used in vehicle production. Therefore, the use of components made from polymers [2], composite materials [3,4], and low-density metals such as aluminum [5,6] and magnesium [7,8] has become increasingly common in automobile bodies, particularly due to oil crises and environmental concerns. However, it is nearly impossible to ensure both economic feasibility and passenger safety with these types of materials. This necessity has made the production and development of high-strength steels indispensable. With the rise in passenger safety standards and the need to reduce environmentally harmful emissions (emission rates), the industry has been driven to search for materials that are both lightweight and capable of meeting required passenger safety standards. Consequently, the desire to produce lighter vehicles has spurred greater research and development into Advanced High Strength Steels (AHSS). Since the late 1990s, new generation steels have been widely used in the automotive industry, leading to reductions in both material thickness and vehicle weight.

For the automotive sector, it is crucial that the high-strength steels produced not only have high strength values but also retain ductility and weldability, particularly for spot welding [9] and laser welding [10-12]. Although initially

developed for the automotive industry, these steels also serve as raw materials applicable across various other industries. Steel manufacturers are known to continuously conduct R&D to develop high-strength, formable, and ductile materials.

Due to substantial increases in the strength of steel grades, less steel is required to achieve the same load-bearing performance as lower-strength grades. This makes steel a viable material for vehicle lightweighting, thereby enhancing fuel efficiency. Numerous studies [13-16] focused on vehicle mass reduction through the use of high-strength and advanced high-strength steels.

Significant reductions in vehicle weight have been observed due to the new AHSS grades developed by companies in their own R&D departments. Figure 1 illustrates the weight reduction achieved in a car door using innovative AHSS from ArcelorMittal, one of the world's largest steel producers.

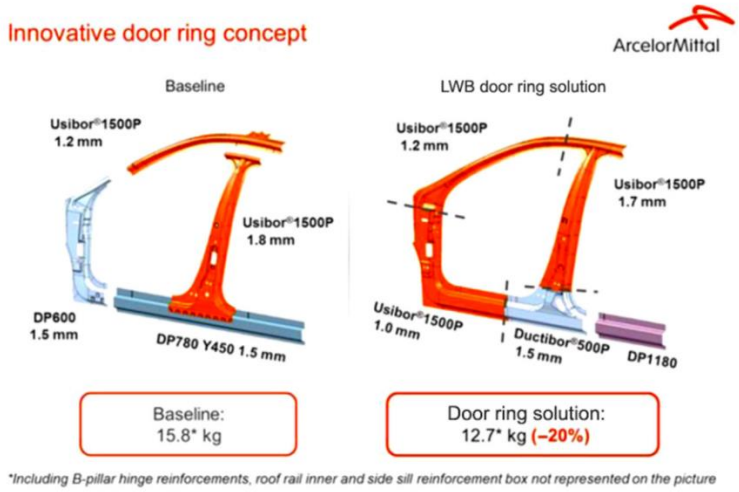

Figure 1. Innovative door ring concept of Arcelor Mittal [17]

3. New Generation Steels Used In The Automotive Industry

3.1. High Strength Low Alloyed Steels (HSLA)

High-strength low-alloy (HSLA) steel is an alloy steel known for its superior mechanical properties and enhanced corrosion resistance compared to carbon steel. Unlike other types of steel, HSLA steels are designed to achieve particular mechanical characteristics rather than adhere to a defined chemical composition.

Hot-rolled HSLA sheet steels are widely utilized in components like chassis parts, front-side rails, engine mounts, wheels, rims, discs, and suspension parts. Cold-rolled HSLA steel, on the other hand, is frequently applied in areas where high formability is not essential [18].

HSLA steels represent a distinct group of carbon steels that are enhanced with microalloying elements like vanadium (V), niobium (Nb), or titanium (Ti), providing them with superior mechanical properties. The yield strength of certain HSLA steels can reach up to 690 MPa, which is more than double the strength range (170–250 MPa) of standard carbon steels. The exceptional strength of HSLA steels is attributed to microstructural characteristics, including grain refinement, precipitation hardening, and the control of inclusion shapes [18]. In much the same way, today's vehicle bodies widely incorporate HSLA steel grades to fulfill the economic and technical requirements of weight reduction alongside enhanced mechanical performance. To meet these objectives, most HSLA steels are alloyed with Nb. The addition of Nb in HSLA steels contributes to higher strength, mainly through grain refinement. In interstitial-free high-strength steels, Nb also serves as a stabilizing element [18, 19]. For this reason yhr other name of HSLA is micro-alloyed steel.

3.2. Dual-Phase Steel (DP)

Due to their high strength, excellent formability, good weldability, ease of availability, and cost advantages, DP steels are among the most widely used types in the AHSS class. The combination of good formability (or ductility) and high strength in DP steels results from their unique microstructure. Dual-phase steel gets its name from the two phases present in its microstructure: ferrite and martensite. Ferrite provides ductility to the structure, while martensite contributes high strength [20,21,22]. Figure2 shows the microstructure of DP steel. It was previously mentioned that DP steels consist of two phases, ferrite and martensite. Due to heat treatments and alloying elements, as shown in Figure 2, retained austenite (RA) can also be present in the microstructure.

DP steels exhibit superior ductility compared to HSLA steels at the same strength level. Generally, they contain a maximum of 0.2% C, 1.5% Mn, and 0.5% Si, and may also include low amounts of alloying elements such as Cr, Mo, Nb, V, and N. In the alloying elements present, manganese aids in the transformation to martensite during rapid cooling. Chromium and molybdenum lower the transition temperatures, while silicon acts as a solid solution hardener. Elements such as Nb, V, and Ti contribute to precipitation hardening and control the grain size [23]. In low-strength dual-phase steels, the soft ferrite phase is continuous, which provides the steel with ductility.

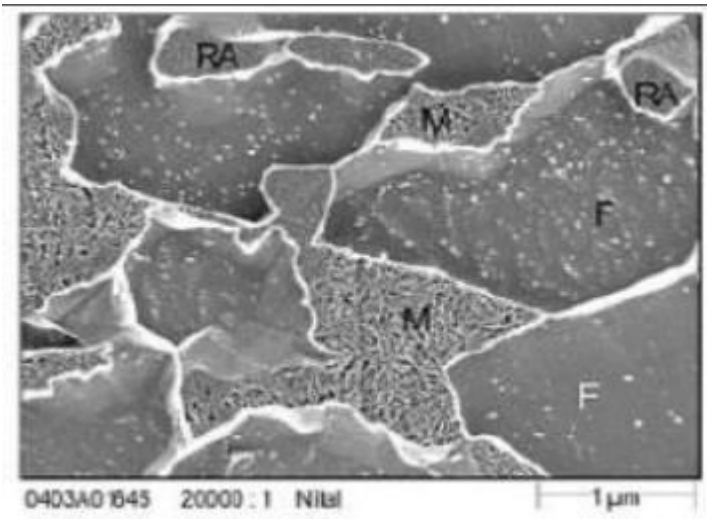

Figure 2. Microstructure of DP steel (M: martensite, F:ferrite, RA: retained austenite) [23]

3.3. Martensitic Steel

To obtain martensitic steel, the austenite formed during hot rolling or annealing is completely transformed into martensite during the cooling process. The martensitic transformation begins when the austenite grains reache the martensite start temperature (Ms) and continue until the lower transformation final temperature (Mf) are reached. In generally, martensitic steel has less than 2% alloying elements due to provide a good weldability behaviour. Martensitic steel is used as side impact beams, bumpers, structural components, and electric vehicles (EV) battery enclosures in automotive industry [24]. Figure 3 shows an EV battery housing component made from martensitic steel. Yield stresses can reach up to 1700 MPa, while tensile strengths can go up to 2000 MPa. However, elongation percentages are quite low (around 3%). To produce the final product with martensitic steels, cold rolling is performed after hot rolling following annealing to achieve the desired strength values and surface smoothness. Martensitic steel provides a good corrosion resistance by using electro galvanized coating.

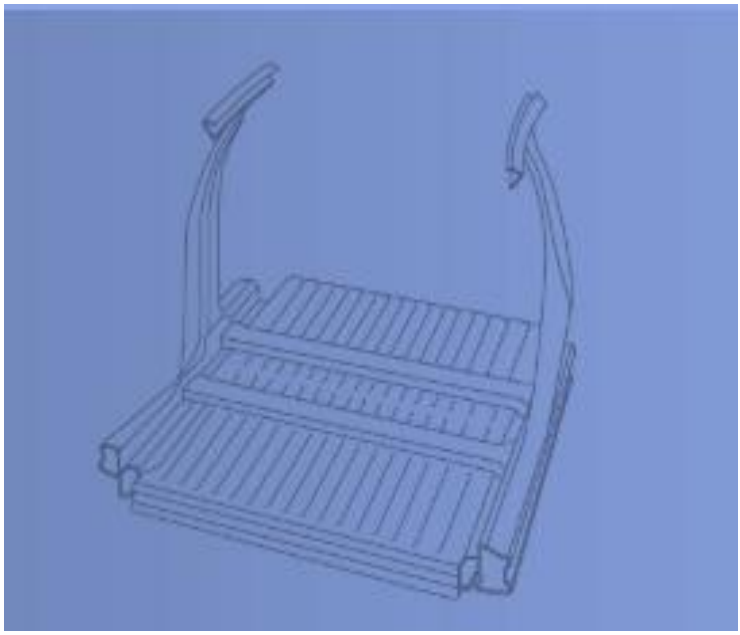

Figure 4. EV battery housing component [24]

3.4. Quenching and Partitioning Steel

Quenching and partitioning (Q&P) steel refers to a category of steels, such as C–Si–Mn, C–Si–Mn–Al, or similar compositions, that undergo the innovative Q&P heat treatment process. In automotive applications, Q&P steel aims to provide a new class of ultrahigh-strength steel with enhanced ductility, helping to improve fuel efficiency while ensuring passenger safety. Its final microstructure, consisting of ferrite (in cases of partial austenitization), martensite, and retained austenite, offers an exceptional balance of strength and ductility. This makes Q&P steel an integral part of the next generation of advanced high-strength steels (AHSS) designed for automotive use [25-27]. Numerous studies [28-30] have explored the correlation between the properties and microstructures of Q&P steels undergoing different heat treatments. These studies have demonstrated that the ultrahigh strength of Q&P steel is derived from martensite laths, while its excellent ductility is linked to the TRIP effect of retained austenite during deformation. Figure 5 shows this relationship. In Figure 5, It is observed that as the voltage increases, the white parts decrease, that is, the retained austenite decreases. To maximize the retention of austenite fractions during the Q&P process, the formation of carbides (whether transition carbides or cementite) should be minimized, as carbides act as carbon 'sinks,' limiting the

partitioning of carbon into austenite. The formation of cementite can be effectively inhibited through alloying with elements such as Si, Al, or P [28].

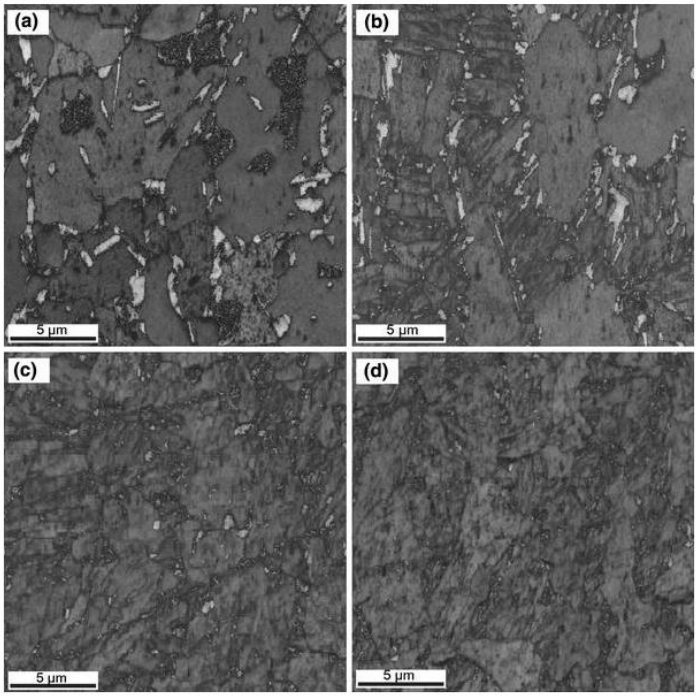

Figure 5. Q&P steel tension tested at 0 °C (32°F). White corresponds to retained austenite. (a) 0, (b) 1, (c) 5, and (d) 10% strain [25]

3.5. TRansformation Induced Plasticity (TRIP) Steel

Transformation Induced Plasticity (TRIP) steels have a microstructure composed of a ferrite matrix along with varying amounts of retained austenite, martensite, and bainite [31]. This microstructure is shown in Figure 6. The production process for TRIP steels usually involves an isothermal holding step at an intermediate temperature to form some bainite. The elevated silicon and carbon levels in TRIP steels contribute to substantial amounts of retained austenite in the final microstructure. The significant forming properties of this group of steels are primarily derived from specifically tailored microstructural components of retained austenite. Austenite is unstable at room temperature under equilibrium conditions. Retaining an austenitic microstructure at room temperature requires a specific chemical composition and a controlled thermal process. During sheet forming, the deformation provides the energy needed to transform austenite into martensite [32,33]. Due to limited time and temperature, significant carbon diffusion from the carbon-rich austenite does not occur,

leading to the formation of high-carbon (and high-strength) martensite after transformation. As deformation continues, the transformation to high-strength martensite progresses, provided there is still retained austenite available for conversion. In TRIP steels, retained austenite gradually transforms into martensite as strain increases, leading to an elevated work hardening rate at higher strain levels. This phenomenon is referred to as the **TRIP Effect** [31]. Compared to DP and HSLA steels, TRIP steels provide higher ductility at the same stress levels due to the TRIP effect. This comparison is shown in Figure 7.

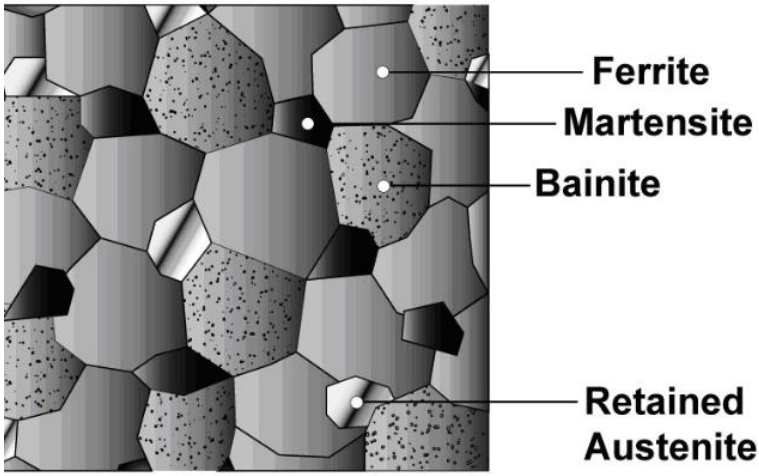

Figure 6. TRIP steel microstructure: ferrite, martensite, bainite and retained austenite [31]

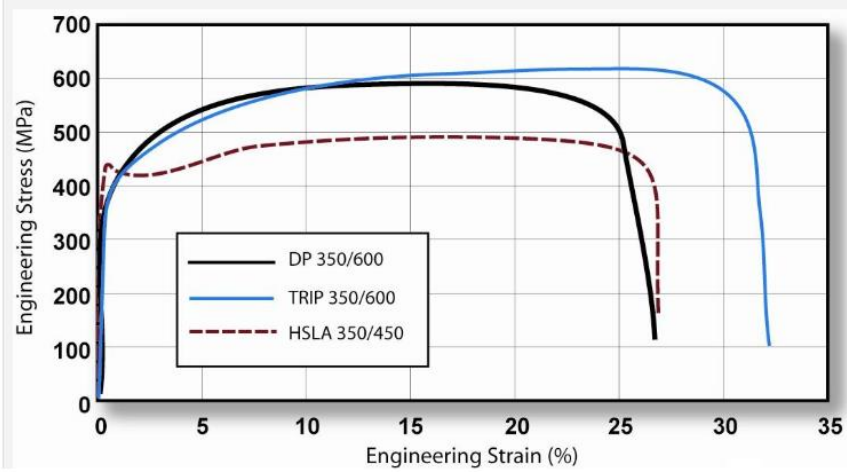

Figure 7. Compairing of stress and strain of HSLA, DP and TRIP steels [31]

3.6. Twinning Induced Plasticity (TWIP) Steels

TWIP steel represents a category of high and ultra-high strength steels known for their exceptional ductility, high strain hardening, significant uniform elongation, and remarkable ultimate tensile strength. These steels are widely studied and developed for industrial uses, including the automotive sector, LNG shipbuilding, oil and gas exploration and transportation, as well as non-magnetic structural applications, thanks to their combination of ultra-high strength, excellent ductility, and outstanding energy absorption capacity. TWIP steels maintain a fully austenitic phase at room temperature due to their high manganese content (15–30%), which delays phase transformation during cooling. Moroever, the Al content is in excess of 3%, and the Si content is in the range of 2–3% (by weight). C also increase the stability of austenite at room temperature. The primary deformation mechanism during plastic deformation is the formation of twins within the grains [34-36]. TWIP steel is anticipated to provide ultra-high strength for structural reinforcement, exceptional ductility for easier press forming, and excellent energy absorption for enhanced crash performance, which is vital for vehicles. Furthermore, widespread adoption of TWIP steel could lead to reduced vehicle weight, lower greenhouse gas emissions, significantly improved fuel efficiency, and enhanced passenger safety. Under plastic deformation, twin bands form within the austenite. Once the volume of deformation twins within the grain becomes saturated, the twins reduce effective glide sitance of dislocation which causes Dynamical Hall-Petch Effect. The combined effects of the TWIP mechanisms enhance plasticity, leading to a high work hardening rate and tensile elongations of up to 65% [34]. Figure 8 shows the Dynamical Hall-Petch Effect.

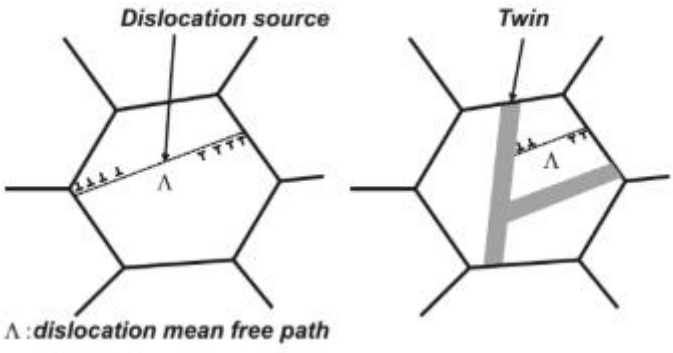

Figure 8. The Dynamical Hall-Petch Effects [34]

Conclusion

The automotive industry has witnessed remarkable advancements in materials science, particularly in the development of high-performance steels. As global demands shift towards more sustainable and fuel-efficient transportation solutions, the evolution of new generation steels, such as Advanced High Strength Steels (AHSS), Dual-Phase (DP) steels, Transformation-Induced Plasticity (TRIP) steels, and Twinning-Induced Plasticity (TWIP) steels, has become crucial in meeting these goals. These steels not only offer exceptional strength-to-weight ratios but also provide an excellent combination of ductility, formability, and energy absorption, which are critical for improving vehicle performance, safety, and sustainability.

One of the primary motivations behind the development of these new generation steels is the urgent need to reduce vehicle weight without compromising safety standards. As the need for better fuel efficiency and lower carbon emissions intensifies, these innovative steels play a pivotal role in reducing material thickness and vehicle mass, contributing to lighter and more energy-efficient vehicles. The ability to achieve ultrahigh strength while maintaining formability through unique mechanisms such as phase transformation, twinning, and dislocation control sets these steels apart from conventional materials, making them ideal candidates for the automotive sector.

The TRIP effect and the TWIP effect, for example, significantly enhance the work hardening capacity and overall ductility of the steels, enabling them to absorb greater amounts of energy during collision scenarios. This leads to improvements in crashworthiness, which is vital for passenger safety. Furthermore, the combination of high strength and superior ductility in steels like DP and TRIP steels allows them to be used effectively in lightweight automotive structures that do not compromise on safety, durability, or performance.

In addition to their mechanical properties, new generation steels like TWIP and Q&P steels show promise for reducing environmental impact. Their ability to absorb more energy during impact, combined with their reduced weight, directly translates to improved fuel efficiency and lower carbon footprints. As the automotive industry continues to prioritize sustainability, these steels will be key to achieving lower emissions, improved fuel mileage, and reduced environmental impact throughout a vehicle's lifecycle.

Despite these advancements, there are challenges in the widespread adoption of these new materials, including the cost of production, processing requirements, and the complexity of integrating these advanced steels into existing manufacturing processes. However, continued research and development,

combined with the growing demand for fuel-efficient and safe vehicles, will likely accelerate the adoption of these high-performance steels.

Looking forward, the potential applications of these steels extend beyond automotive use into sectors such as shipbuilding, aerospace, and energy, where high strength and lightweight materials are essential. The ongoing progress in alloy design, thermomechanical processing, and heat treatments will continue to push the boundaries of what is possible in steel manufacturing, enabling even more optimized materials for future generations of vehicles and industrial applications.

In conclusion, the development of new generation steels marks a significant leap forward in material science and engineering. With their exceptional properties and diverse applications, these steels will play a central role in shaping the future of the automotive industry, contributing to safer, lighter, and more fuel-efficient vehicles. As research continues to refine these materials and manufacturing processes, the potential for even greater advancements in performance, sustainability, and safety remains vast, promising a bright future for automotive and other high-performance industries.

REFERENCES

[1].https://data.tuik.gov.tr/Bulten/Index?p=Karayolu-Trafik-Kaza-Istatistikleri-2023-53479

[2]. Pashkova, O., Nardid, L., Rudnieva, E., & Zarubyna, M. (2020). Characteristic of Modern Polymer Materials and their Application in the Automotive Industry. Theory and Practice of Forensic Science and Criminalistics, 21(1), 388-410.

[3]. Akkaş, M. (2022). Synthesis and characterization of MoSi2 particle reinforced AlCuMg composites by molten salt shielded method. Türk Doğa ve Fen Dergisi, 11(4), 11-17.

[4]. Turayev, S., Tuychiyev, X., Sardor, T., Yuldashev, X., & Maxsudov, M. (2021). The importance of modern composite materials in the development of the automotive industry. Asian Journal of Multidimensional Research (AJMR), 10(3), 398-401.

[5]. Kilicaslan, M. F., Elburni, S. I., Yilmaz, Y., & Akkaş, M. (2022). Effects of B addition on the microstructure and microhardness of melt-spun Al-7075 alloy. Advances in Materials Science, 22(2), 5-18.

[6]. Cavezza, F., Boehm, M., Terryn, H., & Hauffman, T. (2020). A review on adhesively bonded aluminium joints in the automotive industry. Metals, 10(6), 730.

[7]. Musfirah, A. H., & Jaharah, A. G. (2012). Magnesium and aluminum alloys in automotive industry. Journal of Applied Sciences Research, 8(9), 4865-4875.

[8]. Em Akra, K. M., Akkaş, M., Boz, M., & Seabra, E. (2020). The production of AZ31 alloys by gas atomization method and its characteristics. Russian Journal of Non-Ferrous Metals, 61, 332-345.

[9]. Nayak, S. S., Hernandez, V. B., Okita, Y., & Zhou, Y. (2012). Microstructure–hardness relationship in the fusion zone of TRIP steel welds. Materials Science and Engineering: A, 551, 73-81.

[10]. Hong, K. M., & Shin, Y. C. (2017). Prospects of laser welding technology in the automotive industry: A review. Journal of Materials Processing Technology, 245, 46-69.

[11]. Assunção, E., Quintino, L., & Miranda, R. (2010). Comparative study of laser welding in tailor blanks for the automotive industry. The International Journal of Advanced Manufacturing Technology, 49, 123-131.

[12]. Perka, A. K., John, M., Kuruveri, U. B., & Menezes, P. L. (2022). Advanced high-strength steels for automotive applications: arc and laser welding process, properties, and challenges. Metals, 12(6), 1051.

[13]. Refiadi, G., Aisyah, I. S., & Siregar, J. P. (2019). Trends in lightweight automotive materials for improving fuel efficiency and reducing carbon emissions. Automotive Experiences, 2(3), 78-90.

[14]. Singh, A. K., & Kumar, D. S. (2024). Simulation of Automotive Components to Optimize Best Application from Different Grades of Steel Using Finite Element Method (FEM). Engineering Science & Technology, 270-290.

[15]. Li, Z., Chang, Y., Rong, J., Min, J., & Lian, J. (2023, June). Edge fracture of the first and third-generation high-strength steels: DP1000 and QP1000. In IOP Conference Series: Materials Science and Engineering (Vol. 1284, No. 1, p. 012021). IOP Publishing.

[16]. Li, Z., Chang, Y., Rong, J., Min, J., & Lian, J. (2023, June). Edge fracture of the first and third-generation high-strength steels: DP1000 and QP1000. In IOP Conference Series: Materials Science and Engineering (Vol. 1284, No. 1, p. 012021). IOP Publishing.

[17].https://automotive.arcelormittal.com/Solutions_lightweighting/S_in_motion/SinMotionGeneral

[18]. Garcia, C. I. (2017). High strength low alloyed (HSLA) steels. In Automotive Steels (pp. 145-167). Woodhead Publishing.

[19]. Mohrbacher, H., & Klinkenberg, C. (2007, February). The role of niobium in lightweight vehicle construction. In Materials science forum (Vol. 537, pp. 679-686). Trans Tech Publications Ltd.

[20]. Sezgin, C. T., & Hayat, F. (2020). The microstructure and mechanical behavior of TRIP 800 and DP 1000 steels welded by electron beam welding method. Soldagem & Inspeção, 25, e2526.

[21]. Li, X., Roth, C. C., & Mohr, D. (2019). Machine-learning based temperature-and rate-dependent plasticity model: application to analysis of fracture experiments on DP steel. International Journal of Plasticity, 118, 320-344.

[22]. Sezgin, C. T. (2017). Otomotiv Endüstrisinde Yeni Nesil Çelik Kullanımının Önemi. Akademia Mühendislik ve Fen Bilimleri Dergisi, 1(3), 205-210.

[23]. Hofmann, H., Mattissen, D., & Schaumann, T. W. (2009). Advanced cold rolled steels for automotive applications. Steel Research International, 80(1), 22-28.

[24].https://www.ssab.com/en/brands-and-products/docol/automotive-steelgrades/martensitic-steel

[25]. Wang, L., & Speer, J. G. (2013). Quenching and partitioning steel heat treatment. Metallography, Microstructure, and Analysis, 2, 268-281.

[26]. Edmonds, D. V., He, K., Rizzo, F. C., De Cooman, B. C., Matlock, D. K., & Speer, J. G. (2006). Quenching and partitioning martensite—A novel steel heat treatment. Materials Science and Engineering: A, 438, 25-34.
[27]. Chen, P., Li, X. W., Wang, P. F., Wang, G. D., Guo, J. Y., Liu, R. D., & Yi, H. L. (2022). Partitioning-related microstructure evolution and mechanical behavior in a δ-quenching and partitioning steel. Journal of Materials Research and Technology, 17, 1338-1348.
[28]. De Moor, E., Lacroix, S., Clarke, A. J., Penning, J., & Speer, J. G. (2008). Effect of retained austenite stabilized via quench and partitioning on the strain hardening of martensitic steels. Metallurgical and Materials Transactions A, 39, 2586-2595.
[29]. Thomas, G., Speer, J., Matlock, D., & Michael, J. (2011). Application of electron backscatter diffraction techniques to quenched and partitioned steels. Microscopy and Microanalysis, 17(3), 368-373.
[30]. Santofimia, M. J., Zhao, L., & Sietsma, J. (2008). Model for the interaction between interface migration and carbon diffusion during annealing of martensite–austenite microstructures in steels. Scripta Materialia, 59(2), 159-162.
[31].https://ahssinsights.org/metallurgy/steel-grades/3rdgen-ahss/transformation-induced-plasticity-trip/
[32]. Chatterjee, S., Murugananth, M., & Bhadeshia, H. K. D. H. (2007). δ TRIP steel. Materials Science and Technology, 23(7), 819-827.
[33]. Tomita, Y., & Iwamoto, T. (1995). Constitutive modeling of TRIP steel and its application to the improvement of mechanical properties. International Journal of Mechanical Sciences, 37(12), 1295-1305.
[34]. De Cooman, B. C., Estrin, Y., & Kim, S. K. (2018). Twinning-induced plasticity (TWIP) steels. Acta Materialia, 142, 283-362.
[35]. De Cooman, B. C., Kwon, O., & Chin, K. G. (2012). State-of-the-knowledge on TWIP steel. Materials Science and Technology, 28(5), 513-527.
[36]. De Cooman, B. C., Chin, K. G., & Kim, J. (2011). High Mn TWIP steels for automotive applications. New trends and developments in automotive system engineering, (1), 101-128.

Chapter 8

IN NEW GENERATION BUILDING MATERIALS: AUTOCLAVED AERATED CONCRETE, PRODUCTION PROCESS AND PROPERTIES

Selçuk MEMİŞ[1]

[1]1 Doç.Dr.; Kastamonu Üniversitesi, Mühendislik ve Mimarlık Fakültesi, İnşaat Mühendsiliği Bölümü, smemis@kastamonu.edu.tr ORCID No:0000-0002-2588-9227

1. CONCRETE

Concrete is a composite construction material obtained by homogenously mixing cement, aggregates, water, and, when necessary, admixtures in specific proportions, which hardens over time, losing its plasticity and gaining high strength. In other words, concrete is defined as a composite construction material obtained by mixing cement, concrete aggregates, water, and appropriate admixtures in specific proportions, based on calculations and in accordance with a particular production technology, which is initially in a plastic state and, through the hydration of cement, hardens over time, taking the desired shape and becoming solid.

By varying the proportions of the materials that make up concrete (water, cement, sand, gravel), concrete with different strengths can be produced. Additionally, it is possible to obtain concrete with different properties by using specially manufactured cements, special aggregates (lightweight aggregates, heavy aggregates), admixtures, and specific curing conditions. Concrete with different characteristics can be grouped into three categories based on their density, strength, and production location.

The density of hardened concrete is the ratio of the dry mass of the concrete to its apparent volume. Concrete density varies depending on the source, type, and granulometric structure of the aggregates used. Based on this, concrete is classified into three categories: lightweight, normal, and heavy concrete..

According to TS EN 206-1, the properties of concrete classified into three categories can be defined as follows:

1. **Lightweight concrete**: Concrete with a unit weight in the dry state (oven-dry) ranging from 800 kg/m³ to 2000 kg/m³.
2. **Normal concrete**: Concrete with a unit weight in the dry state (oven-dry) ranging from 2000 kg/m³ to 2600 kg/m³.
3. **Heavy concrete**: Concrete with a unit weight in the dry state (oven-dry) greater than 2600 kg/m³.

1.1 Lightweight Concrete

Lightweight concrete has been defined in various ways in different sources, but in short, it is concrete with an oven-dry density ranging from 0.8 to 2.0 kg/dm³, produced using lightweight aggregates (such as pumice, diatomite, etc.), or with materials above a 4 mm sieve being lightweight aggregates, and materials below a 4 mm sieve consisting of natural sand and/or crushed lightweight aggregates. According to another definition, lightweight concrete is described as concrete used in applications where both strength and properties like lightness and thermal insulation are desired, with unit weights ranging from 400 to 2000 kg/m³. A further definition by Memiş (2013) describes lightweight concrete as a material that can be produced either by using lightweight aggregates instead of traditional aggregates,

using only coarse aggregates, or by expanding the cement binder (such as in aerated concrete).

The advantages of lightweight concrete are listed below:

- It provides cost savings in reinforcement for elements under bending.
- The manufacturing conditions for prefabricated structural elements are improved.
- Structures made with lightweight concrete are less affected by earthquakes.
- It offers better thermal insulation.
- It has better resistance to freezing-thawing and fire.
- Prestressed structural elements under bending require a larger critical span.

However, despite these advantages, lightweight concrete has some drawbacks, including:

- A higher void ratio.
- Lower strength compared to conventional concrete.
- Higher shrinkage.
- Requires more care during placement.

Despite its positive and negative aspects, lightweight concrete is an important construction material that can be used in place of normal concrete, provided that sufficient compressive strength is achieved, or depending on the application areas. This allows for a low unit weight and high thermal insulation.

The most common method in the production of lightweight concrete is the use of lightweight aggregates. Lightweight aggregate is an important material used to reduce the unit weight of concrete, and it can be used in both load-bearing and non-load-bearing applications. To reduce the unit weight of concrete, part or all of the normal-weight aggregate can be replaced with lightweight aggregates that have a lower unit weight. While pumice is the most commonly used aggregate in lightweight concrete production, other natural lightweight aggregates such as slag and diatomite are also used. The main purpose of using lightweight aggregates in lightweight concrete is to obtain materials with high thermal insulation properties and low unit weight.

The production of materials similar to lightweight concrete, using lightweight aggregate with lime or pozzolanic binders, dates back to before 3000 B.C. However, after cement became widely used as a binding material, lightweight concrete has gained significant importance in many applications, especially in the last seventy years, with numerous classifications made based on compressive strength. This is due to the use of lightweight aggregates with varying strength levels in lightweight concrete production. Additionally, lightweight concrete can be classified into three groups based on production methods. These methods are;

1. Using porous lightweight aggregate instead of normal-weight aggregate: These types of lightweight concrete are named according to the type of lightweight aggregate used. Examples include load-bearing concretes like expanded clay and shale, as well as insulation or medium-strength concretes like perlite concrete and pumice concrete.

2. Creating large voids in the concrete through physical or chemical methods: One of the most common methods to achieve this is by using air-entraining admixtures. These types of concretes are known as aerated concrete, foamed concrete, or air-entrained concrete..

3. Creating large voids in the concrete by removing fine aggregates: These types of concretes are typically referred to as no-fines concrete. The coarse aggregates are bonded together with a cement paste that is 1-3 mm thick, with a cement dosage ranging from approximately 70 kg/m³ to 130 kg/m³.

It is also noted that due to the lower mechanical properties of lightweight concrete compared to normal concrete, lightweight concrete production can be classified in two ways:

a) Lightweight concretes produced with natural and/or lightweight aggregates:

- Perlite concrete
- Concrete made with blast furnace slag
- Vermiculite concrete
- Expanded clay and shale concrete
- Tuff, fly ash, and pumice (or scoria) concrete
- Concrete made with wood shavings or wood chips

b) Lightweight concretes produced with chemical admixtures:

- Concrete produced by adding air-entraining agents to fresh concrete
- Concrete produced by adding aluminum powder along with cement to fresh concrete
- Concrete produced by adding hydrogen peroxide and bleaching powder to fresh concrete

Lightweight concretes have been produced using various methods from past to present. As explained above, these methods include the use of lightweight aggregates, chemical foaming, using only coarse aggregates without sand, and generating gas through chemical reactions. The main principle in using chemical foam is the expansion of the binding paste to create gas bubbles.

1.1.1. Air void formation methods in lightweight concrete production

The amount of air in the concrete (Fig. 1) can vary depending on several factors. These factors include the materials used in the concrete (such as the amount of

cement, fly ash, and slag as supplementary binders), their chemical composition and fineness, chemical admixtures (such as plasticizers, retarders, etc.), the quantities of aggregates, their particle size and gradation, the chemicals in the mixing water, the water-cement ratio, the water content and consistency, production methods (such as the order of material addition), mixer capacity, mixing time and speed, as well as construction methods and site conditions.

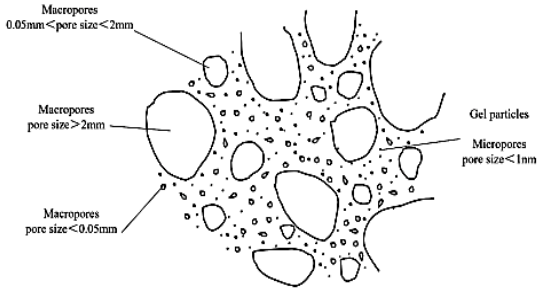

Figure 1. Air gaps trapped in concrete

There are various methods for pore formation in lightweight concrete. The most accepted methods include foam generation, air-entraining, and interconnected pore formation.

The foam generation method is done by mixing whipped foam material into a cement or lime mortar. Commonly used foam materials include adhesive resin foam (pine resin and glue solution), refined resin foam (plant-based soap content, saponin), aluminosulfate foam (paraffin sulfonic acid), hydrolyzed blood foam (a mixture of blood and iron sulfate), hydrolyzed keratin foam (processed waste materials like hair, feathers, horns), and detergents. This method is economical and allows controlled pore formation without chemical reactions, as the foam materials are mechanically mixed into the mortar.

The air-entraining method is a chemical process where chemicals are added to semi-hardened cement or lime mortar to directly increase volume and pore formation. The most well-known chemicals used are powdered aluminum, air-entraining hydrogen peroxide, bleaching agents, and calcium carbide. These chemicals react within the mixture to produce oxygen, hydrogen, or acetylene gas, which gives the concrete its porous structure. Aluminum powder is the most commonly used air-entraining agent.

The interconnected pore formation method combines both foam generation and air-entrainment techniques. The first of these methods involves adding air-entraining chemical agents to the mixture or mixing whipped foam into semi-hardened mortar. The other method involves adding excess water, which leads to void formation as the water evaporates. The following air-entraining additives can be used in the production of lightweight concrete:

1. Tree resin salts (from pine logs)
2. Synthetic detergents (from petroleum fractions)
3. Lignosulfonates (from the paper industry)
4. Petroleum acid salts (from petroleum refining)
5. Protein salts (from animal hides)
6. Oily and resinous acids and salts (from the paper industry and animal hides)
7. Organic salts of sulfonated hydrocarbons (from petroleum refining)

Most of the air-entraining materials used come from the first group, particularly the substance derived from pine logs, known commercially as Vinsol Resin. Additionally, synthetic detergents belonging to the aryl-alkyl-sulfonate group are also widely used in large quantities.

The methods mentioned above are used to create air voids in concrete, and the lightweight concretes produced using these methods are classified as "Gas Concrete" and "Foam Concrete." In these processes, gas concrete is produced by expanding the mixture during production with the help of additives. This type of concrete is commonly used in the building materials industry, and products from companies like Ytong and Çimtaş are examples of this material. Foam concrete, on the other hand, is produced by foaming the fresh mixture through various additives and processes. The difference between gas concrete and foam concrete has been briefly explained by Just and Middendorf (2009) and Liu et al. (2023) in Figure 2.

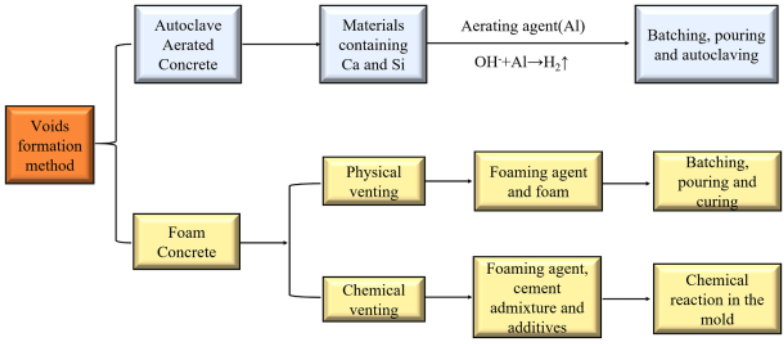

Figure Error! No text of specified style in document. The classification of aerated concrete

In the production of gas concrete or foam concrete, expansion-inducing additives are incorporated into the mixture using two methods. The first method involves mixing the additive into a mortar made of cement and water. The second method involves preparing a mortar with sand, cement, water, and any available mineral additives, and then, after achieving the desired consistency, adding expansion agents

like aluminum powder or hydrogen peroxide to the mixture. The second method is generally preferred in gas concrete production.

1.1.2. Classification of lightweight concrete

The classification of lightweight concrete is generally based on unit weight and compressive strength (Fig. 3). However, its classification varies according to the standards of different countries.

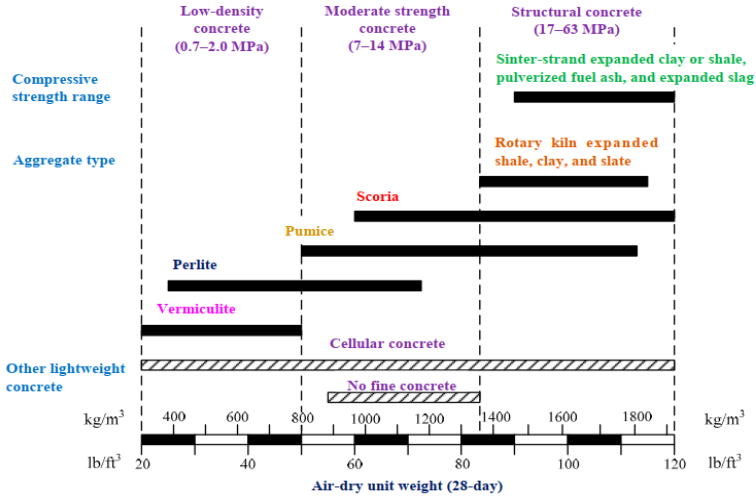

Figure 3 Unit weight and classification of lightweight concrete

a. Structural Lightweight Concrete: According to the ASTM (C330-77) standard, structural lightweight concrete is classified as having a 28-day compressive strength of no less than 17 MPa and a unit weight ranging between 1350–1900 kg/m³. The primary purpose of structural lightweight concrete is to reduce the dead load caused by the self-weight of concrete in reinforced concrete structures. Reducing the dead load of a structure decreases the effects of both static and dynamic loads, enabling smaller cross-sections for load-bearing elements and enhancing the cost-efficiency of the structure.

b. Semi-Structural Lightweight Concrete: As per the ASTM (C330-77) standard, semi-structural lightweight concrete has a 28-day compressive strength between 7–17 MPa. This type of concrete is categorized between structural and insulating lightweight concretes in terms of thermal insulation properties. Semi-structural lightweight concrete is commonly used in constructing structural elements like walls and roof panels, where distributed load transfer is more relevant than concentrated loads. Using semi-structural lightweight concrete in such elements provides thermal insulation and time savings alongside load transfer efficiency.

c. Insulating Lightweight Concrete: Non-structural lightweight concrete, with a unit weight ranging from 300–800 kg/m³, is designed primarily for high thermal insulation. According to the ASTM (C330-77) standard, this type of concrete must have a minimum 28-day compressive strength of 2.5 MPa. Insulating lightweight concretes are typically used in manufacturing non-load-bearing wall infill elements.

Changes in the dry unit weight of lightweight concrete directly impact its mechanical and thermal properties. While lower weight enhances thermal insulation, higher weight reduces it.

Lightweight concretes can also be classified into two groups based on their binding agents:

1. Foamed or aerated concretes made with cement.
2. Foamed or aerated silicates made with lime.

The classification of lightweight concretes also varies depending on national standards. These differences are outlined in Table 1 according to TS, ASTM, and DIN standards.

Table 1. Lightweight concrete classes according to different standards

Standards	Unit Weight (kg/m^3)	Strength (MPa)
TS 2511	≤ 1900	≥ 16
ASTM C330	≤ 1840	≥ 17
DIN 1045	≤ 2000	≥ 16
ACI 213R	≤ 1840	≥ 17
CEB -FIB	≤ 1900	≥ 16

Table 2. Lightweight concrete classes according to TS 206-1

Compressive strength class	Minimum characteristic cylinder strength, fck (N/mm^2)	Minimum characteristic cube strength, fck (N/mm^2)
LC 8/9	8	9
LC 12/13	12	13
LC 16/18	16	18
LC 20/22	20	22
LC 25/28	25	28
LC 30/33	30	33
LC 40/44	40	44
LC 45/50	45	50
LC 50/55	50	55
LC 55/60	55	60
LC 60/66	60	66
LC 70/77	70	77
LC 80/88	80	88

Lightweight concretes are concretes with a unit volume weight not exceeding 1840 kg/m^3 and a 28-day cylinder compressive strength exceeding 17 MPa. Although the unit volume weight of lightweight concrete can be up to 1900 kg/m^3 in standard values that vary by country, in practice the range of change is between 300–1840 kg/m^3.

The classification of lightweight concretes is made according to the compressive strength as well as the unit volume weight. The classification of lightweight concretes regarding the compressive strength is given in Table 2 according to TS EN 206-1.

2. Autoclaved Aerated concrete (AAC)

Autoclaved aerated concrete, also known as AAC or gas concrete, is a lightweight material compared to traditional concrete or masonry. It is highly insulating due to the air bubbles within its structure, which give it excellent thermal properties. Classified as a type of lightweight concrete, it is named "gas concrete" because of these air voids.

AAC is produced by mixing fine silica aggregate and an inorganic binder (lime or cement) with a pore-forming agent, which lightens the mixture. The material is then hardened using steam curing, resulting in a porous lightweight concrete. In the literature, AAC is recognized as a lightweight construction material that belongs to the lightweight concrete category. It is composed of varying proportions of silicon, sand, cement, lime, and aluminum. Al-Kahaled (2002) defined AAC as a lightweight building material achieved by combining different elements to complete structural systems.

According to TS 453, AAC is described as porous lightweight concrete obtained by adding a pore-forming admixture to a mix prepared with finely ground silica aggregate and an inorganic binder (lime and/or cement), followed by steam curing (Figure 6).

Due to the air bubbles in its structure, this material is named “Autoclaved Aerated Concrete - AAC” in English, “Porenbeton” in German, and referred to as “Otoklavlı Gaz Beton” in Turkish. Commonly abbreviated as "gaz beton" in Turkish, it is a lightweight concrete construction material used in the form of blocks or larger panels and slabs.

In the industrial production of AAC, silica-rich materials such as sand, quartzite, or fly ash are typically used as the siliceous aggregate. Aluminum powder or paste serves as the pore-forming agent. Compared to traditional concrete or masonry, AAC is significantly lighter. The air bubbles in its structure grant it excellent thermal insulation properties, as well as resistance to earthquakes and fire, making it a widely used material in the construction industry.

Despite its original name "gas concrete," minor variations in its composition have led to alternative names such as foamed concrete, cellular concrete, aerated concrete, and autoclaved cellular concrete.

AAC is a lightweight construction material developed in Sweden, capable of being manufactured using locally available materials. It exhibits excellent thermal properties and is commonly used for roofing or flooring components, as well as wall elements. Additionally, AAC offers several advantages over other building materials due to its unique properties, including:

- High Thermal Insulation: AAC provides excellent thermal insulation (Figure 4), making it a practical and economical material for wall construction.
- Advanced Manufacturing Standards: AAC available in the market is produced in modern facilities using advanced technology.
- Environmentally Friendly: It is an eco-friendly material that supports sustainable construction practices.
- High Fire Safety Performance: AAC offers superior fire resistance, ensuring enhanced safety.
- Lightweight Property: Its lightweight nature helps reduce the impacts of earthquakes by minimizing the structural load.
- Ease of Workability: AAC can be easily processed to desired dimensions or reshaped as needed, enhancing its versatility.
- Time and Cost Efficiency**:** Its easy application reduces labor costs and saves time during construction.

These features make AAC a highly advantageous and efficient material for modern construction projects.

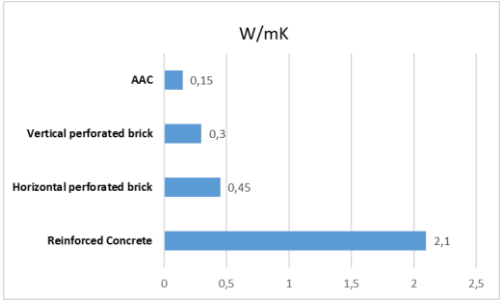

Figure 4. Thermal insulation coefficients of some building materials**.**

One of the primary components of AAC is quartzite, a rock formed by the strong binding of quartz sand grains with natural silica-based cement. Quartzite exists in two main types: sedimentary and metamorphic. It is characterized by its high

strength, durability, and abrasiveness. However, it is also challenging and costly to grind.

For this reason, quartzite production is typically considered after quartz sand and sandstone, which share the same chemical composition but are purer and easier to process. The chemical composition of quartzite, like quartz, sandstone, and quartz sand, is predominantly SiO_2. However, it may contain small amounts of feldspar, mica, clay, magnetite, hematite, garnet, rutile, limestone, and other minerals.

In AAC production, the quartzite used must meet specific quality standards:

- SiO_2 content should be at least 90%.
- Fe (iron) content should not exceed 2%.

The strict requirements for quartzite in AAC production ensure the material's optimal performance, contributing to its strength, thermal insulation properties, and overall quality.

2.1. History of AAC

Throughout the 12000 years of human history, structures like the Egyptian pyramids and Mayan temples were built using natural and traditional materials. Compared to these ancient feats, the use of autoclaved aerated concrete (AAC) as a construction material emerged much later. The idea of artificially producing lightweight and porous materials for construction dates back to the late 10th century.

The development of porous materials began after the invention of cement and concrete. The first patent for producing porous mortar by adding a gas-generating additive was issued in 1889. However, the use of these materials for lightweight concrete only gained traction in 1914 when American inventors Aylsworth and Dyer patented the addition of aluminum powder, zinc powder, or other metallic powders mixed with calcium hydroxide to cement-based mortar as a foaming agent. Later, in 1929, Americans Adolf and Pohl patented the use of hydrogen peroxide and sodium or calcium hypochlorite as alternative agents to achieve similar reactions.

The discovery of AAC as a type of lightweight concrete began in 1919–1920 with the addition of aluminum powder to concrete mortar. This process demonstrated the positive effects of steam curing under pressure (autoclaving) on the hardening of concrete.

In 1923, Swedish architecture professor Johan Axel Eriksson inadvertently discovered AAC while working on porous concrete samples. He placed samples in an autoclave to accelerate the curing process. The resulting material, characterized by hydrogen bubbles formed during chemical reactions, became known in the literature as gas concrete. The invention was named after the small Swedish town where Eriksson developed the material. Combining “Yxhult” (the town’s name) and the Swedish word for concrete, “Betong,” the commercial trademark YTONG was

patented in 1924. After further refinement between 1924–1929, AAC gained popularity in the market and became widely recognized.

The material's success expanded globally, particularly in Europe, the Americas, and Asia. Companies like Ytong, Hebel, and H+H Celcon played significant roles in developing the market. These brands remain prominent players in the European AAC market today.

In the global market, AAC has found extensive use in the construction industry due to its superior properties, such as thermal insulation and a unit density that is one-fifth that of conventional concrete. As a result, its adoption has steadily increased, supported by various manufacturers operating under different brand names. Notable examples include Durox in the Netherlands, Siporex in Sweden, and Termalite in the United Kingdom.

In Türkiye, AAC was first introduced in the 1950s through imports from Germany. The first AAC production facility in Türkiye was established in 1965 in Istanbul. Since then, over the past 75 years, the use of AAC in the construction industry has grown significantly. Today, Türkiye is among the leading countries in terms of both production capacity and potential usage of AAC.

With its wide acceptance, AAC is now manufactured in several provinces across Türkiye (Fig. 5), contributing to the country's construction sector with its energy-efficient and lightweight building solutions.

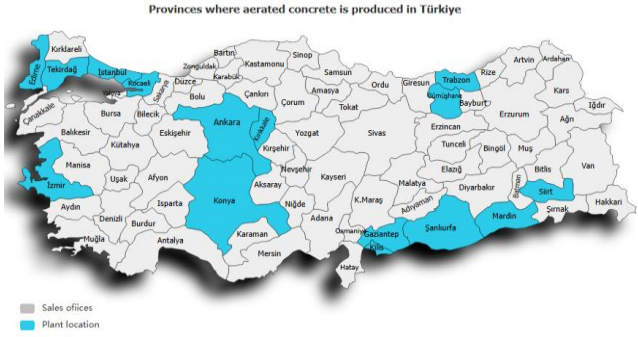

Figure 5 Türkiye's provinces where AAC is produced

Türkiye’s annual consumption of approximately 4.3 million m^3 ranks fourth in Europe as a result of its high usage potential. Today, AAC is produced under various names in many countries around the world, with an annual production of approximately 16 million m^3.

2.2. Types of autoclaved aerated concrete (AAC)

The types of AAC are classified into two categories, based on their chemical and mechanical processes. In the chemical process, expansion occurs through the

reaction of metallic powders, while the mechanical process relies on the creation of gaps between the particles by foam materials that enable the expansion. However, the classification of aerated concrete is made according to the treatment it undergoes during the curing process, and three different types are produced. These include:

- AAC cured under pressure steam
- AAC cured under high heat and steam
- AAC cured in open air

2.3. AAC raw material and production process

AAC is a porous building material with quartzite as its raw material and cement and lime as its binders. These materials are finely ground to a powder-like consistency in a ball mill and, in the final stage, mixed with water and aluminum powder before being transferred to casting molds. Experimental studies by Lidman in 1931 and Shalbergs in 1937 demonstrated that materials such as fly ash, a siliceous material, could replace quartzite. They patented this process, showing the potential for using alternative materials.

A common aspect of these studies is the reaction between burnt lime and water, releasing high heat that reacts with aluminum powder to generate hydrogen gas. This gas, produced by the fine aluminum particles, causes the aerated concrete mix to expand, giving it its primary characteristic: a micro-porous structure.

The production process as preparing a flowable mixture by blending ground lime, ground quartzite, and cement with water. Once the mixture reaches the required temperature and viscosity, a pore-forming slurry is added. In AAC production, sand, lime, cement, gypsum, water, and an expansion agent are used to create a porous structure in the concrete. Aluminum powder, constituting 0.05%-0.08% of the total solid volume, is used as the expansion agent.

The production begins by measuring and mixing precise amounts of these materials. Pouring this mixture into molds initiates multiple chemical reactions. The importance of these reactions lies in aluminum powder reacting with calcium hydroxide and water, leading to hydrogen gas release. This gas forms bubbles within the slurry, increasing its volume. The result is an expanded and porous concrete structure (Fig. 6).

The production process of AAC is similar to the manufacturing of clay-based wall products or prestressed concrete, while the structural components of the materials used in AAC resemble those of conventional concrete. Interestingly, the AAC production process can be likened to bread-making and can be summarized in five main steps (as illustrated in Fig. 7):

a) Combination and mixing of raw materials
b) Addition of expansion agent

c) Rising, shaping, pre-curing, and cutting
d) Final curing in autoclave.
e) Packaging and transportation

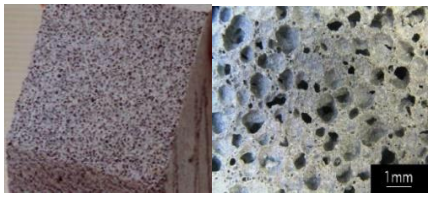

Figure 6. Porous structure of AAC

a) Combination and mixing of raw materials

Autoclaved aerated concrete (AAC) production begins with raw materials including silica, cement, lime, and water. The silica used as aggregate can be derived from finely ground quartz sand or fine sand, which may replace quartz sand. Additionally, materials such as fly ash, slag, or mining waste can be used alongside silica as aggregates.

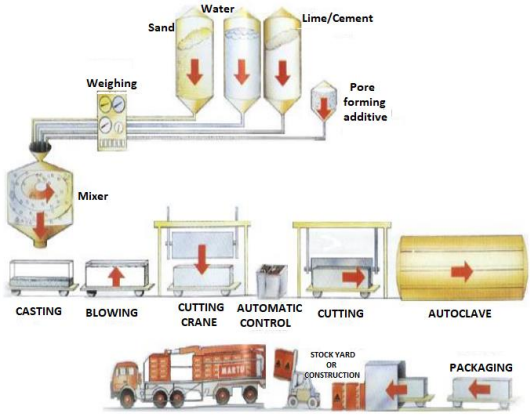

Figure 7 Schematic production process of AAC

These materials are mixed as fine aggregates, and their particle size gradation is critical. Coarse or poorly graded materials hinder the effectiveness of the expansion agent used in the second step of the production process. Cement usage follows the same principles as in conventional concrete production, serving as the binding element that holds aggregates and additives together.

Through the hydration reaction between cement and water, the mixture solidifies into a hardened material. In AAC production, all these materials are mixed with water to form the initial slurry.

b) Addition of expansion agent

In the autoclaved aerated concrete (AAC) production process, the expansion agent is added to the concrete mixture to increase its volume, much like yeast is added to dough in bread-making to make it rise. The purpose of this addition is to create numerous small hydrogen bubbles in the mixture, similar to the carbon dioxide produced by yeast in dough. This is achieved by the reaction of aluminum powder or paste, used as the expansion agent, with lime and water in the mixture.

Additionally, other chemical additives such as metallic powders (e.g., aluminum or zinc), liquid hydrogen peroxide (H_2O_2), or mechanical foaming agents (foam-forming substances) can also be used to induce expansion.

The pore formation mechanism in AAC due to chemical reactions involving aluminum additives can be summarized as follows:

- The aluminum reacts with water and calcium hydroxide, releasing hydrogen gas.
- This hydrogen gas creates microscopic bubbles within the mixture, leading to the desired porous structure.

In the AAC production process, expansion occurs through the addition of an expansion agent to the concrete mixture, similar to how yeast is added to dough in bread-making to make it rise. The goal is to produce numerous small hydrogen bubbles in the mixture, analogous to the carbon dioxide generated by yeast in dough. This is achieved by the reaction of aluminum powder or paste, used as the expansion agent, with lime and water in the mixture.

Additionally, other chemical additives, such as metallic powders (e.g., aluminum or zinc), liquid hydrogen peroxide (H_2O_2), or mechanical foaming agents, can be used to facilitate expansion.

The mechanism of pore formation in AAC resulting from the chemical reactions involving aluminum additives can be summarized as follows:

$$CaO + H_2O \rightarrow Ca(OH)_2 + 278\ Kcal/kg$$

$$2\ Al + 3\ Ca(OH)_2 + 6\ H_2O \rightarrow 3\ CaO\ .\ AI_2O_3 + 3H_2 + 3676\ Kcal/kg$$

(Aluminum Powder + Lime + Water → Tricalcium Hydrate + Hydrogen)

The hydrogens formed as a result of this process move out of the mixture (Fig. 8a) and are replaced by air. This process occurs when hydrogen, a lighter gas, rises and replaces air, which is denser. Additives such as aluminum powder should be added to the mixture as a swelling agent and mixed thoroughly, ensuring equal distribution throughout. The aim here is to ensure that the material expands approximately 2-5 times its normal volume as a result of the formation of hydrogen bubbles (Fig 8b),

providing an equal volume increase throughout the material. This volume increase depends on the lime added to the mixture as well as the aluminum powder or paste.

The mechanism of void formation is similar to that of aluminum additive for hydrogen peroxide additive. However, the formation of pores in concrete occurs as a result of a binary reaction due to the weak oxygen bonds in the chemical structure of hydrogen peroxide, and these reactions are given below.

$$Ca(OH)_2 + H_2O_2 \rightarrow CaO_2 + 2H_2O$$

(Hydrated Lime + Hydrogen Peroxide → Calcium Peroxide + Water)

$$CaO_2 + 2H_2O \rightarrow 2\ Ca(OH)_2 + O_2$$

(Calcium Peroxide + Water → Slaked Lime + Oxygen)

Both additives provide less swelling and a higher density material, while more swelling provides a lower density material. Although the lower density is due to the presence of more microscopic air bubbles, this provides higher heat resistance properties in the material.

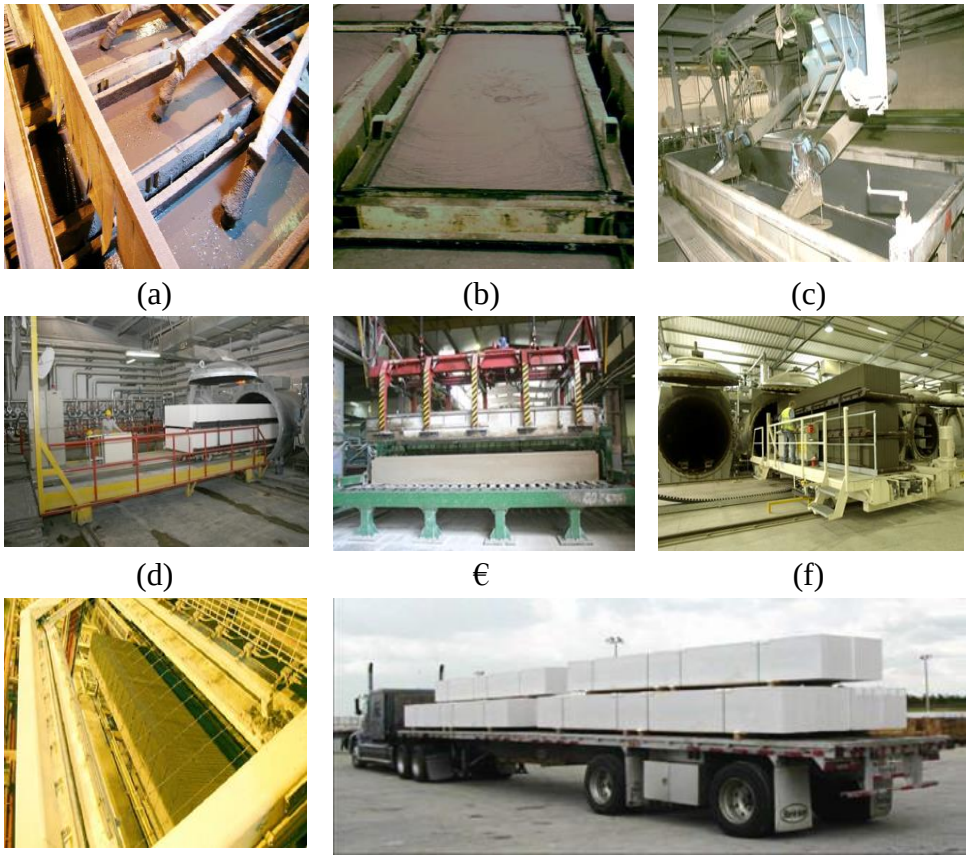

(a) (b) (c)

(d) € (f)

(g) (h)

Figure 8. AAC production process

c) Rising, shaping, pre-curing, and cutting

The hydrogen bubbles formed by the reaction of aluminum powder added to the slurry mixture cause the material to expand to at least twice its original volume. This process occurs within a period of 30 minutes to 4 hours, during which the mixture begins to solidify.

After mixing, the slurry is poured into molds placed on casting carts, filling only 2/3 of their capacity (Fig. 8c), and left to expand. A few hours later, as the chemical reactions progress, hydrogen bubbles form, causing the mixture to rise. The partially solidified AAC block is then transferred to a cutting machine (Fig. 8d). In the final step, the cut blocks are subjected to a steam curing process for approximately 10 hours. Once these steps are completed, the AAC production process is finalized, and the blocks are packaged.

After the expansion agent is mixed into the slurry, the mixture is poured into metal molds designed to allow the material to rise. If the AAC is to be cast as panels or slabs, steel reinforcements are placed in the mold before the mixture is poured. The mixture is typically poured into molds measuring 20 feet (6.10 m) x 4 feet (1.22 m) x 2 feet (0.61 m) and left for a few hours to undergo initial expansion. This pre-curing phase ensures that the material retains its shape once removed from the mold. The cured blocks can then be cut into desired shapes using a device with fine wires (Fig. 8e). Standard AAC block sizes include 8 inches (20 cm) in width, 24 inches (61 cm) in length, and thicknesses ranging from 4 to 12 inches (10-30 cm). Larger blocks can be cut into solid brick-like units, similar to concrete masonry units. However, unlike concrete masonry units, AAC materials can be cut into larger sizes due to their lighter weight.

d) Final curing in autoclave

The autoclave can be defined as a robust, pressurized, hot steam chamber (Figure 8f). During the curing process of autoclaved aerated concrete (AAC), the autoclave operates similarly to a pressure cooker. At this stage, the blocks are cured with high-pressure steam, allowing the chemical reaction between cement and water—hydration—to occur rapidly, resulting in a significant gain in strength.

This process enables the quartz sand to react with calcium hydroxide, continually forming calcium silicate hydrate, the compound responsible for the material's physical strength properties. The high-pressure steam curing in autoclaves is the key to AAC's combination of low density and high compressive strength.

After cutting, the casting carts are transferred to the autoclaves, where the material is cured under saturated steam conditions at 12 atm pressure and 190°C for 10-12 hours. By the end of this process, the material achieves its final strength and dimensional stability.

Witmann (1992) and Holt and Reivo (2005) describe the reactions that occur in the autoclave as follows:

$$Ca(OH_2) + SiO_2 + x\,H_2O \rightarrow CaO.SiO_2.xH_2O$$

Lime + Silica + Water → Monocalcium Silacate Hydrate

The purpose of steam curing AAC is to reach the hardness that normal concrete can reach by subjecting it to water curing at 21°C for 28 days, in a time varying between 8-14 hours through autoclaving. The hardening process begins as a result of the calcium hydrosilicate and aluminum hydrosilicate formed in the material. When a certain level of strength is reached, it is cut to the desired dimensions (Figure 8g) by means of special steel wires in an automatic cutting machine.

e) Packaging and transportation

The aerated concrete, which has been cured for approximately 12 hours, is removed from the autoclave and shipped to the market through a packaging and transportation process (Fig. 8h). However, there must also be a process for the material coming out of the autoclave to cool down. The idea that the time until packaging is sufficient for cooling or that a cooling phase should be experienced before packaging varies from manufacturer to manufacturer.

2.4. Properties of AAC

Under this heading, the physical, chemical and mechanical properties of aerated concrete will be discussed.

2.4.1.Physical characteristics

Regarding the physical properties of AAC material, material color and internal structure, specific gravity, porosity, thermal conductivity, thermal expansion, melting point, shrinkage, equilibrium humidity, water absorption and drying, vapor permeability, frost resistance, fire resistance, sound insulation and sound absorption properties (Table 3) are explained below.

Material Internal Structure, Color, and Surface Texture: The structure of the autoclaved aerated concrete (AAC) material is characterized by circular macro-pores ranging between 0.5-1.5 mm in diameter. These macro-pores are surrounded by micro-pores. Depending on the type of siliceous raw material used, AAC can be white, gray, or pink in color. Since quartzite is commonly used, it is typically white. The surface texture can be smooth or striped-rough, depending on the properties of the steel wires used in the cutting machines.

Specific Gravity: The average specific gravity of the AAC material without voids is 2.60 kg/dm³.

Porosity: The porosity of AAC varies inversely with its dry unit weight.

Table 3. Some properties of AAC

Unit Weight t/m^3	Porosity %	Thermal Conductivity W/m°K	Modulus of Elasticity Kg/cm^2	Shear Stress Kg/cm^2
0.31-0.40	85-88	0.08-0.09	3 800	0.8
0.41-0.50	81-85	0.12	7 500	0.8
0.51-0.60	77-81	0.14	12 500	0.8-1.2
0.61-0.70	71-77	0.18	20 000	0.8-1.2
0.71-0.80	69-73	0.19	42000	1.2

Thermal Conductivity: Due to the micro and macro pores that constitute 80% of gas concrete, its thermal conductivity value is low.

Thermal Expansion: The thermal expansion coefficient of AAC is 0.008 mm/m°C in the temperature range of 20-100°C.

Specific Heat: The specific heat capacity is 0.24-0.26 Kcal/kg°C when the material contains 2-5% equilibrium moisture by weight.

Melting Point: AAC begins to sinter (vitrify) around 1000°C and starts melting at approximately 1100-1200°C.

Shrinkage: AAC undergoes volume reduction as the moisture content decreases and gains volume as the moisture content increases.

Equilibrium Moisture: Building materials release the moisture absorbed during production, transportation, and construction over time, reaching a stable moisture level called equilibrium moisture. This level varies slightly based on the dry unit weight of AAC and the relative humidity of the environment.

Water Absorption and Drying: The primary reason for the water absorption of artificial stone materials is the capillary structure formed as excess production water is expelled from the material. During production, only a small portion of the water added to the mixture remains chemically bonded, while the rest is expelled through evaporation. Approximately 50% of the added water is expelled in gas concrete.

The rate at which water is expelled is significant; faster drying leads to a more developed capillary structure. In AAC production, the amount of expelled water is minimal because there is no drying or firing process. Instead, chemical curing occurs in high-pressure steam, resulting in a weak capillary structure that limits water movement through the pores.

The amount of moisture contained in a building material that is saturated with water determines the water capacity of that material. As the water capacity in building materials approaches the total amount of voids, the material becomes sensitive to freezing and loses its thermal insulation properties due to the effect of moisture. It is stated that approximately 60% of the voids in AAC material remain dry even when saturated with water.

Vapor Permeability: Due to its porous structure, AAC has a low vapor permeability resistance (μ = 5-7), which represents the ratio of the resistance to vapor transfer of the material per unit thickness to that of an air layer of the same thickness. This property allows the material to "breathe" easily in construction. However, in frost-prone regions, if AAC walls are left unprotected, this characteristic can significantly damage the material's structure.

Frost Resistance: In standard concrete, water typically resides in the gel and capillary pores within the cement paste, as well as in and between the aggregates. When water in the aggregates freezes, its volume increases by approximately 9%. If there are no voids to accommodate this expansion, the concrete reaches a critical saturation point, leading to high stresses caused by hydraulic pressure. This can result in cracking, loss of strength, and even spalling of the concrete surface.

Under normal conditions, the maximum moisture content of water-saturated AAC is approximately 30-35% by volume. Considering that the total void volume of AAC is 70-85% by volume, there is sufficient dry space within the material to accommodate the expansion of ice crystals. This provides the material with excellent frost resistance.

However, in cases of sudden frost following heavy rainfall, critical moisture levels may be exceeded in sharp edges, corners, and profiles, leading to frost damage in these areas. Protecting the material with a surface coating during winter months is an effective solution to this issue.

Fire Resistance: AAC is considered non-combustible and provides the highest hourly fire resistance (Fig. 9) per centimeter thickness among all construction materials. It is ideal for fireproofing steel columns and beams, making it an excellent choice for use in fire protection systems.

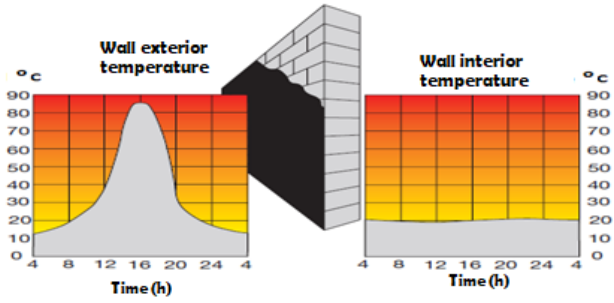

Figure 9. Temperature change of AAC with time

Sound Insulation: Due to the highly porous structure of AAC materials and the ability of sound energy to easily convert into heat energy within these pores, the average sound insulation values of AAC materials are approximately 2 dB higher

than those of some other construction materials when compared on a per-unit weight basis.

Sound Absorption: When sound energy strikes the surface of a material, a portion is absorbed depending on the type of material and surface texture, while the remainder is reflected (Fig. 10). The sound absorption coefficient, defined as the ratio of absorbed sound energy to incident sound energy, increases as it approaches 1, indicating better sound absorption. When the coefficient reaches 1, all incoming sound energy is absorbed.

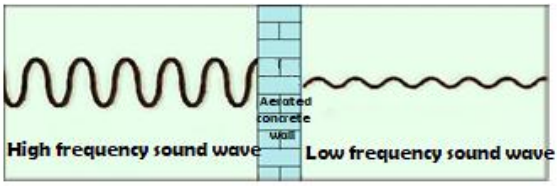

Figure 10. Schematic view of the sound absorption property of AAC

AAC, with its porous surface and high porosity, is a good material for sound absorption. Within the frequency range of 125-4000 Hz, AAC exhibits a sound absorption coefficient ranging from 0.10 to 0.27.

2.4.2. Chemical properties

In terms of its chemical properties, it is possible to examine AAC under two headings: its resistance to chemical factors and its dissolution in water.

Resistance to Chemical Agents: AAC has an alkaline structure composed of silica hydrates, with a pH value ranging from 9.5 to 11.0. This makes it susceptible to acidic environments. Sulfuric acid, hydrochloric acid, and acetic acid can damage the material's structure, while chlorides, sulfates, and nitrates can harm the reinforcement. For this reason, AAC should be protected from seawater. In environments with intense and continuous exposure to chemically aggressive substances, AAC must be safeguarded with surface coatings resistant to these chemicals.

Solubility in Water: The hydro-silicates that provide strength to AAC are insoluble in water. However, if other components used in production (such as sand, lime, cement, or water) contain water-soluble salts, these salts can crystallize on the material's surface under specific environmental conditions, leading to efflorescence. Efflorescence is primarily influenced not by the amount of soluble salts but by the rate of capillary water movement within the AAC and the drying speed on the surface.

2.4.3. Mechanical properties

The mechanical properties of concrete, such as compressive strength, tensile strength, shear strength, and modulus of elasticity, are also applicable to gas concrete. Additionally, AAC possesses unique mechanical characteristics, as described below:

Compressive Strength: The compressive strength of AAC depends on its dry unit weight and moisture content. According to TS 453, the compressive strength of AAC materials is determined using the cube test. In this test, 15x15x15 cm cubes are dried until they reach 10% moisture by weight, after which they are tested for failure under compression. AAC loses strength as its moisture content increases, with a strength reduction of up to 35% observed between fully dry and water-saturated states.

Tensile Strength: The tensile strength of AAC is approximately 1/6 of its compressive strength, ranging from 2 to 12 kg/cm².

Modulus of Elasticity: The modulus of elasticity of AAC varies depending on its dry unit weight and cube strength.

Flexural-Tensile Strength: The flexural-tensile strength of AAC is about 1/5 of its compressive strength, ranging from 3 to 15 kg/cm².

Shear Strength: The maximum allowable shear stress in AAC is 1.2 kg/cm².

Creep: AAC exhibits creep under continuous loading. Studies have shown that the creep of AAC within permissible load limits is less than that of dense concrete. This is because AAC completes its chemical bonding during autoclaving. In contrast, dense concrete undergoes crystal changes under load and continues to experience chemical changes over a long period.

2.5. Areas of use of AAC

The use of AAC, which has been used in Europe for years and has increased in our country in recent years, is widespread in the construction sector. The AAC produced is used in the form of building elements (mortared and glued wall blocks, heat blocks, hollow blocks, insulation plates, door and window lintels, partition elements, ready-made walls, carrier roof and floor elements).

2.6. Classification of AAC components and elements

AAC building elements are categorized into five classes based on the presence of reinforcement, compressive strength, specific gravity, the binder used for bonding, and the type of blocks.

This classification is as follows:

a) Based on the presence of reinforcement:

- Non-reinforced AAC (Building material)
- Reinforced AAC (Building element)

b) Based on compressive strength (Table 4):

- G1: 1.5 N/mm²
- G2: 2.5 N/mm²
- G3: 3.5 N/mm²
- G4: 5.0 N/mm²
- G5: 7.5 N/mm²

c) Based on specific gravity:

- Group 0.4 kg/dm³
- Group 0.5 kg/dm³
- Group 0.6 kg/dm³
- Group 0.7 kg/dm³
- Group 0.8 kg/dm³

d) Based on the binder used for bonding:

- Bonded with adhesive (T)
- Bonded with mortar (H)

e) Based on the type of blocks:

- Plain blocks
- Interlocking blocks
- Tongue-and-groove blocks

In addition to this classification, special purpose hollow blocks, insulation plates, door and window lintels, floor plates, roof panels and vertical and horizontal wall elements (Fig. 11) are also produced.

AAC materials are also classified as non-reinforced building materials and reinforced building elements. These are:

a) Non-reinforced building materials:

- Wall blocks
- Plain blocks
- Interlocking blocks
- U-blocks
- Hollow core blocks
- Insulation blocks

b) Reinforced building elements:

- Load-bearing elements:
  - Floor slabs
  - Roof slabs
  - Vertical wall elements
  - Lintels
- Non-load-bearing elements:

- Horizontal wall elements
- Vertical wall elements
- Partition wall elements

Table 4. Characteristic properties of AAC according to their compressive strength

Class	Average Minimum Compressive Strength Kgf/cm^2 (N/mm^2)	Minimum Compressive Strength Kgf/cm^2 (N/mm^2)	Unit weight (kg/dm^3)	Average Unit Weight (kg/dm^3)	Class Sign	
G1	15 (1.5)	10 (1.0)	0.4	0.31 - 0.40	G	1/0.4
			0.5	0.41 - 0.50	G	1/0.5
G2	25 (2.5)	20 (2.0)	0.4	0.31 - 0.40	G	2/0.4
			0.5	0.41 - 0.50	G	2/0.5
G3	35 (3.5)	30 (3.0)	0.5	0.41 - 0.50	G	3/0.5
			0.6	0.51 - 0.60	G	3/0.6
G4	50 (5.0)	40 (4.0)	0.6	0.51 - 0.60	G	4/0.6
			0.7	0.61 - 0.70	G	4/0.7
G5	75 (6.0)	50 (5.0)	0.7	0.61 - 0.70	G	6/0.7
			0.8	0.71 - 0.80	G	6/0.8

a. Non-reinforced building materials

These materials can be divided into four groups: wall blocks, hollow blocks, U-blocks and insulation plates.

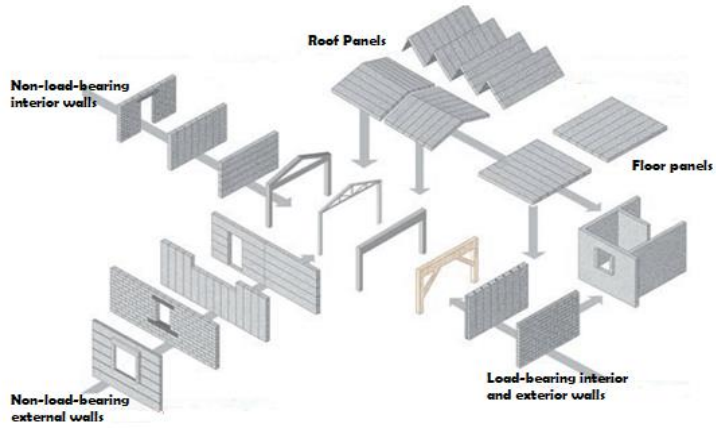

Figure 11. AAC building elements

Wall blocks: They are used in lightweight masonry structures with a thin plaster in the construction of masonry walls and in the construction of infill walls in reinforced concrete structures (Fig. 12). There are two different production types in the production of wall blocks: plain block and interlocking block.

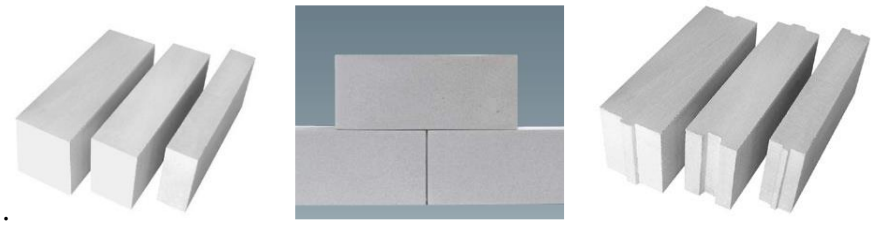

Figure 12. Plain wall block and interlocking wall blocks

Hollow block: AAC hollow block are building materials produced in sizes 40x30 cm, 40x60 cm from 20 cm to 60 cm thick. Hollow block (Fig. 13) is used as hollow block filling material especially in serrated floors where high average heat insulation value is required.

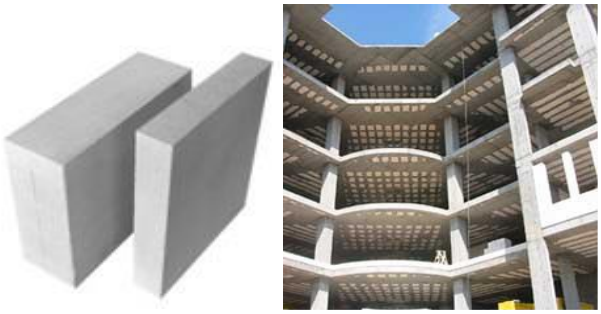

Figure 12. Hollow blocks

U blocks: They are used instead of wooden formwork (Fig. 14) in the production of reinforced concrete bonding, columns or beams that must be inside the walls. They are used especially in the production of the upper reinforced concrete bonding of masonry structures, ensuring a homogeneous surface on the inner and outer walls. In addition to this use, they can also be used in the production of intermediate bonding on high walls, the production of the upper bonding of roof shield walls, the production of chimneys, the concealment of rain downpipes and the concealment of reinforced concrete surfaces in the construction of fire walls.

Figure 14. U blocks

Insulation blocks: Insulation plates (Fig. 15) are used to insulate surfaces that are walked on, to insulate old or new external walls with insufficient thermal insulation, and to insulate horizontal or vertical concrete external surfaces.

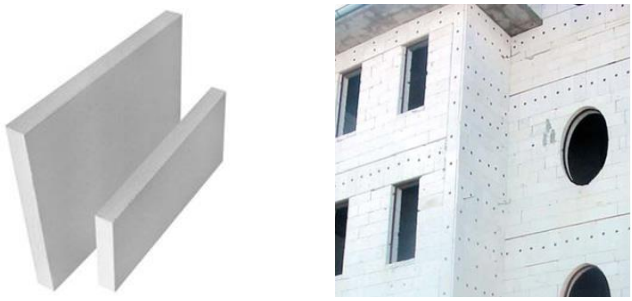

Figure 15. Insulation plates

b. Reinforced building elements

Reinforced AAC elements are produced with double-row steel mesh reinforcement and are profiled in various forms, including plain, tongue-and-groove, dovetail, and free-channel designs. These elements eliminate the need for formwork, rebar preparation, and setting time during construction, thus saving labor and time. Thanks to these advantages, construction with these elements can be carried out under all weather conditions.

Although reinforced structural elements are categorized as load-bearing and non-load-bearing, they can be further examined under four main categories: roof and floor elements, vertical and horizontal wall elements, partition wall elements, and lintels.

Roof and Floor Elements: AAC floor and roof slabs (Fig.16) are structural elements with thicknesses ranging from 10 cm to 30 cm and lengths up to the building's full span. They are used to form roofs and floors on wooden, concrete, or steel supports in both masonry and frame constructions.

Roof slabs are prefabricated reinforced structural elements designed primarily for solid roofs in industrial buildings and residential structures. These slabs can be used

for various roof applications, including flat, sloped, ventilated, and non-ventilated designs.

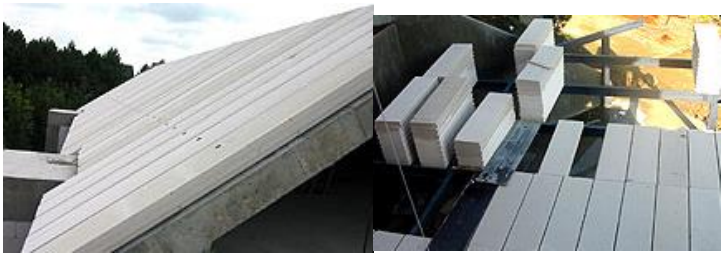

Şekil 16. Roof and floor Elements

Load-Bearing Vertical and Horizontal Wall Elements: These elements are used as load-bearing internal and external walls (Fig. 17), and are produced in thicknesses ranging from 15 cm to 25 cm, with a maximum height of 3 meters. They are designed to withstand wind loads of up to 90 kg/m². These elements are used for load-bearing internal and external walls in residential buildings up to three full stories and in structures where dynamic loads are not significant. Vertical wall elements are placed on a reinforced concrete plinth, which is raised approximately 30 cm above the ground level.

Figure 17. Horizontal and vertical load-bearing wall elements

Partition Wall Elements: AAC partition panels are structural elements produced in thicknesses ranging from 10 cm to 25 cm, with a maximum length of 6 meters, and can withstand wind loads of up to 90 kg/m². These elements are produced in longitudinal, beveled (to remove sharp edges for sloped surfaces), or non-beveled, rectangular or tongue-and-groove profiles.

Lintels: Lintels are AAC structural elements (Fig. 18) used above doors and windows, produced with reinforcement. Lintels are placed with equal overhangs on both sides. Non-load-bearing lintels are supported with a minimum overhang of 15 cm, while load-bearing lintels require a minimum overhang of 20 cm. They are anchored using AAC adhesive or cement mortar.

Figure 18. Lintels

3. Conclusion

AAC products offer several advantages over other similar wall materials, which can be categorized into benefits in design, construction, and performance. In design, AAC simplifies the planning process by reducing the thickness of exterior walls and allowing for slimmer building supports. During construction, its easy workability, precise dimensional production, light weight, and suitability for packaged transportation contribute to significant time and cost savings. As a building material, AAC stands out with its wide range of properties, offering the strength and stability of a solid material despite its light weight. It possesses adequate compressive strength, excellent thermal insulation, balanced heat storage, and diffusion behavior, making it an ideal choice for energy-efficient construction. Furthermore, its fire resistance, shape stability, low water absorption, and minimal susceptibility to freezing enhance its durability and longevity. The material's sound insulation properties, non-toxic composition, seismic resistance, and environmental friendliness make it a safe and sustainable option for modern buildings. Additionally, its ease of cleaning, repair, and low maintenance costs further solidify its value as an effective and efficient building material.

In conclusion, autoclaved aerated concrete (AAC) stands out as a superior building material compared to other similar wall products, offering significant advantages in design, construction, and performance. Its contributions to design include facilitating easier project planning, reducing exterior wall thickness, and enabling slimmer structural elements. In construction, AAC’s lightweight, ease of handling, precision manufacturing, and convenient packaging streamline building processes.

REFERENCES

Aamr-Daya, E., Langlet, T., Benazzouk, A., and Queneudec , M., (2008). Feasibility Study of Lightweight Cement Composite Containing Flax By-product Particles: Physico- Mechanical Properties, Cement and Concrete Composites, Vol: 30, pp: 957-963

Abdullah. K., Hussin. M.W., Zakaria. F., Muhammad. R., Hamid. Z.A., (2006). POFA: A Potential Partial Cement Replacement Materials in Aerated Concrete. Proceeding of the 6th Asia-Pasific Structural Engineering and Construction Conference. Malaysia.

Aidan, A., Shareefdeen, Z., Bogdanov, B., Markovska, I., Rusev, D., Hristov, Y., Georgiev, D., (2009). Preparation and Properties of Porous Aerated Concrete, Chemical Technologies, Biotechnologies and Food Technologies, vol.48, book 9, http://conf.uni-ruse.bg/bg/docs/cp09/9/9-4.pdf

Albayrak, M., Yörükoğlu, A., Karahan, S., Atlıhan, S., Aruntaş, H.Y., Girgin, İ., (2007). Influence of Zeolite Additive on Properties of Autoclaved Aerated Concrete, Building and Enviroment, vol.42, pp.: 3161-3165.

Al-Kahaled, G., (2002). Hebel Design Analysis Program, Master Thesis, Faculty of the School of Architecture, University of Southern California.

Anonymous, (2011a). 5th. International AAC Conference Securing a Sustainable Future, http://www.aerconaac.com/TECHNCAL%20MANUAL%5Caacinternational.pdf

Anonymous, (2011b). High-Strength Structural Lightweight Concrete, http://www.light concrete.com/images/LightConcrete.pdf

Anonymous, (2012a). Production Process, Turkish Aerated Concrete Producers Association http://www.tgub.org.tr/Default.asp?L=TR&mid=236

Anonymous, (2012b.) Autoclaved Aerated Concrete (AAC, Aircrete), http://www.understanding-cement.com/autoclaved-aerated-concrete.html

Anonymous, (2018). Aerated Concrete, Turkish Construction Industry Report. http://tgub.org.tr/raporlar

Anonymous, (2021). TS EN 206+A2, Concrete - Specification, performance, production and conformity, Turkish Standards Institution, Ankara.

Anonymous, (2022). TS 13655/T1, Specification for masonry units - Foamed concrete masonry units, Turkish Standards Institution, Ankara.

Anonymous, (2024a). Aerated Concrete, Catalog. Turkish YTONG Industry Inc., www.ytong.com.tr

Anonymous, (2024b). Aerated Concrete, Production Process, http://tgub.org.tr/uretim-sureci

Anonymous, (2024c). Autoclaved Aerated Concrete https://medium.com/@dante.hunter/hebel-autoclaved-aerated-concrete-the-worlds-most-innovative-building-material-be2d129e8c5f

Anonymous, (2024d). Block_Construction_Brochure, www.hebel.co.nz

Anonymous, (2024e). Turkish Construction Industry Report, Turkish Construction Materials Industrialists Association – İMSAD, https://imsad.org/dflip/Uploads/Files/Yapi_Sektoru_Raporu_2023_web.pdf

Anonymous, (2024f). Unreinforced Building Materials, www. ytong.com.tr

Araujo, E.G., Tenerio J.A.S., (2005). Cellular Concrete with Addition of Aluminum Recycled Foil Powders, Materials Science Forum, vol: 498-499, pp:198-204.

Arslan, M., (2008). Construction Technologies 2 (First Edition), Seçkin Publishing, Technical Books Series:23, Ankara.

Bagheri. H., (2006). Prestressed Hybirds of AAC and HPC the BCE (Block Composed Element Building System, A Conceptual Study, Licentiate Thesis, Royal Institute of Teknology, School of Architecture and the Built Enviroment, Stockholm, TRITA-ARK-For Skings Publication.

Beben, D., Manko, Z.Z., (2011=. Influence of Selected Hydrophobic Agents on Some Properties of Autoclaving Cellular Concrete (ACC), Construction and Building Materials, vol.25, pp.: 282–287.

Cabrillac, R., Fiorio, B., Beaucour, A., Dumontet, H., Ortola, S., (2006). Experimental Study of the Mechanical Anisotropy of Aerated Concretes and of the Adjustment Parameters of the Introduced Porosity, Construction and Building Materials vol.20, pp.: 286–295.

Chen, H.-J.; Chang, W.-T.; Tang, C.-W.; Peng, C.-F. A., (2023), Feasibility Study on Textile Sludge as a Raw Material for Sintering Lightweight Aggregates and Its Application in Concrete. *Appl. Sci. 13*, 6395. https://doi.org/10.3390/app13116395

Chen, Y., Li, F., Xu, B., (2006). Use of Clayish Crushed Stone for Production of

Damla, N., Çevik, U., Kobya, A.I., Çelik, A., Grieken, R.V., Kobya, Y., (2009). Characterization of Gas Concrete Materials Used in Buildings of Turkey, Journal of Hazardous Materials vol:168 , pp.: 681–687.

Demir, A., (2012). Fly Ash Aerated Concrete Research, http://www.e-kutuphane.imo. org.tr/pdf/13568.pdf

Domingo, E. R., (2008). An Introduction to Autoclaved Aerated Concrete Including Design Requirements Using Strength Design, Department of Architectural Engineering & Construction Science, College of Engineering, Kansas State Univercity, http://krex.k-state.edu/dspace/bitstream/2097/543/1/EricDomin go 2008.pdf

Ekmekyapar, T., Örüng, İ., (1997). Construction Material Information. Atatürk University Faculty of Agriculture Offset Facility, 151, Erzurum.

Erdoğan, T. Y., (1995). Materials Forming Concrete-Aggregates. METU, pp:162. Ankara.

Erdoğan, T.Y., (2003). Concrete. METU Development Foundation and Publishing Inc.., Ankara.

Ersoy, H.Y., (2001). Composite Material, Literature Publishing, Literature Publications: 66, İstanbul

Goual, M.S., Bali, A., Queneudec, M., (1999). Effective Thermal Conductivity of Clayey Aerated Concrete in The Dry State: Experimental Results and Modelling, J. Phys. D: Appl. Phys. Vol.32, pp.: 3041–3046.

Guglielmi, P.O., Silva, W.R.L., Repette, W.L., Hotza, D., (2010). Porosity and Mechanical Strength of an Autoclaved Clayey Cellular Concrete, Advances in Civil Engineering, Doi: 10.1155/2010/194102.

Hauser, A., Eggenberger, U., Mumenthaler, T., (1999=. Fly Ash From Cellulose Industry as Secondary Raw Material in Autoclaved Aerated Concrete, Cement and Concrete Research vol.29, pp.: 297–302.

Holt, E., Raivio, P., (2005). Use of Gasification Residues in Aerated Autoclaved Concrete, Cement and Concrete Research, vol:35, pp:796-802.

Jasicza, J., Zielinski, K., (2006). Effect of Protein Additive on Properties of Mortar, Cement and Concrete Composites, vol:28, pp:451-457.

Just, A., Middendorf, B., (2009). Microstructure of High-Strenght Foam Concrete, Materials Characterization, vol. 60, pp.: 741-748

Kömürlü, R., Önel, H., (2007). Use of Aerated Concrete Building Products in Residences, YTU Faculty of Architecture E-Journal, vol:2, issue:3

Kurama, H., Topçu, İ.B., Karakurt, C., (2009). Properties of the Autoclaved Aerated Concrete Produced From Coal Bottom Ash, Journal of Materials Processing Technology vol. 209, pp.:767-773.

Liu, X., Zhang, Z., & Wu, P. (2023). Utilization of solid wastes for aerated concrete preparation: Mechanical properties and microstructural analysis. *Journal of Building Engineering*, 108235.

Memiş, S., (2013). Investigating The Usability Of Gas Concrete, Produced Utilizing Various Additives From Erzurum-Pasinler Pumice, On Agricultural Buildings. PhD Thesis, Ataturk University, Institute of Science, Erzurum.

Mostafa, N.Y., (2005). Influence of Air-Cooled Slag on Physicochemical Properties of Autoclaved Aerated Concrete, Cement and Concrete Research, vol. 35, pp.: 1349–1357.

Nambiar, E.K.K, Ramamurthy, K., (2006). Influence of Filler Type on the Properties of Foam Concrete, Cement & Concrete Composites, vol. 28, pp.: 475–480.

Narayanan, N., Ramamurthy, K., (2000). Structure and Properties of Aerated Concrete: A Review, Cement & Concrete Composites, vol. 22, pp.: 321-329.

Önal, M., Can, Ö., Tokgöz, H., Koçak, A., (2007). An Experimental Study on Reinforcement Adherence and Compressive Strength in Swelling Aerated Concrete Panel, Journal of Engineering and Science, vol:25, issue:2

Özyıldırım, Ç., (2007), The Role of Air Entraining Admixtures in Concrete Durability, 2nd Symposium on Chemical Admixtures in Structures, Proceedings Book, pp. 37-51.

Puttappa, C.G., Rudresh., İbrahim, A., Muthu, K.U., Raghavendra, H.S,, (2008). Mechanical Properties Foamed Conctere, Internatıonal Conference on Construction and Building Tecnology, vol.43, pp.: 491-500, Malaysia.

Ramamurthy, K., Narayanan, N., (2000). Influence of Composition and Curing on Driying Shrinkage of Aerated Concrete, Materials and Structures, vol.33, pp.:243-250.

Rundai, G., 1963, Lightweight Concrete, Publishing House of the Hungarian Academy of Sciences, Budapest.

Serin. G., Çankıran. O., Başyiğit. C., Taş. H.H., Fenkli. M., (2007). Comparison of Physical and Mechanical Properties of Normal, Lightweight and Semi-Lightweight Concrete Blocks. Construction Technologies Electronic Journal. Vol:1, pp.:15-22

Şimşek, O., (2003). Building Materials II (Second Edition). Beta Printing Publishing Inc.., İstanbul.

Şimşek, O., (2009). Concrete and Concrete Technology (Third Edition), Technical Sciences Series:10, Ankara.

Topçu, İ.B., Uygunoğlu, T., (2007). Properties of Autoclaved Lightweight Aggregate Concrete, Building and Environment, vol.42, pp.:4108–4116.

Türkçü, H.Ç., (2010). Construction, Principles – Materials – Methods – Solutions, Birsen Publishing Co. Ltd., Istanbul. pp 154-169.

Uğur. İ., (2003). An Analysis on Improving the Engineering Properties of Lightweight Concretes with Crushed Stone Aggregates, III National Crushed Stone Symposium, Istanbul.

Uluata, A. R., (1981). Concrete Materials and Concrete, Ataturk University, Faculty of Agriculture, Erzurum,

Ungkoon, Y., Sittipunt, C., Namprakai, P., Jetipattaranat, W., Kim, K., Caharinpanitkul, T., (2007). Analysis of Microstructure and Properties of Autoclaved Aerated Concrete Wall Construction Materials, J. Ind. Eng. Chem., Vol. 13, No. 7, pp.: 1103-1108.

Ünal, O., Demir, İ., Güçlüer, K., Aker, A., Başpınar, M.S., (2011). Investigation of the Usability of Fly Ash and Silica Fume in Aerated Concrete Production, Ready Mixed Concrete Congress,www.thbb.org/Files/File/[439-448].pdf

Visagie, M., (2000). The Effect of Micrustructures on Properties of Foamed Concrete, Master Thesis, Structural Engineering, University of Pretoria, South Africa.

Witmann, F.H., (1992). Advances in Autoclaved Aerated Concrete, 3rd International Symposium on Autoclaved Aerated Concrete, Switzerland.

Yıldırım, T., (2002). Aerated Concrete Sector Profile Researchı. www.ito.org.tr/Dokuman/ Sektor/1-35.pdf

Chapter 9

WATER TREATMENT PROCESSES TODAY AND IN THE FUTURE

Temel Kan BAKIR[1*]

[1] Department of Chemistry, Faculty of Science, Kastamonu University, Kastamonu, Turkey
*Correspondence: temelkan@kastamonu.edu.tr
https://orcid.org/0000-0002-7447-1468

INTRODUCTION

Water, which plays an important role in industrial processes, has a direct impact on efficiency, equipment life and energy consumption, whether used in cooling systems, steam production or factory production processes. The quality of the water used can be improved by water treatment processes that are maintained within the correct physical and chemical parameters. Water treatment is a series of chemical and physical processes applied to ensure efficient and safe operation of industrial systems by increasing the quality of water.

Industrial water treatment chemicals play a critical role in these processes. Water treatment chemicals are an important requirement in ensuring water safety, improving water quality and increasing the efficiency of industrial processes. The increasing industrial demand in our world ensures the growth of the market for these chemicals every day. At the same time, the pollution of groundwater increases the use of chemicals for water treatment. Not only increasing water pollution, but also problems such as global warming indicate that this sector will grow. However, challenges such as high costs and competition from alternative technologies will require innovation and the development of other cost-effective solutions to meet the global demand for clean water.

Use of Water Resources

Water, one of the basic elements of life used to meet various needs such as agriculture, industry and energy production, is formed from water resources found on the surface and underground. Sustainable management of water resources that meet the vital needs of people is very important. Water resources play a vital role in many areas such as irrigation in agriculture, providing drinking water, industry, energy production and the continuity of ecosystems (Minibaş, 2008).

Water resources can be provided from two main sources: surface sources such as rivers, streams, lakes and dams, or underground water sources such as aquifers and wells. In addition to these, a third water source can be considered as atmospheric water sources such as rain and snow water. Streams and rivers, which also provide water displacement depending on changes in the groundwater level, are widely used for energy production and irrigation. Many of the lakes that form large water masses by accumulating water on the surface constitute freshwater sources. Dams built on rivers are water reservoirs and are used both to provide drinking water and to generate electricity (Ulusoy, 2007). Underground water resources are located in the soil without reaching the surface.

Aquifers are water resources located in rock layers that carry water under the soil. Aquifers are usually extracted by wells and used to provide drinking water. Wells are an important source, especially in rural areas, to reach underground water resources. Another example of water resources is rainwater, which is formed when moisture in the atmosphere condenses and falls to the ground. Rainwater collection systems are an important resource, especially in regions with water shortages. Snow in the mountains and glaciers in the poles can melt to form rivers and lakes, and they are important sources of water supply, especially in mountainous regions and cold climates (Özsoy, 2009).

The protection and proper management of water resources are of great importance for future water security. Pollution of water resources, excessive consumption and the decrease of these resources due to climate change cause serious problems. For example, water scarcity in agricultural production can cause yield losses and this may require the reconsideration of agricultural policies (Arslan, 2018). As people's needs change day by day, the factors that threaten water resources may also change. However, the main threats can be listed as shown in Figure 1.

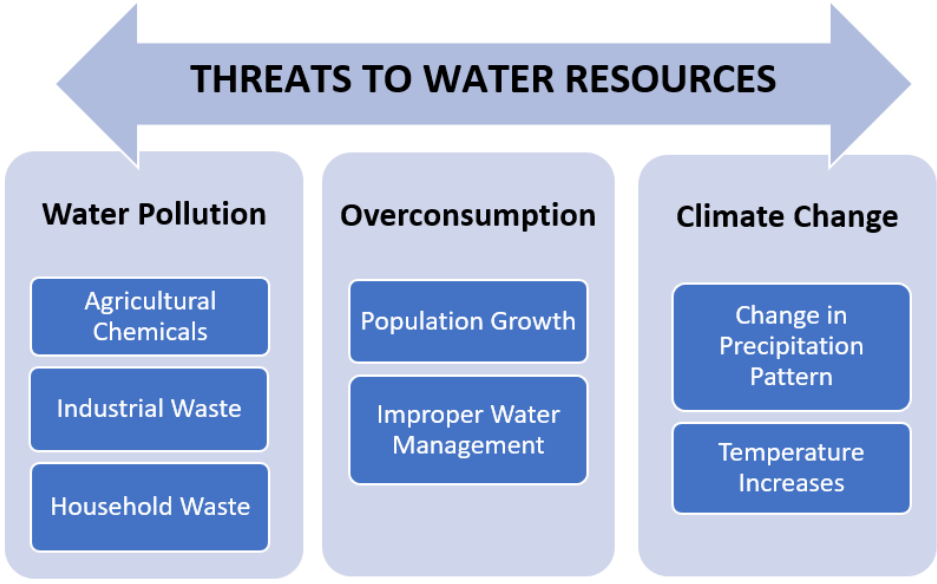

Figure 1: Threats that can disrupt the balance of water resources.

Today, water use in cities, water resource management, climate change, population growth and increasing dependence on surface water in metropolitan areas have become even more critical. As stated in Sarış's study, the increasing

rate of water withdrawal from rivers and the challenges dams face with climate change pose significant risks to water security (Sarış, 2021). In this sense, understanding the behavior of water users, developing environmentally friendly solutions and maintaining the supply-demand balance, emphasizing awareness on consumer behavior and water use are important for future water management strategies (Çiner, 2017). Such studies provide important information on the analysis of precipitation data, the optimum use of water resources and the assessment of the effects of climate change (Özfidaner et al., 2016). This holistic approach can contribute to the adoption of more conscious and sustainable approaches in water use and is of critical importance for the sustainable management of water resources.

Considering the effects of climate change and agricultural activities on water resources, it has been revealed how the concept of basin management is integrated into strategies in Turkey and what role this approach plays in the protection of water resources (Yıldırımer, 2024). Water use in the future requires a more conscious approach at both individual and social levels. In this context, elements such as water footprint analyses (WAS), basin management policies and understanding consumer behavior are of critical importance for the sustainable management of water resources. Batan provides important data on how water use can be optimized under drought conditions with the WAS analyses he conducted in Şanlıurfa province (Batan, 2021).

Water scarcity is a growing global concern, and industries are turning to innovative solutions such as industrial desalination and industrial wastewater treatment to address this challenge. Industrial water treatment is a critical component of sustainable industrial practices that address both environmental concerns and operational efficiency. The importance of this area is underlined by the increasing demand for water in industrial processes. As of 2011, this demand accounted for approximately 24% of total water consumption in many countries, of which a staggering 80% was used in the circulation of cooling water (Liu and Zhou, 2012).

One of the main issues in industrial water treatment is the need to reduce pollution and improve water reuse. For example, the textile industry has been identified as a significant contributor to water pollution, requiring continuous monitoring and advanced treatment technologies to effectively manage wastewater (Rabbi et al., 2018). As industrial organizations face increasing regulatory pressures and public scrutiny regarding their environmental impacts, effective water treatment strategies are becoming important not only for compliance but also for resource conservation and economic viability. Conventional water treatment methods are often inadequate in cases of high

contamination. Therefore, the use of innovative solutions such as anaerobic fluidized bed reactors and aerobic moving bed reactors is inevitable (Rabbi et al., 2018). The recycling of treated wastewater is recognized as a viable strategy to alleviate freshwater scarcity, especially in water-stressed regions (Boysen et al., 2020; Intaraburt et al., 2022). In this sense, the economic impacts of water treatment cannot be ignored and the development of innovative materials and technologies for wastewater treatment is of vital importance (Anikin and Shilkov, 2018). Furthermore, the integration of nanotechnology into water treatment processes has shown promising results in increasing efficiency and reducing costs, but these technologies need further validation on larger scales to reach their full potential (Jassby et al., 2018).

Ensuring water reuse in industrial areas can significantly reduce factories' dependence on natural water resources (Bauer et al., 2019). Thus, industrial water management helps preserve our freshwater resources with sustainable practices and offers new opportunities for water reuse and recycling in various sectors. Ultimately, the economic value of water in an industrial context highlights the need for effective water management strategies that balance environmental stewardship with economic viability (Ku and Yoo, 2011). From the oil industry to mining, from manufacturing to agriculture, many businesses are looking for new ways to reduce their water footprint, increase efficiency, and minimize environmental impact. In this respect, a good understanding of today's raw water processing and treatment technologies allows us to foresee how new water technologies will improve water management in industries.

Water in the world's hydrological cycle can be provided from four main sources: rainwater, surface water, groundwater, and seawater. It is not correct to think that these resources will meet the needs of all humanity forever without depletion. After the rapidly increasing population and urbanization, it is important to purify and reuse water polluted as a result of drinking, agricultural use and industrial activities or to release it in a way that will not harm nature. Thus, water included in the recycling from natural sources can be recovered with lower cost and higher percentage efficiency. The conversion of raw water taken from natural sources into utility water or industrial water form can be summarized in Figure 2.

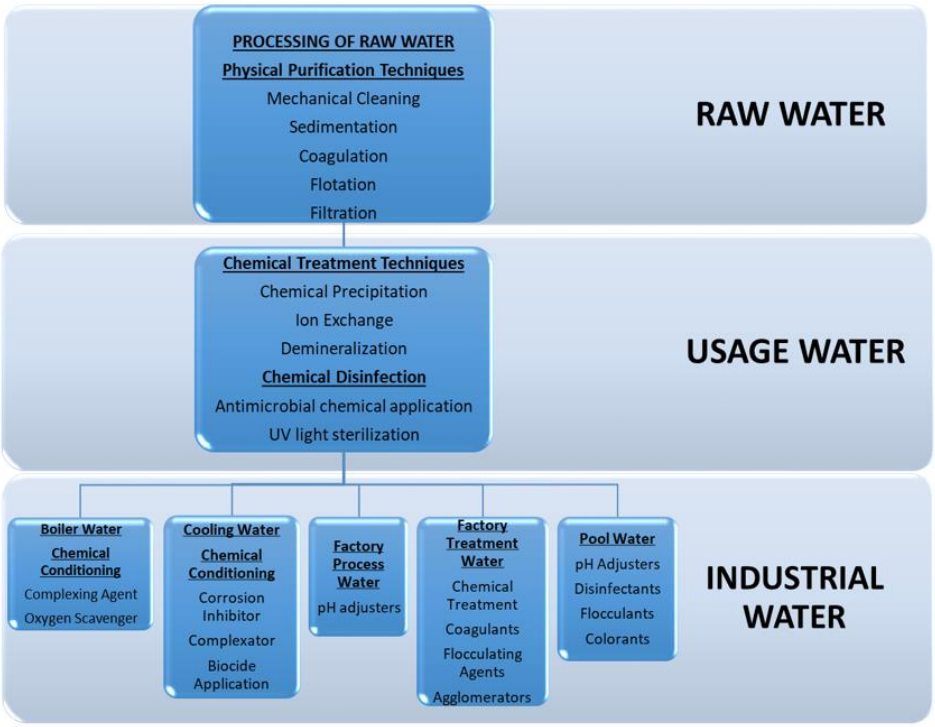

Figure 2: Stages of processing raw water by physicochemical means

The treatment process of water taken from the source is a critical process aimed at ensuring the safety and quality of drinking water and the effective management of wastewater. Regardless of the source, physical filtration is essential as the primary process. In fact, physical treatment is a method used in many stages of water treatment procedures. Physical filtration will both act as a barrier in capturing suspended solids and contaminants and will also undertake a cost-reducing task for the chemical and physical treatment processes to be applied later. At this stage, whether in wastewater treatment or raw water processing, physical filtration processes such as Mechanical Cleaning, Sedimentation, Coagulation, Flotation and cartridge filtration can be used. However, physical filtration processes are not sufficient for the removal of dissolved solids. Therefore, in addition to physical filtration in water, chemical treatment processes must also be applied. Physicochemical treatment techniques such as precipitation with chemical addition, ion exchange, reverse osmosis or demineralization can also be used. Chemical treatment techniques are applied not only for the removal of dissolved ions or molecules, but also for the removal of biological pollution. At this stage, sodium hypochlorite, hydrogen peroxide,

chlorine dioxide, sodium metabisulphite or ozone gas applications are commonly made.

After applying one or both of the physical or chemical treatment methods, water suitable for many areas such as people's drinking water needs, factory process water needs, agricultural and food industry water needs is obtained. It is possible to use the obtained water after these stages by applying simple water conditioning techniques in areas such as factory process water. However, in industrial branches where heating and cooling systems are important, such as the iron and steel industry, thermal power plants, nuclear energy facilities, textile dyeing industry, chemical treatment of water requires complex interventions that must be carried out very carefully.

Water Conditioning Processes

Water is needed in every area of industry, just like in homes and cities. Water conditioning is very important in the phase where utility water meets industrial needs. In particular, the conditioning of boiler feed water, cooling water and industrial process water is necessary for the sustainability of industrial production.

Water conditioning is a process carried out to keep the pollutants and dissolved substances contained in water at a certain level, thus increasing efficiency in industrial systems, protecting pipelines, heat exchangers, boilers and other equipment and preventing malfunctions. This process requires the use of various chemicals to regulate the hardness, acidic or basic properties of water, the amount of microorganisms and other chemical parameters.

In applications such as heat exchanger systems where heat transfer is provided, the use of chemicals is inevitable in order to prevent deposit formation. Especially in high-pressure steam boilers, impurities in water can form boiler scale in the form of sediment on the boiler walls. This not only reduces heat transfer efficiency, but can also cause crevice corrosion and boiler perforation. This situation causes the boiler temperature and pressure to drop and the boiler pipes to scorch due to the liquid leaking from the cracks. For this reason, it is desired that the boiler usage water is close to pure water or has soft water properties. In high-pressure steam boilers that feed electricity production systems such as turbines, it is not enough to remove the hardness of the boiler feed water alone. In such systems, it is desired that there are no dissolved salts that cause the boiler water conductivity to increase.

Boiler Water Conditioning

The conditioning of boiler systems that meet the hot water or steam needs in many industrial areas begins with the shaping of the feed water. Factories make their boiler selections in line with their needs at the first stage. In industrial flame tube steam boiler systems, soft water obtained by removing Ca+2 and Mg+2 ions from raw water is mostly used. In industries where the steam demand is higher and needs to be provided faster, water tube boiler systems are preferred. These systems require great sensitivity in terms of water conditioning. Because it is not enough to provide feed water in the form of soft water to such systems. No matter how purified the boiler feed water is, the impurity concentration in the boiler increases due to evaporation. Depending on the boiler pressure, it is desired that the total dissolved salt concentrations, silicate and hydroxyl alkalinity are within certain values. In boiler water conditioning, processes such as oxygen removal, pH adjustment and removal of impurities by blowing should be carried out in order to prevent deposit formation and corrosion and to ensure pure steam production. Therefore, the use of chemical conditioners is necessary in boiler water treatment. In boiler water systems, the removal of dissolved oxygen, which causes pitting corrosion in particular, can be reduced to a certain value with mechanical systems such as deaerators, but it can be reduced to the desired levels with chemical methods. For this purpose, oxygen-binding chemicals such as sodium sulfite, hydrazine, carbohydrazide, and diethyl hydroxylamine are used. Chemicals are also used to prevent the formation of boiler deposits and to ensure that the boiler pH value remains within optimum ranges. These include complexing compounds such as sodium metaphosphate, disodium hydrogen phosphate, and/or trisodium phosphate, which hold calcium and magnesium and prevent them from forming hard deposits. Coordinated phosphate compounds also hydrolyze in the boiler water, ensuring that the boiler water remains in the alkaline region. These compounds can also form films on clean pipe surfaces, thus delaying metal corrosion. Chemical use is not only used for boiler interior conditioning, but is also used to protect environments where the vapor phase condenses (condensate lines, turbine blades, etc.) from corrosion. Volatile compounds such as ammonia, morpholine, hydrazine and cyclohexylamine are used to prevent corrosion caused by the formation of carbonic acid in pure water formed by condensation of steam. These chemicals do not increase the amount of dissolved solids in the boiler and can therefore be used in high-pressure and single-pass boilers. This conditioning technique is generally used in drum boilers to adjust the pH of condenser and feed water and to neutralize carbon dioxide. In this system, amines also provide protection to turbines with their volatile properties. However, the inability to buffer the boiler water environment makes

pH adjustment difficult. Therefore, it is very important to remove or retain hard deposit-forming impurities entering the boiler water. Removal of certain contaminants such as dissolved silica is another critical aspect of industrial boiler water treatment. Silica can cause hard deposit formation in boilers and turbines, leading to operational inefficiencies and increased maintenance costs (Sasan et al., 2017). Therefore, effective silica removal techniques are required to maintain the integrity of industrial systems. In addition, the presence of heavy metals in industrial wastewater poses significant environmental risks and requires stringent treatment protocols to meet regulatory standards (Fayomi et al., 2016). Today, these heavy metal or dissolved silica impurities that pollute boiler waters are no longer a problem by using an effective chemical treatment method. The use of organic or inorganic based complexing agents, especially used in boiler water treatment, prevents the accumulation potential of ions that can cause permanent and temporary hardness.

Cooling Water Conditioning

Cooling water is indispensable for large-scale industries such as thermal power plants, iron and steel factories and nuclear power plants. Since these facilities require a large amount of cooling water, they are installed in areas close to water sources such as lakes, streams or the sea. Since the hourly water usage in these facilities is high, the conversion of raw water to soft or pure water is costly. Softening of water from streams or ponds is possible with the use of cold lime-soda, hot lime-soda, lime and cation exchangers. For facilities using sea water, water purification methods such as reverse osmosis are needed. In both cases, industrial chemicals are needed for the regeneration, cleaning and operation of these facilities.

The use of softened or pure water in cooling systems requires a good chemical conditioning program. In particular, it is desired that the temperature difference of the cooling water does not exceed 10-15 °C in heat transfer systems within the facility. In systems where the temperature difference is high, the formation of hardness deposits or the possibility of corrosion increases. Therefore, total hardness inhibitor and corrosion inhibitor chemicals should be added to the cooling system water. In cases where the cooling process is provided by tower systems open to the atmosphere, there is a constant new water supply to the system due to evaporation loss. Thus, the water concentrated in the cooling system contains more salinity and impurities. These impurities, which cause the conductivity to increase, must be removed from the system with daily blowdowns.

In cooling waters, coordinated phosphate compounds as well as bases such as sodium hydroxide are used to maintain the pH value between 7.5-9.0. Sometimes, pH-controlled sulfuric acid dosing can be done. In these systems, corrosion rate and total hardness values must be constantly controlled and kept in balance. For this purpose, stable conditions are determined using the Langelier index sign. Cathodic and anodic inhibitors are used to control the corrosion rate in cooling systems. Inhibition in a cooling water can be achieved by adsorbing on the metal surface and forming a film layer or by reacting with the metal and forming a solid film on the metal surface. In addition, the inhibitor can react with molecules that can cause corrosion in water and dampen their effects. Molybdates, chromates, zinc salts, nitriles, polyphosphates and medium phosphates are the main inhibitors used in cooling water systems.

Cooling waters of tower systems open to the atmosphere may contain dissolved gases such as saturated oxygen and carbon dioxide. It is important to control these with chemical conditioning. However, the problems of these systems open to the atmosphere are not only hardness formation and corrosion. At the same time, microorganisms that reproduce in cooling water cause mechanical problems as well as health problems. Semi-permeable films formed by microorganisms cause corrosion by creating oxygen chambers. Chemical disinfection process is applied to remove biological pollution in all usage waters and is also used in cooling systems. Chlorine is a widely used disinfectant that plays a vital role in protecting public health by reducing the risk of waterborne diseases (Gitis and Hankins, 2018). Chemicals such as copper salts, mercury salts and chlorine can be added to cooling systems periodically in order to prevent microorganisms and algae. In addition to these, it is also possible to use potassium permanganate and quaternary ammonium compounds that have a biocide effect. However, chlorine use should be managed carefully due to the potential health risks associated with its by-products (Masmali et al., 2023). Additionally, the continuous addition of disinfectants to water lines has been shown to keep bacterial numbers within acceptable limits, although it presents difficulties in controlling resistant microorganisms such as Legionella (Leoni et al., 2015).

Table 1: Inhibitors used in various environments and their approximate dosages (Yalçın and Gürü, 2002)

Corrosive Environments	Inhibitor type	Metal to be protected	Approximate dosage	Usage Requirement
Drinking Water	Polyphosphate $Ca(OH)_2$	Fe, Zn, Cu, Al	5-10 ppm pH>8	Complex Generators pH Adjusters
Cooling Waters	$Ca(HCO_3)$ Na_2CrO_4 $NaNO_2$ Na_2HPO_4 Morpholine	Fe, Zn, Cu	10 ppm % 0,1 %0,05 % 1 % 0,2	pH Adjusters Anodic Inhibitor Complex Builders and Filmmakers Complex Builders and Filmmakers Complex Builders and Filmmakers
The boilers	Na_2HPO_4 Polyphosphate Morpholine Hydrazine Ammonia Octadecylamine Sodium Polymethacrylate	Fe	10 ppm 10 ppm Sufficient dose Sufficient dose According to pH Sufficient dose	pH Adjusters Complex Generators Oxygen Scavengers Oxygen Scavengers pH Adjusters Oxygen Scavengers Dispersants

The Future of Chemical Water Treatment Technology

In the future, the use of treatment chemicals will be reshaped in line with environmental sustainability goals. The integration of sustainability practices into corporate strategies will provide a more effective approach to the management of these chemicals (Risteska, 2023). Companies will need to conduct sustainability reporting and independently secure these reports to minimize the impacts of these chemicals on the environment (Temiz et al., 2022).

The future of chemical water treatment technology will show significant changes in areas such as sustainability, digitalization, energy efficiency and the development of alternative technologies. It can be said that this technology has great potential in terms of protecting water resources and using water more efficiently. However, new solutions and innovations are needed to make chemical water treatment systems more environmentally friendly and energy efficient. One of the developments in this area is the increasing use of reverse osmosis in water treatment. This increase is improved by pretreatment, membrane permeability, energy efficiency and chemical optimization regulations. However, reverse osmosis is not the only way to desalinate water. Researchers are constantly working on new studies in this field of water treatment methods. For example, a team led by Shihong Lin has developed a new saltwater treatment method called electrodialytic crystallization. This newly published innovative approach has the potential to significantly reduce energy consumption and costs associated with saltwater crystallization. Recent studies have also highlighted the importance of optimizing chemical dosing in water treatment systems to improve water quality while minimizing costs. For example, the chemical composition of the water source significantly affects the amount of treatment chemicals required (Santana

et al., 2014). We can examine how chemical water treatment technology will evolve and develop in the future under several main headings:

-Environmental Sustainability and Green Chemicals

The future of chemical water treatment technology will move towards developing environmentally friendly and sustainable solutions. Some chemicals used today for water treatment, such as chromates, can harm the environment or create difficulties in water recovery processes. In the future, the effectiveness of environmentally friendly and biodegradable green chemicals is being examined by research. Especially in the context of environmental sustainability, natural, biological and biotechnological solutions are also emerging as innovative approaches to water treatment. For example, the discovery of natural flocculating agents obtained from plant materials offers a promising alternative to traditional chemical coagulants. These natural substances not only reduce the environmental impact of water treatment, but can also be used for various applications thanks to their biodegradability (Cortes-Perez et al., 2021).

Nowadays, the integration of advanced technologies such as photocatalysis for the removal of persistent pollutants in water is also being investigated (Choi et al., 2023). Despite advances in water treatment chemicals and technologies, management of some chemical contaminants continues to pose risks, especially in areas such as hemodialysis where water purity is crucial (Mineshima et al., 2018).

-Digitalization and Automation

With the advancement of technology, automation applications in water treatment systems have increased. Using smart sensors, artificial intelligence (AI) and machine learning (ML), water quality can be monitored instantly and more efficient and precise control is provided. Especially in boiler systems, cooling systems, wastewater treatment systems and pools, chemical usage can be optimized in every area where water is used, and a safe and accurate water treatment process can be applied.

-Specialized Water Treatment Needs

Industrial water treatment applications are creating more specialized water quality requirements. Chemical water treatment technology will need to become more flexible to provide specific chemical solutions to meet the needs of different sectors, especially in areas such as wastewater treatment and water recovery.

-Energy Efficiency and Carbon Footprint

In the future, industrial facilities may make improvements to their chemical water treatment processes to increase energy efficiency and reduce their carbon footprint. Water treatment chemicals that operate at lower temperatures for less energy and fewer chemicals, or solutions that will allow more efficient use of waste heat, can be developed.

-Development of Smart Chemicals and Alternative Technologies

In the future, it is expected that alternative technologies will develop that can replace chemical water treatment or reduce chemical consumption. For example, processes such as membrane technologies, photodynamic processes and electrocoagulation can disinfect water without chemical additives. Chemical use can be controlled and costs can be reduced thanks to smart devices and software. In addition, some physical and biological method applications such as reverse osmosis, ultraviolet light or electrochemical methods can be tried to be used instead of chemical water treatment. In this process, the needs created by global climate change make water recovery important and water resources management and supply security gain importance, and increasing water scarcity necessitates more efficient and effective use of water. Chemical water treatment technology will play an important role in water recovery and reuse by reducing industrial water use with the production of new smart chemicals.

The future of treatment chemicals will be shaped in line with sustainability principles and companies are expected to fulfill their environmental, economic and social responsibilities in this process. In this context, sustainability reporting and transparency will be among the key elements that will determine the way companies manage these chemicals (Aksoy, 2019; Saygılı et al., 2020).

CONCLUSION

As a result of global warming and climate change, clean water resources are gradually decreasing. In the future, desalination studies in water will gain importance. The reduction of high energy consumption spent for obtaining pure water and the use of environmentally friendly chemicals for membrane cleaning should be encouraged.

Safe and trouble-free operation of pressurized steam boilers in a business and continuous control of the water cycle are possible with the use of water treatment chemicals. Important industrial organizations employ chemists and chemical engineers in shifts to ensure the control and correct management of cooling systems. The water treatment chemical expenses required for a trouble-free water cycle of businesses are naturally increasing. In the future, the budget that

industrial organizations will allocate for chemicals such as hardness inhibitors and oxygen scavengers used for boiler water conditioning and water treatment chemicals such as microorganism inhibitors, hardness and corrosion inhibitors used for cooling water conditioning will constitute a very significant cost.

In addition, effective use of water treatment chemicals is necessary to provide safe drinking water and discharge wastewater in the future. The development of innovative treatment methods and optimization of chemical processes are important for addressing the challenges associated with water quality management. Industrial water treatment encompasses environmental protection, resource conservation and economic efficiency. As industries continue to evolve in response to global water challenges, the adoption of innovative treatment technologies and sustainable practices will be crucial to ensuring the long-term viability of industrial operations. We must not forget that the protection and efficient use of water resources is of vital importance not only for present generations but also for future generations.

REFERENCES

Aksoy, F. (2019). İşletmelerde sürdürülebilirlik raporlama çerçeveleri. Muhasebe Bilim Dünyası Dergisi, 21(2), 324-346. https://doi.org/10.31460/mbdd.459841

Anikin, Y. and Shilkov, V. (2018). Modern materials and technologies of industrial wastewater treatment. Russian Journal of Construction Science and Technology, 4(2), 22-26. https://doi.org/10.15826/rjcst.2018.2.004

Arslan, Ö. (2018). Su kıtlığına maruz bırakılmış c3 ve c4 bitkilerinin fotosentetik aktivitelerinin belirlenmesi. Iğdır Üniversitesi Fen Bilimleri Enstitüsü Dergisi, 8(4), 47-54. https://doi.org/10.21597/jist.402367

Batan, M. (2021). Kuraklıkla mücadele eden şanlıurfa ilinde su kullanımının planlanması: su ayak izi analizleri. Gazi Üniversitesi Mühendislik-Mimarlık Fakültesi Dergisi, 36(4), 2135-2150. https://doi.org/10.17341/gazimmfd.790928

Bauer, S., Dell, A., Behnisch, J., Chen, H., Bi, X., Nguyen, V.A., Linke, H.J., Wagner, M. (2019). Water-reuse concepts for industrial parks in water-stressed regions in south east asia. Water Science & Technology Water Supply, 20(1), 296-306. https://doi.org/10.2166/ws.2019.162

Boysen, B., Cristóbal, J., Hilbig, J., Güldemund, A., Schebek, L., & Rudolph, K. (2020). Economic and environmental assessment of water reuse in industrial parks: case study based on a model industrial park. Journal of Water Reuse and Desalination, 10(4), 475-489. https://doi.org/10.2166/wrd.2020.034

Choi, M., Singh, N., Son, S., Kim, J.H., Kang, M., Park, S.H., Choi, D.H., Hong, C.S., Kim, J.S. (2023). A post-synthetically modified porous organic polymer for photocatalytic water purification. Materials Chemistry Frontiers, 7(10), 2085-2092.

Çiner, F. (2017). Consumer behaviours and awareness in water usage - as a sample of field study in nigde city,turkey. Pamukkale University Journal of Engineering Sciences, 23(9), 1019-1026. https://doi.org/10.5505/pajes.2017.13245

Cortes-Perez, C., Pérez-Montalvo, L., Puello-Silva, J., Pasqualino, J., Lambis-Miranda, H. (2021). Synthesis and characterization of a coagulating agent from plantain peel starch (musa paradisiaca), as adjuvant in water treatment. Water Air Soil Pollut, 234:316. https://doi.org/10.1007/s11270-023-06323-7

Fayomi O.S.I., Olukanni D.O., Fayomi G.U., Joseph O.O., Popoola A.P.I. (2016), In-situ evaluation of the degradable carbon influence for industrial

waste water treatment. *AIP Conf. Proc.* 1758 (1): 020020. https://doi.org/10.1063/1.4959396

Gitis, V. and Hankins, N. (2018). Water treatment chemicals: trends and challenges. Journal of Water Process Engineering, 25, 34-38. https://doi.org/10.1016/j.jwpe.2018.06.003

Hayri Yalçın, Metin Gürü, (2002), Su Teknolojisi, Palme Yayıncılık, Ankara 2002, ISBN 975-8624-14-8.

Intaraburt, W., Sangsanont, J., Limpiyakorn, T., Ruangrassamee, P., Suttinon, P., Suwannasilp, B. (2022). Feasibility study of water reclamation projects in industrial parks incorporating environmental benefits: a case study in chonburi, thailand. Water, 14(7), 1172. https://doi.org/10.3390/w14071172

Jassby, D., Cath, T., Buisson, H. (2018). The role of nanotechnology in industrial water treatment. Nature Physics, 13(8), 670-672. https://doi.org/10.1038/s41565-018-0234-8

Ku, S. and Yoo, S. (2011). Economic value of water in the korean manufacturing industry. Water Resources Management, 26(1), 81-88. https://doi.org/10.1007/s11269-011-9905-z

Leoni, E., Dallolio, L., Stagni, F., Sanna, T., D'Alessandro, G., & Piana, G. (2015). Impact of a risk management plan on legionella contamination of dental unit water. International Journal of Environmental Research and Public Health, 12(3), 2344-2358. https://doi.org/10.3390/ijerph120302344

Liu, Y. and Zhou, J. (2012). Research of the operating parameters from reducing industrial water conductivity through electro sorption technology. Applied Mechanics and Materials, 229-231, 2522-2526. https://doi.org/10.4028/www.scientific.net/amm.229-231.2522

Masmali, I., Khalid, A., Shuaib, U., Razaq, A., Garg, H., Razzaque, A. (2023). On selection of the efficient water purification strategy at commercial scale using complex intuitionistic fuzzy dombi environment. Water, 15(10), 1907. https://doi.org/10.3390/w15101907

Mineshima, M., Kawanishi, H., Ase, T., Kawasaki, T., Tomo, T., Nakamoto, H. (2018). 2016 update japanese society for dialysis therapy standard of fluids for hemodialysis and related therapies. Renal Replacement Therapy, 4(1). https://doi.org/10.1186/s41100-018-0155-x

Minibaş, T., (2008), Globalizmde Suyun Ekonomi Politiği, www.turkelminibas.net, ErişimTarihi: 04.11.2008

Özfidaner, M., Şapolyo, D., Topaloğlu, F. (2016). İç anadolu bölgesi yağış verilerinin gidiş analizi. Nevşehir Bilim ve Teknoloji Dergisi, 0(0), 161. https://doi.org/10.17100/nevbiltek.33972

Özsoy S. (2009). Su ve Yaşam: Suyun Toplumsal Önemi, T.C. Ankara Üniversitesi Sosyal Bilimler Enstitüsü Çalışma Ekonomisi ve Endüstri İlişkileri Anabilim dalı, Ankara-2009.

Rabbi, M., Hossen, J., Sarwar, M., Roy, P., Shaheed, S., Hasan, M. (2018). Investigation of waste water quality parameters discharged from textile manufacturing industries of bangladesh. Current World Environment, 13(2), 206-214. https://doi.org/10.12944/cwe.13.2.05

Risteska, M. (2023). Kurumsal iletişim açısından sürdürülebilirlik yönetimi uygulamaları: türkiye ve kuzey makedonya karşılaştırması. The Journal of International Scientific Researches, 8(3), 367-392. https://doi.org/10.23834/isrjournal.1335210

Santana, M., Zhang, Q., Mihelcic, J. (2014). Influence of water quality on the embodied energy of drinking water treatment. Environmental Science & Technology, 48(5), 3084-3091. https://doi.org/10.1021/es404300y

Sarış, F. (2021). Evaluation of domestic water supply and use statistics of turkey. Coğrafi Bilimler Dergisi, 19(1), 195-216. https://doi.org/10.33688/aucbd.883794

Sasan, K., Brady, P., Krumhansl, J., Nenoff, T. (2017). Removing dissolved silica from waste water with catechol and active carbon. United States, 2007. https://doi.org/10.2172/1340632

Saygılı, E., Yargı, S., Erginer, D. (2020). Halka açık şirketlerin sürdürülebilirlik raporları analizi: Borsa İstanbul'da bir uygulama. Yönetim ve Ekonomi Dergisi, 27(2), 239-261. https://doi.org/10.18657/yonveek.599794

Temiz, H., Şeker, Y., Özdemir, F. (2022). Sürdürülebilirlik raporlaması ve bağımsız güvence kararlarının belirleyicileri. Eskişehir Osmangazi Üniversitesi İktisadi ve İdari Bilimler Dergisi, 17(3), 862-892. https://doi.org/10.17153/oguiibf.1147346

Ulusoy, K., (2007), Küresel Ticaretin Son Hedefi: Su Pazarı, Kristal Kitaplar Yayınevi, Ankara, 2007.

Yıldırımer, S. (2024). Havza yönetimi yaklaşımlarında uluslararası alanda yaşanan gelişmelerin türkiye'deki politika ve strateji belgelerine yansımaları. Anadolu Orman Araştırmaları Dergisi, 10(1), 78-90. https://doi.org/10.53516/ajfr.1465516

Zhang, X., Yao, Y., Horseman, T., Wang, R., Yin, Y., Zhang, S., Tong, T. Lin, S. (2023). Electrodialytic crystallization to enable zero liquid discharge. Nature Water, 1(6), 547-554.

Chapter 10

EFFICIENCY IN SMART RAIL TRANSPORTATION SYSTEMS

Eyyüp TAŞKAYA[1]
Bahadır Furkan KINACI[2]

[1] Lec., Karabuk University, https://orcid.org/0000-0002-7188-4638
[2] Lec., Karabuk University, https://orcid.org/0000-0001-6872-2630

1. INTRODUCTION

Rail systems are ideal for both intra-city and inter-city transportation and are open to development. Rail systems can carry both freight and passengers. This transportation system consists of vehicles, infrastructure and superstructure. Sustainability, high capacity and safety advantages distinguish it from other transportation methods (Aksu & Kaplan, 2022).

Rail systems offer advantages such as sustainability, high passenger and freight transport, high capacity, low accident rates and renewable energy use. However, there are problems such as high investment costs, long construction periods and maintenance, business management and costs required for the smooth operation of the systems put into operation in vehicle technology and infrastructure construction (Coto-Solano, 2024).

Rail transportation has long been the most preferred transportation method due to its advantages over other transportation methods. New applications for resource efficiency, sustainability and system security have emerged with the development of intensive transportation systems. As a result of these applications, the efficiency of the rail transportation system has become one of the most effectively discussed topics in the literature.

To evaluate the efficiency of rail transportation systems, it is necessary to first evaluate the efficiency of infrastructure, superstructure, vehicles and businesses. The traceability structure, which is one of the most important factors affecting efficiency, reduces the downtime by keeping maximum vehicles in the business, works with maximum occupancy and selects efficient maintenance techniques.

For all the reasons mentioned, efficient system management, effective use of resources and passenger satisfaction, which are addressed with the economic, environmental and social aspects of rail transportation systems, help cities achieve sustainable transportation goals (Özarpa, Kınacı, & Avcı, 2022).

2. SMART TRANSPORTATION SYSTEMS

Intelligent transportation system technologies enable the collection, storage, processing and application of information in real time using advanced electronic, information and communication technologies applied to roads, vehicles and subsystems. The developed systems provide safer transportation, more efficient capacity use, more mobility, more energy management and a more environmentally friendly working environment.

Intelligent transportation systems, as in all systems, meet the expectation of being cleaner, safer and more efficient in transportation systems. The interopera-

bility structure of intelligent transportation systems allows them to find application in all areas of land, air, sea and railway transportation and to be integrated into all systems and subsystems used (Tektaş & Tektaş, 2022).

Intelligent transportation systems have various advantages. These can be listed as; optimizing transportation times, reducing traffic accidents and related loss of life and property, reducing environmental bans, enabling more efficient travel with less energy in road transportation systems based on fossil fuel use, providing road and route information, providing automatic and faster collection of toll collection results, instant detection of traffic rule violations by vehicle users, ensuring that they are effectively informed about meteorological events that may affect transportation, ensuring the effectiveness of emergency management systems and applications, providing information and efficiency increase with vehicle-to-vehicle communication, vehicle-to-infrastructure communication, vehicle-to-driver communication systems, providing ease of transportation by analysing big data collected from the environment and infrastructures, increasing electric and hybrid changes and facilitating the transition to smart energy systems Greer Liz, Fraser Janet, Hicks Drennan, Mercer Mike, & Thompson Kathy (2018).

3. SMART RAIL TRANSPORTATION SYSTEMS

With the development of digital technologies such as smart railways and transportation systems, it is now possible to manage controllable vehicle and station systems with both physical and virtual connections. Controlling these systems from specific centres helps to protect these systems from problems such as failure, accident, data loss, time and income loss. It also provides experience to develop new, more efficient designs and systems. While intra-city and inter-city freight and passenger transportation is carried out by railway systems, numerous system control centres serve as supervisors (López-Aguilar, vd., 2022).

Intelligent rail transport systems have the potential to become a cornerstone in cities of the future, enabling multimodal transport and empowering new service models such as mobility as a service (Butler, Yigitcanlar, & Paz, 2021). Technologies such as ubiquitous computing, edge computing, artificial intelligence (AI), and blockchain, as well as fast data networks on 4G and 5G, have yet to take the potential of rail transport to the next level. To realize the full potential of context-aware environments such as smart stations or smart wagons, progressive sensorization of railway stations, wagons, and rails will strengthen these systems. Using a large number and variety of digital devices, large amounts of heterogeneous

data can be collected and analysed to obtain advanced information and provide effective services in real time (López-Aguilar et al., 2022).

The increase in digitalization, developments in smart transportation systems and the integration of rail systems into these systems have enabled all kinds of controllable systems to be controlled through virtual and physical connections. While managing smart rail systems from control centres reduces possible accidents, malfunctions, data losses and financial disruptions, it has facilitated the development of more optimum and efficient designs and structures through the experiences gained. Intra-city and inter-city freight and passenger transportation is carried out by railway networks where various systems are controlled by control centres. In common applications, station control centre's act as sub-control centres of the primary control centre and manage vehicle and road systems (including line safety systems, signalling and switching systems) along the line via various communication infrastructures such as GPRS, fibre optic and LAN. In applications, road systems and station control systems managed from the central control centre vary depending on the status of the infrastructure and the scale of the line (Hahn, Munir, & Behzadan, 2021; Kelarestaghi, Foruhandeh, Heaslip, & Gerdes, 2021; Tektaş & Tektaş, 2019). The network architecture and substation control centres connected to the main control centre are shown in Figure 1.

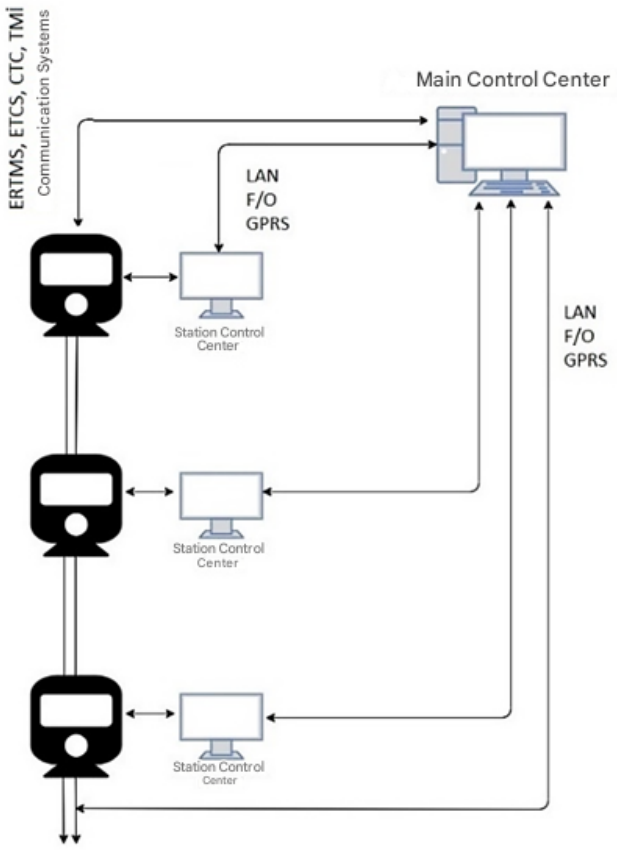

Figure 1. Substation control centres and network architecture connected to the main control centre (ÖZARPA, AVCI, & KINACI, 2021)

Station control systems provide comfort, control, vehicle navigation and security systems control in connection with the main control centre in developed smart structures. Security, control and comfort systems in the station are lighting, escalator, ventilation, camera, ticket control, elevator and security systems. Outside the station, security, vehicle movement, control and comfort systems and switch, signal and road control systems are managed. The structures created have station management systems that interface with the main control centre to manage vehicle navigation, security, control and comfort systems. Lighting, stairs, ventilation, cameras, elevators, ticket control and security systems in the station are managed. Vehicle movement, security, comfort and external control systems in the station are managed together with switch, signal and road control systems. (ÇODUR & TOPDAĞI, 2018; Ulvi & Akdemir, 2019). Figure 2 shows the architecture of the systems controlled at the station.

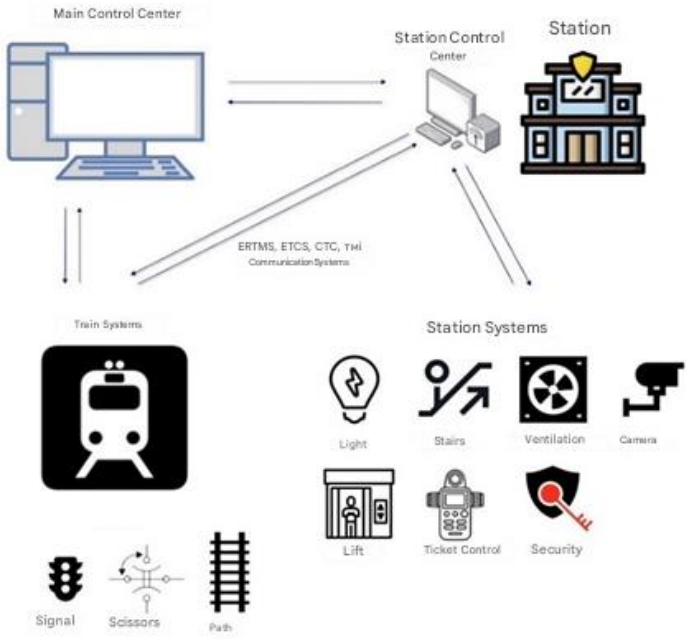

Figure 2. Systems controlled at the station in smart rail system applications

Various comfort, navigation and control systems in rail cars can be managed from central control and station control centres. These systems manage all passenger operations and conduct basic navigation planning and movement procedures by connecting with central control along the route. Figure 3 shows the systems that can be managed in the rail car.

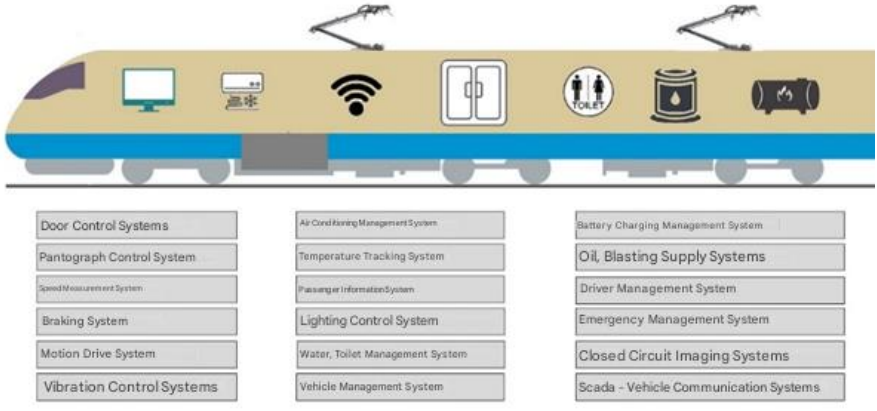

Figure 3. Systems that can be controlled in smart rail system vehicles

4. RELATIONSHIP BETWEEN RAIL SYSTEMS AND EFFICIENCY

Efficiency is defined as obtaining optimum benefit within a system and has an important place today, especially in relation to energy use and environmental pollution. The risks associated with the spread of technologies that increase energy resources, urban density and pollution necessitate the design of efficient systems and the increase in efficiency in existing systems. Examining the parameters that increase efficiency in industrial systems reveals the importance of maintenance practices, initial purchasing criteria, employment of qualified personnel, institutional framework, public awareness, use of smart technologies, integration with various systems, innovative orientation, central management, planning and energy technology. The efficiency of existing systems increases their longevity, customer satisfaction, ease of participation, strategic planning possibilities and reduces failure rates and operational expenses. (Gallego-García, Gejo-García, & García-García, 2021). The smart applications to be used are important in terms of the interaction and efficiency that smart railway system technologies bring.

4.1. Transport Efficiency in Rail Transportation Systems

Efficiency means obtaining maximum output using minimum resources. A system is expected to provide maximum performance, sustainability, capacity and revenue while minimizing costs, human resources, facilities, maintenance and repairs (Kahya & Polat, 2007). Equation 1 shows the efficiency in a mathematical way.

$$Efficiency = \frac{\text{Output}}{\text{Input}} \tag{1}$$

When calculating efficiency in smart rail systems, Equation 2, which is derived from the efficiency calculation in Equation 1, is used.

$$Efficiency = \frac{\text{Transport Performed}}{\text{Standard Carrying Capacity}} \tag{2}$$

Equation 2 expresses the volume of passenger and freight transport obtained by considering the actual transport, maintenance, repair, failure, delay and interruptions used in the calculation of the efficiency of rail systems. The term standard transport capacity refers to the maximum passenger and freight volume that a rail system can carry at full capacity within a certain time. In a study published in the literature, the efficiency of the rail transport systems of 19 different countries that are members of the OECD (Organization for Economic Co-operation

and Development) was examined using the amounts of "Passenger-Km" and "Tonne-Km" carried. (Oum, Tae Hoon, & Chunyan Yu, 1994). The calculation of "Passenger-Km" and "Load Tonne-Km" values for unit quantity is shown in Equations 3 and 4. The calculations made in the equations are used to determine the transportation quantities carried out in the efficiency calculation.

$$1\ (passenger)\ x\ distance\ (1\ km)\ =\ 1\ passenger - Km \quad (3)$$
$$1\ (tonne) load\ x\ distance\ (1\ km)\ =\ 1\ load\ (tonne) - Km \quad (4)$$

During the evaluation of the factors affecting the efficiency of rail systems, the ratio of the carrying capacity of the vehicles and infrastructure to the current carrying value is taken into consideration. While making the carrying capacity evaluations, the literature on efficiency, which addresses labour productivity models and design applications, has been examined and the relevant data has been developed for rail transportation systems. (Kahya & Polat, 2007). Efficiency evaluation allows us to determine the amount of transportation that is realized and not realized, unproductive times, effective transportation amount, standard efficiency, transportation effectiveness and process efficiency. The calculations of the efficiency components are shown in Figure 4. The component calculations are shared in Equation 5-17.

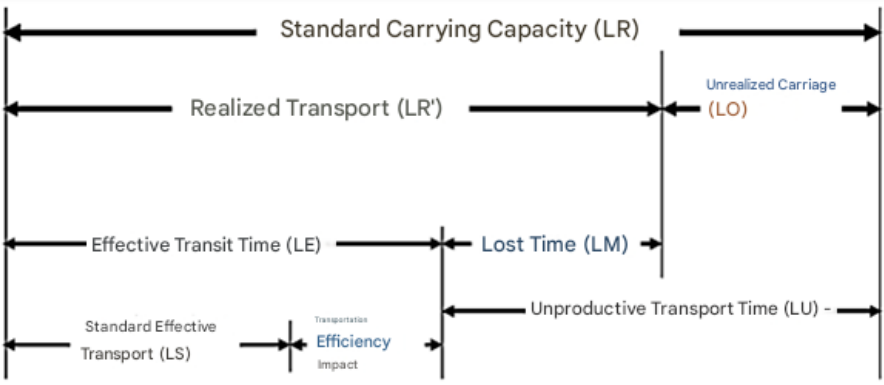

Figure 4. Efficiency components of carrying capacity (ÖZARPA et al., 2022)

$$L_R{}' = L_R - L_O \quad (5)$$
$$L_E = L_R{}' - L_M \quad (6)$$
$$L_M = L_R{}' - L_E \quad (7)$$
$$L_U = L_O + L_M \quad (8)$$

In the above equations, Q is the total amount of transportation performed in a given time for a specified transport system (the total amount of transport realized), L_R the total amount of transport that the existing transport system must perform per unit time (the typical transport capacity used to generate the output Q), L_O, the amount of mandatory and unpredictable transport (due to mandatory loss times such as maintenance, replenishment, absence of passengers or freight), $L_R{}'$, the amount of transport realized within the total capacity,L_E refers to the effective transportation quantities, L_M the loss times during transportation such as road condition and waiting times, L_U the inefficient times and L_S the standard effective transport amount. The overall and specific efficiency of the system can be calculated using the carrying capacity and the amount of transport performed. Equations 9-17 will be used to calculate the ratio of the overall system's overall output carrying capacity.

$$\tau_R = \tau_S \; x \; E_w \; x \; le^{(1)} \; x \; le^{(2)} \quad (9)$$

$$Q/L_R = Q/L_S \; x \; L_S/L_E \; x \; L_E/L_R{}' \; x \; L_R{}'/L_R \quad (10)$$

$$\tau_R = Q/L_R \quad (11)$$

$$\tau_S = Q/L_S \quad (12)$$

$$E_w = L_S/L_E \quad (13)$$

$$le^{(1)} = L_E/L_R{}' \quad (14)$$

$$le^{(2)} = L_R{}'/L_R \quad (15)$$

$$\tau_R{}'' = Q/L_S \; x \; L_S/L_E = Q/L_E \quad (16)$$

$$le^{(0)} = le^{(1)} \; x \; le^{(2)} = L_E/L_R{}' \; x \; L_R{}'/L_R = L_E/L_R \quad (17)$$

In equations; τ_R the efficiency of the whole process (the ratio of the actual amount of transportation to the carrying capacity), τ_S the standard efficiency (the ratio of the amount of transportation performed to the effective transportation), E_w the transportation efficiency (the contribution of the structure to the efficiency), $le^{(1)}$ the ratio of the effective transportation amount to the amount of transportation performed, $le^{(2)}$ the ratio of the actual transportation amount to the standard carrying capacity, $\tau_R{}''$ the process efficiency (the ratio of the standard efficiency to the transportation efficiency), $le^{(0)}$ the effective transportation time to the standard carrying capacity It shows the rate.

Equation 5-17 was used to calculate the efficiency components (Kahya & Polat, 2007). As a result of the theoretical calculations, calculations of all efficiency components of rail transportation systems can be made.

5. CONCLUSION

In this study, smart railway applications used to increase efficiency in rail transportation systems are discussed and equations used to calculate efficiency are evaluated. Today, transportation has become more critical with the increasing population. Like other types of transportation, railway transportation has also increased because it is the most economical and efficient solution. Therefore, increasing transportation to existing facilities appears as the most economical solution. Transportation efficiency can be increased with smart solutions in rail transportation systems. With the development of digital technologies such as smart transportation systems and railways, it has now become possible to manage controllable station and vehicle systems with virtual and physical connections. Controlling these systems from special centre's protects against problems such as failures, accidents, data loss, time and income loss. Thus, efficiency increases and train and freight carrying capacities that can be used with the existing infrastructure can be developed. In addition, more reliable transportation can be provided with instant controls. For this reason, more studies should be conducted in this area and different methods and applications should be developed to increase efficiency. In addition, equations can be considered more comprehensively in future studies and more precise calculations can be made.

REFERENCES

AKSU, E., & KAPLAN, M. (2022). Enhancing Energy Efficiency in Rail System Vehicles. *European Journal of Science and Technology*. doi:10.31590/ejosat.1140257

Butler, L., Yigitcanlar, T., & Paz, A. (2021). Barriers and risks of Mobility-as-a-Service (MaaS) adoption in cities: A systematic review of the literature. *Cities*, *109*, 103036. doi:10.1016/j.cities.2020.103036

ÇODUR, M. Y., & TOPDAĞI, S. (2018). Akıllı Ulaşım Sistemlerinin Kent İçi Toplu Taşımaya Etkisi: Erzurum İli Örneği. *Erzincan Üniversitesi Fen Bilimleri Enstitüsü Dergisi*, *11*(3), 576–586. doi:10.18185/erzifbed.409255

Coto-Solano, M. E. (2024). Demand study of freight transportation via railway of four commodity groups: A case study on Costa Rica's Pacific Coast Route. *Multimodal Transportation*, *3*(4), 100157. doi:10.1016/j.multra.2024.100157

Gallego-García, S., Gejo-García, J., & García-García, M. (2021). Development of a Maintenance and Spare Parts Distribution Model for Increasing Aircraft Efficiency. *Applied Sciences*, *11*(3), 1333. doi:10.3390/app11031333

Greer Liz, Fraser Janet, Hicks Drennan, Mercer Mike, & Thompson Kathy. (2018). *Intelligent Transportation Systems Benefits, Costs, and Lessons Learned*. U.S.

Hahn, D., Munir, A., & Behzadan, V. (2021). Security and Privacy Issues in Intelligent Transportation Systems: Classification and Challenges. *IEEE Intelligent Transportation Systems Magazine*, *13*(1), 181–196. doi:10.1109/MITS.2019.2898973

Kahya, E., & Polat, O. (2007). Bir İşletmenin Mekanik İşler Atölyesi'nde Oranlarla İş Gücü Verimlilik Yönetim Sistemi (WPMR) Tasarımı. *Verimlilik Dergisi*, (2), 9–36.

Kelarestaghi, K. B., Foruhandeh, M., Heaslip, K., & Gerdes, R. (2021). Intelligent Transportation System Security: Impact-Oriented Risk Assessment of in-Vehicle Networks. *IEEE Intelligent Transportation Systems Magazine*, *13*(2), 91–104. doi:10.1109/MITS.2018.2889714

López-Aguilar, P., Batista, E., Martínez-Ballesté, A., & Solanas, A. (2022). Information Security and Privacy in Railway Transportation: A Systematic Review. *Sensors*, *22*(20), 7698. doi:10.3390/s22207698

Oum, Tae Hoon, & Chunyan Yu. (1994). Economic Efficiency of Railways and Implications for Public Policy: A Comparative Study of the OECD Countries' Railways. *Journal of Transport Economics and Policy*, *28*, 121–138.

ÖZARPA, C., AVCI, İ., & KINACI, B. F. (2021). Akıllı Raylı Sistemlerde Kullanılan Alt Sistemlerin Kritik Seviye Analizi. *Demiryolu Mühendisliği*, (14), 143–153. doi:10.47072/demiryolu.937278

ÖZARPA, C., KINACI, B. F., & AVCI, İ. (2022). RAYLI ULAŞIM SİSTEMLERİNDE BAKIM YÖNTEMLERİNİN VERİMLİLİK AÇISINDAN ÖNCELİKLENDİRİLMESİ. *Verimlilik Dergisi*, (4), 643–658. doi:10.51551/verimlilik.988870

Tektaş, N., & Tektaş, M. (2019). Dünyada Akıllı Ulaşım Sistemlerinin Gelecek Hedefleri Japonya Örneğinin İncelenmesi. *Paradoks Ekonomi Sosyoloji ve Politika Dergisi*, *15*(2), 189–210.

Tektaş, N., & Tektaş, M. (2022). National Technology Initiative in Transportation: Intelligent Transportation Systems. In *National Technology Initiative: Social Reflections and Türkiye's Future* (pp. 329–376). Türkiye Bilimler Akademisi Yayınları. doi:10.53478/TUBA.978-625-8352-17-7.ch18

Ulvi, H., & Akdemir, F. (2019). Kent İçi Raylı Sistem Yatırım Ölçütlerinin Üzerine Bir Araştırma: Erzincan Kent İçi Raylı Sistem Örneği. *Journal of International Scientific Researches*, *4*(2), 333–354. doi:10.21733/ibad.552605

Chapter 11

SIGNALLING SYSTEMS USED IN RAIL SYSTEMS

Yusuf YUREKLI[1]
Eyyup TASKAYA[2]
Bahadir Furkan KINACI[3]

[1] Karabuk University, https://orcid.org/0009-0000-4246-4098
[2] Lec., Karabuk University, https://orcid.org/0000-0002-7188-4638
[3] Lec., Karabuk University, https://orcid.org/0000-0001-6872-2630

1. MANAGEMENT SYSTEMS

With the development of rail system technology, efficient use of line capacities, sharing of the same line by different types of transport (freight, passenger) and the need for mutual operability have made much more efficient systems necessary. Different management systems can be encountered in all areas where they are needed. These systems required by rail system technology aim to eliminate accident risks, allocate lower costs, maximum efficiency and maximum transport capacity. The most important management system used in rail system technology, which enables centralized tracking and control of vehicles, provision of line transition information with signal lights, and direction determination with control of switches, is signalling systems. (Yan, Gao, Tang, & Zhou, 2017). In addition to signalling systems, RAMS application and Safety Management systems also appear as important topics.

2. SIGNAL SYSTEMS

The light notification systems manufactured in different types, which all vehicles travelling on the rail system must comply with, located on the right of the lines according to the direction of progress, are called signals. The progress of trains on the railway is done by the guidance of the engineers with these signals. The progress conditions of the train until the next signal are determined by this signal. Transitions between two signals are provided under the conditions determined by the traffic regulations.

Signals are divided into two in terms of appearance: dwarf signal and high signal. High signals; can have 2,3,4 signals. Their height is between 3.8 - 4.2 meters. They are signals located on the main road. Dwarf signals; are signals attached to steel pipes between 0.8 - 0.1 meters. They are placed at the exits of stations and shelter roads. An example of a high triple signal is shared in Fig 1.

Figure 1: High Triple Signal

In terms of their usage, signals are divided into two groups: automatic and controlled signals. These are signals that can be controlled separately by traffic controllers and station control desks. Controlled signals are those used as station entrances and exits and as protection signals. Automatic signals are signals that change automatically according to the notification status of the next signal according to the traffic conditions. Block signals are in this group and are designed to ensure the continuity of train traffic.

Signals in terms of their functions:

- Input Signals: These are the signals that control the entrances to the stations. They are high, 4-lamp, controlled signals.
- Output Signals: These are high or dwarf-controlled signals placed at the exits of the stations.
- Protection Signals: These are the controlled high signals before the input signal of the terminal stations. The 0.5 meter part of the signal pole after the 2 meters from the ground is painted white.
- Approach Signals: These are automatic block signals before entry at stations other than terminal stations. As with protection signals, whitewashing is also done at approach signals.
- Automatic Block Signals: These are the signals placed at the entrances of the blocks between stations. It is controlled with high and three lamps.
- Repeat Signals: It is the type of signal used by the driver on inclined roads where there is no line of sight. It is used to indicate the colour of the signal after it. They are high signals in green and daylight colours with the coloured letter T on them.

2.1. Direct Control Systems

These are systems where systems are directly controlled via a control console or panel. Return data defined as indication is collected by feeding from a different line. It is suitable for use in central lines where local terminal stations are located. It is not preferred for use along the line and is preferred in central stations for fast communication, ease of solution and to save time. Direct control systems are given in Figure 2.

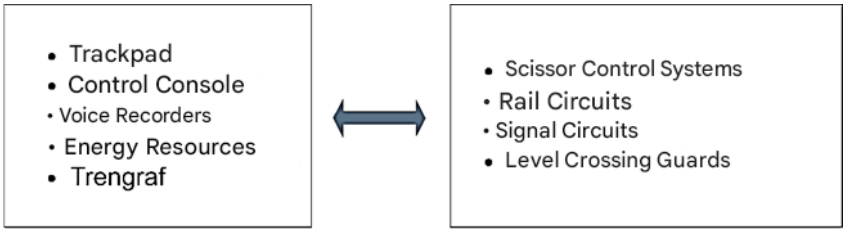

Figure 2: Direct Control Systems

2.1.1. Centrally Controlled Systems

Central control systems are systems that can be accessed along the line through a control centre and manage systematic processes. All kinds of signalling information and line-length data can be monitored from a central panel or monitor. Professional equipment is used to ensure information flow in this system. The train control mechanism is shared in Figure 3.

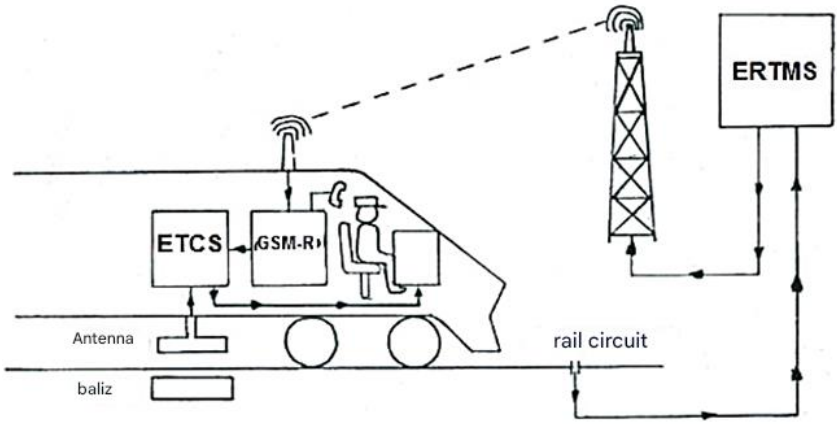

Figure 3: Train Control Mechanism ('ERTMS', 2010)

There are traffic controllers called dispatchers who continue the operations performed on the control panel. These controllers manage the continuous navigation status by routing with the engineer. They create safe areas by ensuring that trains on certain lines are locked with switches and signals. There is a simulation of the entire controlled line in the control centre. Although the great crossings in the areas where trains will pass are opened and closed automatically, they must be constantly monitored by these personnel. The trains that must wait inside the stations are controlled by automatic switch motors by dispatchers without being included in the system to stay in the safe area and their movement requests. Stationary systems are also constantly monitored in central stations. Although the station maneuvering operations are performed by the station personnel, they are

always under the control of the control centre. In case of a notification on the road, the first observation is made by the control centre and the notification is transmitted to the relevant personnel. The traffic control panel is shared in Fig 4.

Figure 4: Traffic Control Panel

2.1.2. Direct Control Systems

To ensure the safe dispatch and management of train traffic in rail systems, the exact location of the trains must be determined. Rail circuits use rails as a conductive circuit complement and provide control over whether there is a busyness in that area according to the completion of the circuit. The railway is used like a simple electrical circuit, acting as a switch in the trains that enter the circuit, giving a busyness on the line and ensuring that traffic is monitored from the control screens. Rails serve as iron bars that enable the transmission of electric current. They have a high current carrying capacity. Breakers are also located on the line against overloading situations. When there is another element on the line that complements the circuit, not only connected to the trains, but it is also understood that there is a problem as a busyness situation. Circuit completion systems continue their existence in signalling systems as a security mechanism. The signalling system rail circuit is shared in Figure 5.

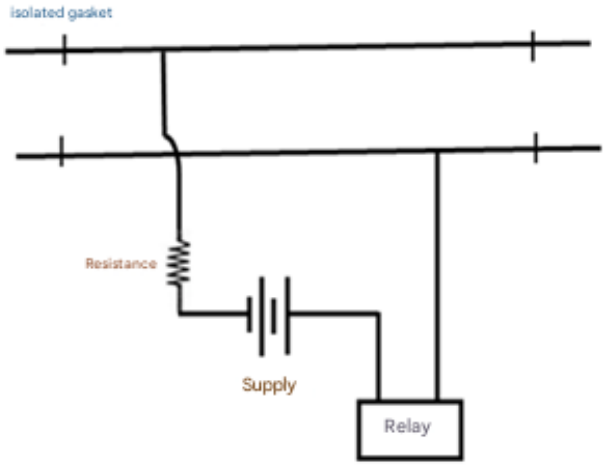

Figure 5: Signalling System Track Circuit

2.1.3. Train Protection System

In systems where trains are managed by signalling, a control mechanism has been developed that eliminates human elements in case of unauthorized and uncontrolled entries. It is a protection system that automatically stops the train in cases where the engineer makes a mistake and continues to move at a red light. In some systems, there are systems that warn the engineer when the permitted speeds are exceeded and then automatically break the train. The first and most common application name of these systems is briefly ATS (Automatic Train Stopping), that is, automatic train stopping system.

Continuity is provided by a system in which the track coil placed inside the rail or on the side of the road next to the signals along the line and the ATS cabin devices placed on the locomotives work together. Automatic braking is performed at safe distances with magnets placed under the locomotives. ATS ground magnets warn the train to stop or slow down according to the colour of the signal by means of vehicle magnets. In the event of a red signal being passed, when the ground magnets warn the coils on the locomotive, the air in the vehicle installation is discharged to the atmosphere, and air is sent from the auxiliary air tanks to the brake cylinders, aiming to stop the train as soon as possible. ATS magnets on the track are shared in Figure 6.

Figure 6: On-Road ATS Magnets

2.1.4. European Train Control Systems

Different signalling systems used in European countries have made it difficult to control the track and on-board equipment. With these difficulties, the development of a central management and control mechanism has become a necessity. Separate on-board equipment for each signalling system has created separate transition difficulties for each locomotive (Bernal, Spiryagin, & Cole, 2019). To solve these problems, with the encouragement of the European Railway Community (CER), a monopoly mechanism that can be formed within the continent in rail system technology has been created by coming together with a uniform system. In this way, train dispatch and management has been taken under control in a wide area and a safer transportation has been provided.

The European Railway Traffic Management System (ERTMS) is a union established to create and spread a standard throughout Europe. These standards are implemented in our country as well as in European countries. Our newly constructed lines and especially our high-speed train lines are manufactured in accordance with European standards. ETCS system components are shared in Figure 7.

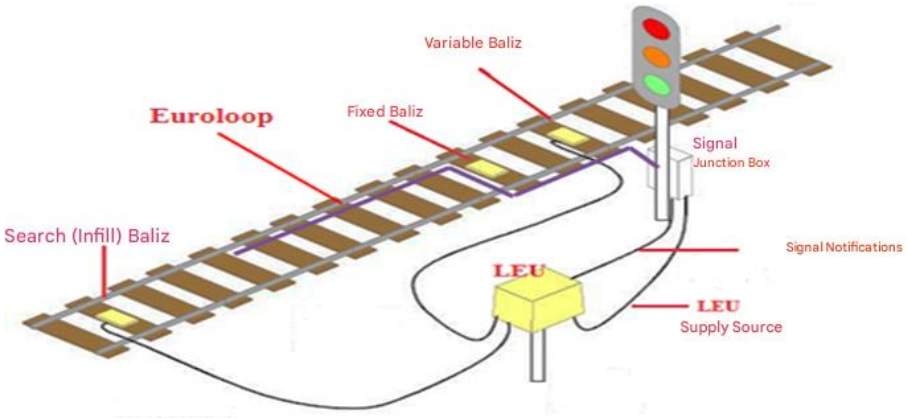

Figure 7: ETCS System Components

ETCS systems consist of road and vehicle interactions, as in automatic train stopping systems. The system consists of signal circuits, line-length electronic unit, rail circuit and radio block system, signal receiver and on-board equipment. The system in the vehicles consists of a receiver and transmitter radar system that monitors the driver's road and speed information, and a panel consisting of sound and/or image recording mechanisms (Yin et al., 2017).

2.2. Safety Management Systems

In recent years, due to the significant increase in railway speeds and traffic density on railway lines, the safe time intervals between train journeys have decreased significantly, creating new and greater risks.

These risks are becoming more apparent, especially in high-speed railway transport. The purpose of establishing a safety management system is to meet the conditions required for safe transport on railways. In railways, which stand out with their travel safety, safety management systems need to be developed to protect and improve this understanding. The general structure of the system and basic safety processes and techniques are determined by the European Commission Directive 2004/49/EC (Sitarz & Chruzik, 2019). This directive was subsequently updated by Directive 2016/798 of the European Parliament and of the Council (EC, 2016). According to the Railway Safety Directive, all railway operators and infrastructure managers must use a safety management system correctly. This is crucial for the success of the regulatory safety framework as a whole (Wu, Ge, & Luo, 2020).

The safety management system is basically created in three stages. The first two stages include hazard analysis and threat assessment. After these two stages, also called risk management, the third is the reduction of risks (Edkins & Pollock,

1996). There should be various elements in the developed safety management systems. First, the basic goals of the system should be well determined and the parameters appropriate to the desired safety level should be determined. To conduct risk assessment, inspection methods should be explained correctly. Personnel training plans should be made regarding hazardous material transportation, railway traffic and maintenance and repair of vehicles. The incidents and accidents that occur should be documented correctly. In addition, the implemented safety management systems should be periodically inspected (Li & Guldenmund, 2018).

2.3. RAMS

RAMS consists of reliability, availability, maintenance and safety components. As railway usage increases, accidents increase, which can cause various problems and interruptions in railway traffic.

RAMS analysis of railway networks helps managers to find key components such as sections and stations that are important for safety and examines how a section or station failure affects the safety of the network. Therefore, RAMS management is an important decision maker in today's global and local railway operations (Zhang, Jia, & Qin, 2021). RAMS management of the railway sector in Turkey is defined by the TS EN 50126-2 standard. This standard describes the necessary RAMS parameters throughout the life cycle of a product or system (Kadıoğlu & Toprak, 2020).

3. CONCLUSION

The significant increase in the speed of railway vehicles and the traffic density on railway lines in recent years requires the correct planning and management of safe time intervals between train trips. This has made signalling and safety systems more important and critical. In this study, signalling systems, which have an important place in railways, are discussed. The importance and use of railway transportation, which is the most efficient transportation method among transportation systems, is increasing day by day. For this reason, signalling systems need to be planned more accurately to achieve more efficient, faster and safer transportation. For this reason, more studies should be conducted in the future on the design and analysis of faster and more reliable signalling and safety systems.

REFERENCES

Bernal, E., Spiryagin, M., & Cole, C. (2019). Onboard Condition Monitoring Sensors, Systems and Techniques for Freight Railway Vehicles: A Review. *IEEE Sensors Journal*, *19*(1), 4–24. doi:10.1109/JSEN.2018.2875160

EC. (2016). Directive (EU) 2016/798 of the European Parliament and of the Council of 11 May 2016 on railway safety. *Official Journal of the European Union*, *138*.

Edkins, G. D., & Pollock, C. M. (1996). Pro-active safety management: Application and evaluation within a rail context. *Safety Science*, *24*(2), 83–93. doi:10.1016/S0925-7535(96)00027-6

ERTMS. (2010). Retrieved 29 November 2024, from https://www.christian-bruun.dk/ERTMS.html

Kadıoğlu, T., & Toprak, T. (2020). RAYLI SİSTEM ARAÇLARINDA RAMS VERİLERİNİ VE TEKNİKLERİNİ KULLANARAK, ARAÇ PERFORMANSINI, BAKIM VE ARIZA GİDERLERİNİ İYİLEŞTİRMEK. *İstanbul Commerce University Journal of Science*, *19*(38), 190–207.

Li, Y., & Guldenmund, F. W. (2018). Safety management systems: A broad overview of the literature. *Safety Science*, *103*, 94–123. doi:10.1016/j.ssci.2017.11.016

Sitarz, M., & Chruzik, K. (2019). AN APPROACH TO THE LEGAL REQUIREMENTS REGARDING RAILWAY TRANSPORT SAFETY MONITORING IN THE EUROPEAN UNION. *Transport*, *34*(3), 163–174. doi:10.3846/transport.2019.8528

Wu, S., Ge, X., & Luo, Y. (2020). *A New Model of Safety Management System for Railway Operation*. In *2020 7th International Conference on Information Science and Control Engineering (ICISCE)* (pp. 1576–1584). IEEE. doi:10.1109/ICISCE50968.2020.00312

Yan, F., Gao, C., Tang, T., & Zhou, Y. (2017). A Safety Management and Signaling System Integration Method for Communication-Based Train Control System. *Urban Rail Transit*, *3*(2), 90–99. doi:10.1007/s40864-017-0051-7

Yin, J., Tang, T., Yang, L., Xun, J., Huang, Y., & Gao, Z. (2017). Research and development of automatic train operation for railway transportation systems: A survey. *Transportation Research Part C: Emerging Technologies*, *85*, 548–572. doi:10.1016/j.trc.2017.09.009

Zhang, Z., Jia, L., & Qin, Y. (2021). RAMS analysis of railway network: model development and a case study in China. *Smart and Resilient Transportation*, *3*(1), 2–11. doi:10.1108/SRT-10-2020-0013